People's Democratic Republic of Algeria

Ministry of Higher Education and Scientific Research
Mohamed El Bachir El Ibrahimi University of Borj Bou Arréridj
Faculty of Mathematics and Computer Science
Department of Mathematics

THESIS
In order to obtain the Doctorate degree in LMD (3rd cycle)
Branch : Applied Mathematics
Option : Modelization, Control and Optimization

THEME

Numerical treatment of stochastic differential equations: Diffusion and jump-diffusion processes with applications

By: Ikram Boukhelkhal

Publicly Defended In : **13/06/2024**

In front of the jury composed of:

Pr. Rebiha Benterki	University of B.B.A	**President**
Dr. Rebiha Zeghdane	University of B.B.A	**Supervisor**
Pr. Arezki Kheloufi	University of Bejaia	**Examiner**
Dr. Smail Addoune	University of B.B.A	**Examiner**
Dr. Imad Eddine Lakhdari	University of Biskra	**Examiner**

2023/2024

Acknowledgement

Abstract

In this dissertation, we deal with the problem of simulating stochastic differential equations driven by Brownian motion or the general Lévy processes. First, we establish the basic theory of stochastic calculus and introduce the Itô-Taylor expansion for stochastic differential equations (SDEs). In addition, we present various numerical schemes derived from the Itô-Taylor expansion. These methods are used to solve the stochastic Lorenz equation, the stochastic Duffing equation, and the Merton model equation. In addition, spectral techniques are adapted for the numerical solution of nonlinear stochastic differential equations. Further, generalized Lagrange interpolation functions are proposed for solving various types of SDEs, offering significant performance improvements.

Keywords: Stochastic differential equation, Brownian motion, jump diffusion, spectral method, numerical solution, collocation method.

Résumé

Dans cette thèse, nous traitons le problème de la simulation des équations différentielles stochastiques dirigées par le mouvement brownien ou les processus généraux de Lévy. Tout d'abord, nous établissons la théorie de base du calcul stochastique et introduisons le développemement d'Itô-Taylor pour les équations différentielles stochastiques (EDS). En outre, nous présentons divers schémas numériques dérivés de développement d'Itô-Taylor. Ces méthodes sont utilisées pour résoudre l'équation stochastique de Lorenz, l'équation stochastique de Duffing et l'équation du modèle de Merton. Par ailleurs, les techniques spectrales sont adaptées à la résolution numérique d'équations différentielles stochastiques non linéaires. De plus, des fonctions d'interpolation de Lagrange généralisées sont proposées pour résoudre divers types d'équations différentielles stochastiques, offrant des améliorations significatives des performances.

Mots clés: Equation différentielle stochastique, mouvement brownien, diffusion par sauts, méthode spectrale, solution numérique, méthode de collocation.

الملخص

نتناول في هذه الأطروحة مشكلة محاكاة المعادلات التفاضلية العشوائية المرتبطة بالحركة البراونية أو عمليات ليفي العامة. أولاً، نؤسس النظرية الأساسية لحساب التفاضل والتكامل العشوائي ونقدم توسعة إيتو-تايلور للمعادلات التفاضلية العشوائية. بالإضافة إلى ذلك، نقدم العديد من الطرق العددية المختلفة المشتقة من توسع إيتو-تايلور. تُستخدم هذه الطرق لحل معادلة لورينزالعشوائية ومعادلة دفينج العشوائية ومعادلة نموذج ميرتون. كما أن الأساليب الطيفية مناسبة أيضًا لحل العددي للمعادلات التفاضلية العشوائية غير الخطية. وبالإضافة إلى ذلك، تُقترح دوال استيفاء لاغرانج المعممة لأنواع مختلفة من المعادلات التفاضلية العشوائية، مما يوفر تحسينات ملحوظة في النتائج.

الكلمات المفتاحية : المعادلة التفاضلية العشوائية، الحركة البراونية، الانتشار القفزي، الطريقة الطيفية، الحل العددي، طريقة التجميع

Contents

List of Figures

List of Tables

Notations

SDE	Stochastic differential equations
SIVIE	Stochastic Ito-Volterra integral equation
$(\Omega, \mathcal{A}, P)$	Probability space
$\mathcal{A}_t$	Filtration
X_t	Stochastic process
N_t	Poisson process
λ	The intensity of Poisson process
$\mathcal{J}_t$	Compound Poisson process.
$\mathcal{N}(\mu, \sigma^2)$	Normal distribution with expectation μ and variance σ^2
$\mathcal{B}_t$	Brownian motion
$\mathcal{G}$	The set of elementry functions
$n(\beta)$	Number of componenets of a multi-index β
$\mathcal{H}$	The sets of adapted right continuous stochastic processes with left hand limite
τ_1, τ_2	Stopping time
$I_\beta(g)$	The multiple Ito integral
Δ	The step size discretization
$\mathcal{J}^{\alpha,\beta}(t)$	Jacobi polynomials
$G_j^L(t)$	Generalized Lagrange functions
δ_{ij}	The Kronecker delta

Introduction

Mathematical models of physical processes in science and engineering are presented in the form of algebraic expressions before they are viewed as differential equations. One of the basic principles of numerical methods is the reduction of a differential equation to an approximation using algebraic equations. This reduction involves replacing a continuous differential equation, whose solution space is generally infinite dimensional, with a finite set of algebraic equations whose solution space is finite-dimensional.

During the last three decades, deterministic chaos theory has rapidly attracted mathematicians, engineers, economists, physicists, biologists, etc. But, this type of "chaos" can only be understood as quasi-chaos, where all states of a system can be predicted and recreated by experimenting. In addition, many experiments in the natural sciences have provided hard evidence of stochastic behavior. Deterministic models can represent idealized situations and can often be corrected by adding stochastic influences.

Because of the irregularity of Brownian motion, stochastic differential equations can only be interpreted in terms of stochastic integral equations. Kiyosi Ito (1915-2008) discovered the difficulty of investigating differential equations with a noise term that does not converge to a unique limit in the mean square sense. To avoid this difficulty, Ito developed a new approach and created a formula called the Ito formula, which is the basis of the Itô calculus and an introduction to stochastic differential equations (SDE) [47, 48, 49, 56]. The passage from ODEs to SDEs is made by incorporating random elements into the differential equation. Randomness can be set in the initial data for the problem, otherwise, the function that describes the physical system can be a random function, and in this case, the differential equation is known as a stochastic differential equation. Stochastic differential equations are basically equations of motion for dynamic systems that evolve according to a probabilistic description. In the last few years, stochastic ordinary differential equations have been widely used in population dynamics, bacteriophage infection, and other fields [10, 26, 66].

Stochastic differential equations (SDEs) driven by the Brownian motion process are im-

portant tools in a wide range of applications, including biology, chemistry, mechanics, economics, physics, and finance [46, 55, 64, 65, 66], these equations are interpreted using Itô calculus [98]. For example, the geometric Brownian motion

$$dX(t) = \mu X(t)dt + \lambda X(t)d\mathcal{B}(t), \quad X(0) = X_0, \tag{1}$$

which is a stochastic process commonly used to model the behavior of asset prices in finance, including in the Black-Scholes-Merton option pricing model, where $X(t)$ represents the asset price at time t, $dX(t)$ represents the infinitesimal change in the asset price, μ is the drift coefficient, representing the average rate of return of the asset over time and λ is the volatility coefficient, representing the standard deviation of the asset's returns. Another important example is Feller's branching diffusion, which is a stochastic process commonly used in mathematical biology to model population dynamics, particularly in the context of branching processes.

$$dX(t) = \alpha X(t)dt + \sigma\sqrt{X(t)}d\mathcal{B}(t), \quad X(0) = X_0 > 0, \tag{2}$$

where $\mathcal{B}(t)$ is the Brownian motion in both examples and here $X(t)$ represents the population size at time t, $dX(t)$ represents the infinitesimal change in the population size, α is the growth rate coefficient, representing the average rate of increase or decrease in the population size over time and σ is the volatility coefficient, representing the standard deviation of the population growth rate.

Stochastic differential equations driven by jump processes have been applied extensively in several fields to model various natural problems [72, 102, 115, 136].

In recent years, time-dependent systems under random effects have attracted much attention in various domains of science. Usually, such dynamical systems can be expressed by SDEs. These equations are formulated by a stochastic process with non-smooth trajectories. Since solving the SDEs can only be done in a particular cases, developing stable numerical techniques for SDEs is a major and rapidly increasing area of research.

Taylor-Itô schemes have been widely used to solve stochastic differential equations (SDEs) for a long time. Their popularity is unlikely to diminish with the increased use of automatic differentiation techniques. The Taylor expansions of exact solutions of SDEs, from which Taylor methods are constructed, can take one of two forms: either as Wagner's Platen series [66, 67, 131] or as B-series [114]. The connection between the two series has been shown in

[32]. The construction of explicit and semi-implicit Taylor schemes can be found in many references [66, 81]. Much research has been done on fully implicit methods in recent years. T. Tian et al.[125] proposed implicit Taylor schemes for SDE. Ahmad et al.[5] created the fully implicit stochastic-α method. Wang et al.[127] designed the split-step backward balanced Milstein methods. [42] built a class of split-step balanced methods. Haining Wen developed the fully-implicit truncated Euler–Maruyama method [133]. Wang et al. [129] presented a family of fully implicit Milstein methods. Haghighi et al. Others recent contributions are given in [6, 7, 54, 77, 82, 111, 128]. In [24], the author suggests an efficient way and powerful class of Runge-Kutta methods for the solution of SDE, this class of methods is the focus of the author's research in the investigation of high-order methods suitable for the numerical solution of SDE. Recently, a lot of work has been devoted to improving Taylor schemes by developing implicit or multi-step techniques or by some spectral methods.

Due to their high accuracy, spectral methods have been widely used in the last decades. Three main types of spectral methods can be applied: collocation, tau, and Galerkin. The choice of the type of method depends fundamentally on the application. Collocation methods are appropriate for nonlinear problems or problems with intricate coefficients. The standard approach, in which the test of functions (polynomials), has major disadvantages. First, the matrices generated by the discretization matrices have an increasing condition number, and thus computational rounding errors. This reduces the expected theoretical exponential accuracy. Furthermore, the discretization matrices are usually fully populated, making it difficult to use efficient algebraic solvers. Several attempts have been made to try to get around these inconveniences of the standard approach. All of these attempts are based on the relatively large flexibility in choosing trial and test functions. In fact, using different weight functions, they are constructed in such a way as to include as much bounded data as possible and, additionally, to decrease the condition number of the matrices. Due to inherent "randomness" within stochastic differential equations (SDEs) and the unpredictable nature of Brownian motion, solving them analytically poses significant challenges. Explicit solutions for SDEs are rare, making it difficult to address them directly. Consequently, there has been a growing focus over the last decade on the advancement of numerical techniques for solving stochastic differential equations. Numerous studies have explored these equations employing a variety of numerical techniques, including cubic B-spline collocation method, the Chebyshev collocation method, Jacobi collocation method,

quadratic B-splines method, the finite difference-Simpsons method, reproducing kernel algorithm, reproducing kernel Hilbert space method, and piecewise optimal fractional reproducing kernel method, a spectral collocation method and Taylor expansion method, Bernstein polynomials, Bernoulli polynomials, block pulse functions, and Chebyshev wavelets [4, 8, 9, 90, 91, 104, 107, 108, 143].

In this thesis, we are mainly concerned with approximations of stochastic differential equations (SDE). The aim is to present recent developments in these numerical methods and include our own works. We first study the classical strong and weak Taylor-Ito schemes to approximate solutions of stochastic differential equations and examine their stability properties. The fundamental question is as follows, how well does the numerical method approximate the characteristics of the analytical solution. Following Higham [45], we consider numerical methods for SDEs, in particular, the Euler-Maruyama method and Milstein method. These methods are constructed from the Ito-Taylor expansion. In our research, we deal with a nonlinear SDE. We estimate the exact solution using Monte Carlo simulation for each method. To demonstrate the effectiveness of the numerical methods, approximate solutions are compared with the analytical solution for different sample trajectories, and some applications are given, including the linear Black-Scholes model, the Duffing equation, the Lorenz system, and the Merton jump diffusion. In addition, we propose a novel approaches to numerically approximate some classes of stochastic differential equations driven by white noise. The presented methods share some particular features with stochastic collocation techniques, and in particular, they exploit the smoothness assumption of the approximated function to achieve fast convergence. The solution of the stochastic differential equation (SDE) is expressed in terms of some basis functions. The coefficients of basis functions can be calculated by solving a system of algebraic equations. Another attraction of this work is the novelty of the numerical methods, which do not belong to the classical methods for solving SDEs. Numerical experiments are performed to demonstrate the accuracy and effectiveness of the new methods.

This thesis is organized as follows: Chapter 1 begins with the concept of stochastic processes, provides some background on probability theory, Itô calculus, and introduces stochastic differential equations. In Chapter 2, we will first look at the classical Taylor Itô methods with some numerical analysis. It discusses numerical methods for approximating stochastic differential equations, we will look at two different pseudo-spectral methods and how to

implement them. In Chapter 3, we propose a new adapted method for numerically solving SDE. The method is based on the stochastic collocation method. We conclude this thesis by summarizing the results obtained in the numerical experiments. Finally, we give a brief overview of some topics of interest that are beyond the scope of this thesis. Some contributions of papers in this dissertation are as follows:

1. In the first work, we focus on Lagrange interpolation polynomials for solving nonlinear stochastic integral equations. In this work, we use an efficient adaptative collocation method solver that is used for a strong solution of SDE. The resulting method is well-suited for dealing with different problems, which we demonstrate through numerical examples and improve some stability issues.

2. In the second work, we concentrate on a novel efficient technique for solving nonlinear stochastic Itô-Volterra integral equations. In this work, we provide an analysis of the error committed by the generalization of interpolation problem to the so-called generalized Lagrange functions. Our analysis provides a novel technique to indicate the efficiency of the Jacobi collocation method for interpolation problems.

To finish this introduction, let us recall that the content of this thesis is the subjects of the papers [22, 23].

Stochastic Calculus

This chapter is devoted to stochastic analysis which is one of the most interesting domain in applied mathematics, which has been and is still studying phenomena in our daily lives and has contributed to solving many problems. The story began in 1827 when Robert Brown was hired to classify plants, so one of his interests was how pollen could be used to classify plants. He put a drop of water on a microscope slide and added pollen to it; like usual, the pollen wiggled and vibrated in the water, but for the first time, Brown wondered why. Many hypotheses came to his mind regarding the movement of pollen in the water. Among these hypotheses was that the movement could be due to the current, that the pollen was alive and moving, or because of the evaporation of water, but all of these hypotheses contradicted the random movement of the pollen, and they all failed during testing of their validity. Brown repeated the same experiment, but with something certain that it was dead, but they continued to notice the vibration, which became not limited to pollen. The only defining feature that all the jiggling specimens have in common is that the motion is random. At that time, atoms and their movement had not been discovered, and there was common disagreement among scientists about the presence of small, invisible particles that move due to changes in pressure and temperature. This hypothesis had a problem from a theoretical standpoint because the theory said that the particles were so small that even the best microscopes at the time wouldn't be able to see them.

Well, in 1905, Einstein came up with a solution to the problem and, in doing so, solved Brown's pollen mystery as well. He figured that even if we couldn't see the tiny particles themselves, we should be able to describe how they interact with something larger that we can see. The atoms theory of Einstein was proven experimentally by the physicist Jean

Perrin in 1926 [103], and he got a Nobel prize for it, even the scientists who were skeptical about the theory's validity were convinced.

A lot of modern technology was made possible by stochastic calculus, especially Brownian motion. In 1976, Norbert Wiener developed the properties of Brownian motion in collected works [134], which is often also called the Wiener process; all of Wiener's study was based on the measure theory, discovered by Lebesgue in 1902 [70].

To understand the dynamics of most SDEs and their solutions, it is important to have some knowledge of probability theory as well as some mathematical principles. Here is a brief introduction to some of these concepts.

1.1   Introduction to stochastic processes

Let $(\Omega, \mathcal{A}, P)$ be a probability space where Ω is a set, $\mathcal{A}$ is a σ-field and P is a probability measure on $\mathcal{A}$. Establishing the definition of random variables constitutes a fundamental aspect of probability theory. A random variable X is a measurable function from a sample space Ω as a set of possible outcomes to a measurable space E. One of the important random variables are Gaussian variables characterized by their normal distribution densities [21, 100]. A generalization of Gaussian variables are Gaussian vectors for which all the linear combination of its components is a Gaussian variable. However, the progression in this field has prompted a move beyond mere satisfaction with random variables alone. In recent years, the development of chaotic models has helped to eradicate the distinction between deterministic and stochastic models. A chaotic model is a deterministic model that is highly susceptible to the values of some parameters in the model and the researchers have claimed that systems normally considered to be stochastic processes as viewed chaotic deterministic systems, for example, a beating heart, a column of rising smoke, a smallpox epidemic.

The necessity to delve into random processes arises when addressing phenomena that evolve over time. While a random variable signifies a singular outcome of a random experiment, a stochastic process encapsulates a collection of random variables distributed across time. The principal motivation for transitioning from random variables to random processes lies in the imperative to model and scrutinize systems or phenomena exhibiting variability and randomness over time or space.

Definition 1.1 *(**Stochastic process**)*

A collection of random variables $\{X_t(w), t \in [0,T], w \in \Omega\}$ is called a stochastic process.

- *When we fix the time t, the stochastic process become a random variable: $X_t = X_t(w), w \in \Omega$.*

- *For a fixed outcome $w \in \Omega$, the application*

$$X : \mathbb{R}_+ \longrightarrow \mathbb{R}^n$$

$$t \mapsto X_t(w),$$

is called a trajectory or realization of stochastic process.

In reality, stochastic processes are used to describe and analyze various phenomena where randomness plays a significant role. Stochastic processes provide a way to understand and quantify the inherent randomness and unpredictability in various systems and phenomena. They offer valuable tools for making probabilistic predictions, optimizing processes, and gaining insights into the behavior of complex systems in the presence of uncertainty. One of the important process in stochastic calculus is the Markov process.

Remark 1.1 *A stochastic process has the Markov property if its future evolution depends only on its current position, for example, assume there is a person who goes to the casino and has 1,000\$. He will play one game every one hour. If he wins, the amount in his hand will be doubled, and if he loses, the amount he has will be divided into two.*

Define the stochastic process as X_t= { his amount at the tth hour }.

In this example, if we want to calculate how much money he will have at $t = 4$, its mean X_4, we need just information about X_3, and we do not need information about how much money he had in X_2 or X_1. This is exactly what the Markov process means.

Definition 1.2 *(**Gaussian process**)*

We say that X_t is a Gaussian process if for all $(t_1, t_2, ..., t_n) \in \mathbb{R}_+^n$ the vector $(X_{t_1}, X_{t_2}, ..., X_{t_n})$ is a Gaussian vector (which means that each linear combination between its components is a Gaussian variable).

It's important to note that the Gaussian distributions are prevalent and useful in many scenarios. In cases where the data significantly deviates from normality, alternative distributions and statistical methods may be more appropriate.

In the theory of stochastic processes, filtrations are fully organized collections of subsets that are used to describe the information available at a given time. Hence play a major role in the formalization of stochastic processes.

Definition 1.3 *(**Filtration**)*

On a probability space $(\Omega, \mathcal{A}, P)$, a collection $\{\mathcal{A}_t, 0 \leq t < \infty\}$ of sub-σ-field on $\mathcal{A}$, such that $\mathcal{A}_s \subset \mathcal{A}_t$ for every $0 \leq s \leq t$ is called a filtration. The space $(\Omega, \mathcal{A}, \mathcal{A}_t, P)$ is called a filtrated probability space.

Example 1.1 *1. One common example of a filtration is in the context of a financial market. Consider a financial market where each day you receive information about the stock prices. The information available to you forms a filtration. Let's denote the information at day t as $\mathcal{A}_t$, representing the sigma-algebra of events known up to and including day t. Here, the filtration $\mathcal{A}_t$ captures the increasing information over time. If you observe stock prices for several consecutive days, $\mathcal{A}_1$ would represent the information available after day 1, $\mathcal{A}_2$ after day 2, and so on. This concept is crucial in stochastic processes and the theory of stochastic calculus, particularly in the modeling of financial derivatives and understanding the evolution of information in dynamic systems.*

2. The natural filtration of stochastic process X_t is defined as $\mathcal{A}_t^X = \sigma\{X_s, s \leq t\}$.

Definition 1.4 *(**Adapted process**)*

The stochastic process $\{X_t, t \geq 0\}$ is adapted to the filtration $\{\mathcal{A}_t, 0 \leq t \leq \infty\}$ if for every $t \geq 0$, X_t is $\mathcal{A}_t$-measurable.

One of the most important types of stochastic processes is the stochastic process with independent increments. In this thesis, we will consider processes with independent increments.

Definition 1.5 *A stochastic process X_t is said to be an independent increasing process if for all $t_1, t_2, ..., t_n$ such that $0 < t_1 < t_2 < ... < t_n$, the random variables $X_{t_1}, X_{t_2} - X_{t_1}, ..., X_{t_n} - X_{t_{n-1}}$ are independent.*

1.2 Brownian motion and the Wiener process

Let given the filtrated probability space $(\Omega, \mathcal{A}, (\mathcal{A}_t)_{t \geq 0}, P)$.

Definition 1.6 *The Brownian motion (also called Wiener process) $\mathcal{B} = \{\mathcal{B}_t, t \geq 0\}$ is a stochastic process that satisfy the following conditions:*

- **Independent increasing process:** *for all $t > s \geq 0$, the random variable $\mathcal{B}_t - \mathcal{B}_s$ is independent of $\mathcal{A}_s = \sigma\{\mathcal{B}_u, u \leq s\}$.*

- *For all $t \geq 0$, $\mathcal{B}_t$ is normally distributed with mean 0 and variance t.*

- **Continuity:** *The process $\mathcal{B}$ is continuous.*

1.2.1 Construction of Brownian motion

Let us start with a simple random walk on a set of integers in discrete time.

Definition 1.7 *(**Random walk process**)*

Suppose that $Y_1, Y_2, \ldots, Y_t, \ldots$ are independent identically distributed random variables, taking the value 1 or -1 with probability $1/2$, then define for each integer $t \geq 1$

$$X_t = \sum_{i=1}^{t} Y_i, \tag{1.1}$$

where $X_0 = 0$, then $\{X_t, t \geq 0\}$ is called simple random walk.

By center limit theorem, X_t converge to $\mathcal{N}(0, t)$ then we will have $\frac{1}{\sqrt{t}} X_t$ converge to $\mathcal{N}(0, 1)$.
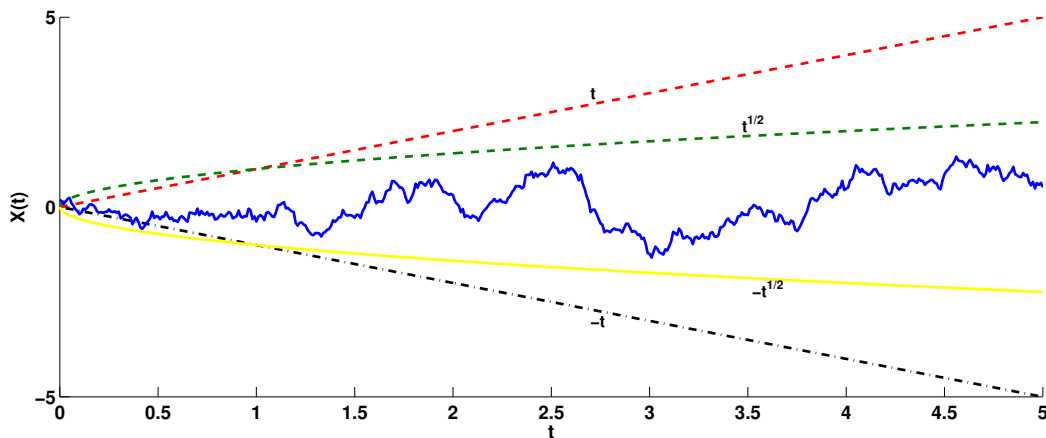
Figure 1.1: The random walk process.

Figure 1.1 shows the trajectory of a random walk process.

If we go back to the movement of pollen in water, if we think of each collision (between molecules and pollen) as one step, then each step will push pollen to the left or the right by accumulating over time, this is a simple random walk. If we lead t to infinity in the Eq. (1.1), we will have a Brownian motion. Figure 1.2-1.4 describe the trajectories of Brownian motion in one, two and three dimensions, respectively.
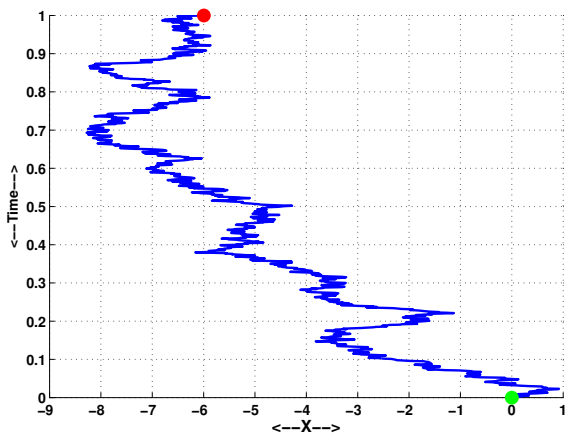
Figure 1.2: Brownian motion in one dimension.
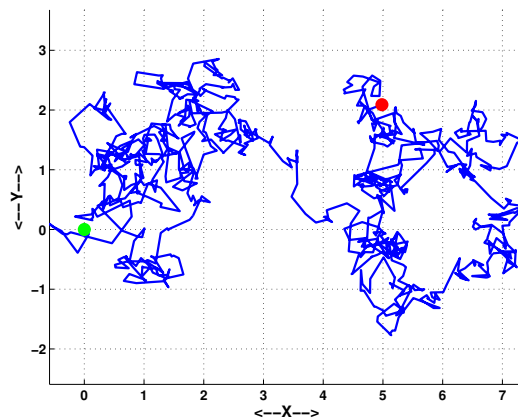
Figure 1.3: Brownian motion in two dimension.
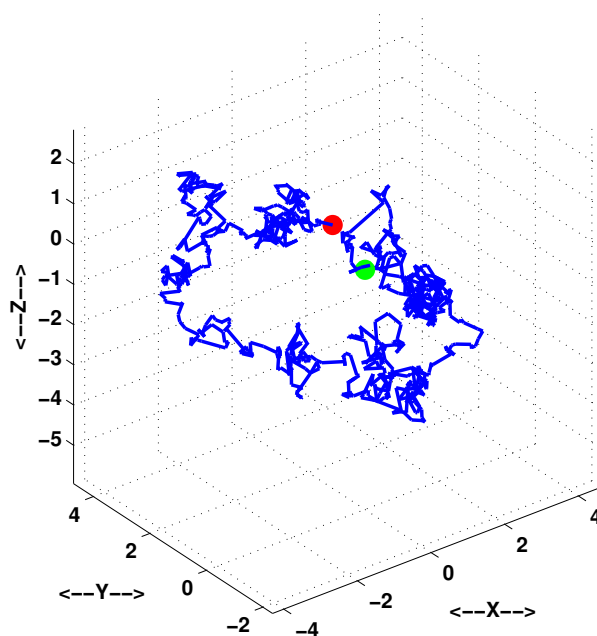
Figure 1.4: Brownian motion in three dimension.

1.2.2   Sample paths properties of Brownian motion

Let $\mathcal{B}_t$ be a Brownian motion, so we have

- $(\mathcal{B}_t)$ is not differentiable at any point, and the trajectory of it passes infinitely many times through all points.

- Stationary: for all $h > 0$, $\{\mathcal{B}_t, t \geq 0\}$ and $\{\mathcal{B}_{t+h}, t \geq 0\}$ have the same distribution.

- One of the important property of Brownian motion is its scaling invariance which modifies the individual Brownian random functions but keeps their distribution invariant.

Theorem 1.1 *[112]* (**Quadratic Variation**)

Let $\{\mathcal{B}_t\}_{t \in [0,T]}$ be a Browniann motion, then we have

$$\lim_{n \to \infty} \sum_{i=1}^{n} \left(\mathcal{B}\left(\frac{i}{n}T\right) - \mathcal{B}\left(\frac{i-1}{n}T\right) \right)^2 = T. \tag{1.2}$$

Proof.

Before we prove the property in Eq.(1.2), let's see the result if we have a continuous differentiable function instead of Brownian motion.

Assume that f is a continuously differentiable function so for a discretisation $t_i = \frac{i}{n}T$, $i \in \{1, 2, .., n\}$, we apply the mean value theorem to each interval $[t_i, t_{i+1}]$, so there exists a point s_i in each interval such that

$$f(t_{i+1}) - f(t_i) = f'(s_i)(t_{i+1} - t_i),$$

so, we have

$$\sum_{i=1}^{n} \left(f(t_{i+1}) - f(t_i)\right)^2 = \sum_{i=1}^{n} \left(f'(s_i)(t_{i+1} - t_i)\right)^2,$$

because f' is continuous in $[0, T]$, it must be bounded. Let M be a bound of f', thus we have

$$\sum_{i=1}^{n} \left(f'(s_i)(t_{i+1} - t_i)\right)^2 \leq \sum_{i=1}^{n} \left(M(t_{i+1} - t_i)\right)^2 \leq \frac{M^2 T^2}{n}.$$

So we abtain

$$\lim_{n \to \infty} \sum_{i=1}^{n} \left(f(t_{i+1}) - f(t_i)\right)^2 = 0.$$

Now let's prove Eq.(1.2).

Let $X_i = \mathcal{B}(t_{i+1}) - \mathcal{B}(t_i)$, so $\quad X_i \sim \mathcal{N}(0, \frac{T}{n})$ and $\sum_{i=0}^{n-1} (\mathcal{B}(t_{i+1}) - \mathcal{B}(t_i))^2 = \sum_{i=0}^{n-1} X_i^2$.

Setting $Y_i = X_i^2$, then

$$\sum_{i=0}^{n-1} (\mathcal{B}(t_{i+1}) - \mathcal{B}(t_i))^2 = \sum_{i=0}^{n-1} Y_i = n \left(\frac{1}{n} \sum_{i=0}^{n-1} Y_i \right),$$

where $Y_i, i = 1 : n$, are a random variables with mean equal to $\dfrac{T}{n}$. Using the strong law of large numbers, the distribution $\left(\frac{1}{n} \sum_{i=0}^{n-1} Y_i \right)$ converge to $\frac{T}{n}$ as $n \to \infty$, so we obtain

$$\lim_{n \to \infty} \sum_{i=0}^{n-1} (\mathcal{B}(t_{i+1}) - \mathcal{B}(t_i))^2 = T. \tag{1.3}$$

■

Remark 1.2 *As a result of quadratic variation we have $(d\mathcal{B}_t)^2 = dt$.*

1.3 Itô integral and stochastic differential equations

1.3.1 Introduction

The discovery of Brownian motion in the early 19th century was the beginning of a new way of thinking about randomness. Early researchers like Thiele in 1880, Bachelier in 1900, and Einstein in 1905 explored its applications in various fields, from analyzing stock markets to understanding particle movement in fluids [14, 30, 38, 99, 124]. In 1931, Kolmogorov carried out a detailed study of Bachelier's research, which led to the development of Markov's theory and defined Kolomogorov's equations [68], giving us tools to study random phenomena systematically. Then, From 1938 to 1940, Doob expanded on these ideas by introducing concepts like time change [126]. The real breakthrough came in 1944 when Itô introduced stochastic integration in his first article [48], he tried to understand and study the Winers' papers. Itô worked to develop and improve the Wiener's ideas in 1951 [50, 51]. This was the beginning of the development of this subject by the initiation of the study of SDEs and the attempt to make sense of the stochastic integral. Mathematical models have been used to describe natural phenomena, and ordinary differential equation modeling is particularly useful for addressing questions about quantities that vary with time. These equations have the following form

$$dx(t) = F(x(t), t)dt, \quad t \in \mathbb{R}, \tag{1.4}$$

for a given initial state x_0. By integrating Eq.(1.4), we get

$$x(t) = x_0 + \int_0^t F(x(s), s)ds. \tag{1.5}$$

In the application of these equations to our physical reality, these functions often model a tangible phenomenon, while their derivatives encapsulate the behavior of these functions. Numerous natural phenomena can be expressed through ordinary differential equations. Simultaneously, there are numerous phenomena characterized by unpredictable behaviors, which we cannot fully isolate from their surroundings. Consequently, random external influences perpetually come into play, exerting control and altering the dynamics of the studied phenomenon. Indeed, the necessity arises to define what are known as stochastic differential equations.

For instance, consider the stock market, particularly in major companies, a subject that has been under examination since 1953, notably by Kendall [57]. The findings from this study revealed the intrinsic difficulty in predicting the behavior of prices, which exhibit random changes over time. As research progressed, it became evident that stock prices could be effectively modeled by a random walk. This phenomenon can be encapsulated in the form of a stochastic differential equation, wherein a key parameter is not deterministic but rather stochastic.

Certainly, let's simplify the explanation. The fluctuation of stock prices in companies is influenced by various factors such as the company's performance, profitability, supply and demand, and other external elements. This relationship can be expressed by the following equation

$$\frac{dX_t}{dt} = K(t)X_t, \tag{1.6}$$

in the given equation, the process X_t represent the share prices, $\frac{dX_t}{dt}$ is the rate of change in the stock price with respect to time and $K(t)$ signifies the rate of price monotony, because $K(t)$ is not precisely known due to its linked with external influences, we can express this as

$$K(t) = \alpha(t) + \gamma noise, \tag{1.7}$$

where γ is a real constant, $\alpha(t)$ is deterministic term and the noise in general can be a Brownian motion. But modeling some phenomena requires considering more general processes, where the noise in Eq. (1.7) can be a Jump process. Due to the inclusion of the noise term, the differential equation is called a stochastic differential equation (SDE).

If the noise is a Brownian motion, so the Eq. (1.6) becomes an (SDE) with the form

$$dX_t = \alpha(t)X_t dt + \gamma X_t d\mathcal{B}_t. \tag{1.8}$$

If the noise is a jump process, then, in this context, the stochastic differential equations with jump diffusion appeared, which took a great importance in applied mathematics, and it is found, for example, in economics, finance, magnetic reconnection, computer vision,...etc. The difference between the SDEs governed by Brownian motion and the SDEs with jumps is that the SDEs consist of a drift part and a diffusion part. The diffusion part is the Brownian motion. As we all know, the Brownian motion satisfies

- Continous paths

- Independent increments

- Stationary increments

So if we don't have the continuous paths condition, then we allow the jumps in the sample path, and that's precisely the SDEs with jump diffusion mean.

1.3.2   Ito integral

To model the Markov process, Itô constructed a stochastic differential equation of the form

$$dX_t = F(X_t, t)dt + G(X_t, t)d\mathcal{B}_t, \tag{1.9}$$

for an initial state X_0. By integrating Eq.(1.9), we will get the stochastic process of the form

$$X_t = X_0 + \int_0^t F(X_s, s)ds + \underbrace{\int_0^t G(X_s, s)d\mathcal{B}_s}_{(I)}. \tag{1.10}$$

In this case, Itô was faced with two problems. First, to define the stochastic part (I), and to link Kolomogorov's research on the Markov process with his explanations.

Knowing that the Brownian motion is nowhere differentiable, so we need to define the integral (I).

Definition 1.8 *Let $\mathcal{G} = \mathcal{G}(W, T)$ be the set of functions*

$$g(t, w) : [0, \infty) \times \Omega \longrightarrow \mathbb{R},$$

that satisfy the conditions

- $(t, w) \mapsto g(t, w)$ is $B \times \mathcal{A}$-measurable, where B is the Borel σ-algebra on $[0, \infty)$.

- $g(t, w)$ is $\mathcal{A}_t$-measurable.

- $E\left[\int_W^T g^2(t, w) dt\right] < \infty$.

The elementary function $\rho \in \mathcal{G}$ is given as

$$\rho(t, w) = \sum_{j=1}^{n_1 - 1} \rho_j(w) \chi_{[t_j, t_{j+1}]}, \tag{1.11}$$

where $\rho_j(w)$ is $\mathcal{A}_j$ measurable and $\chi_{[t_j, t_{j+1}]}$ is the indicator function.

Elementary functions play the role of stepped functions in the Lebesgue integral. It is natural to define **the Itô integral of elementary functions** as

Definition 1.9 *Consider the partition ($W = t_1 < t_2 < ... < t_{n_1} = T$) of the interval $[W, T]$, so*

$$\int_W^T \rho(t, w) d\mathcal{B}_t = \sum_{j=1}^{n_1 - 1} \rho_j(w)(\mathcal{B}_{t_{j+1}} - \mathcal{B}_{t_j}). \tag{1.12}$$

Example 1.2 *Suppose that*

$$\rho_1(t, w) = \sum_{j=1}^{n_1 - 1} \mathcal{B}_{t_j}(w) \chi_{[t_j, t_{j+1}]}, \qquad \rho_2(t, w) = \sum_{j=1}^{n_1 - 1} \mathcal{B}_{t_{j+1}}(w) \chi_{[t_j, t_{j+1}]}.$$

So we have $\int_W^T \rho_1(t, w) d\mathcal{B}_t = \sum_{j=1}^{n_1 - 1} \mathcal{B}_{t_j}(\mathcal{B}_{t_{j+1}} - \mathcal{B}_{t_j})$, because of the independance increments of Brownian motion then

$$E\left[\int_W^T \rho_1(t, w) d\mathcal{B}_t\right] = \sum_{j=1}^{n_1 - 1} E\left[\mathcal{B}_{t_j}(\mathcal{B}_{t_{j+1}} - \mathcal{B}_{t_j})\right] = 0.$$

For $\rho_2(t, w)$, we have $\int_W^T \rho_2(t, w) d\mathcal{B}_t = \sum_{j=1}^{n_1 - 1} \mathcal{B}_{t_{i+1}}(\mathcal{B}_{t_{j+1}} - \mathcal{B}_{t_j})$, then

$$E\left[\int_W^T \rho_2(t, w) d\mathcal{B}_t\right] = \sum_{j=1}^{n_1 - 1} E\left[\mathcal{B}_{t_{j+1}}(\mathcal{B}_{t_{j+1}} - \mathcal{B}_{t_j})\right] = \sum_{j=1}^{n_1 - 1} E\left[(\mathcal{B}_{t_{j+1}} - \mathcal{B}_{t_j})^2 + \mathcal{B}_{t_{j+1}}\mathcal{B}_{t_j} - \mathcal{B}_{t_j}^2\right]$$

$$E\left[\int_W^T \rho_2(t, w) d\mathcal{B}_t\right] = \sum_{j=1}^{n_1 - 1} E\left[(\mathcal{B}_{t_{j+1}} - \mathcal{B}_{t_j})^2 + \mathcal{B}_{t_j}(\mathcal{B}_{t_{j+1}} - \mathcal{B}_{t_j})\right] = \sum_{j=1}^{n_1 - 1} E\left[(\mathcal{B}_{t_{j+1}} - \mathcal{B}_{t_j})^2\right]$$

$$= \sum_{j=1}^{n_1 - 1} t_{j+1} - t_j = T - W.$$

Thus, Itô only allows integrals that correspond to the underlying filtration of sigma algebra of the Brownian motion, since he is aware that it is impossible to integrate all continuous stochastic processes due to the inbounded variation path of the Brownian motion. Therefore, he exploits the independence of the increments of the Brownian motion to construct the **Itô isometry**.

Lemma 1.1 *[98] (**Itô isometry for elementary functions***)*

If $\rho(t, w)$ is a bounded and elementary function then

$$E\left[\left(\int_W^T \rho(t,w)d\mathcal{B}_t\right)^2\right] = E\left[\int_W^T \rho^2(t,w)dt\right]. \tag{1.13}$$

Proof. Let $d\mathcal{B}_j = \mathcal{B}_{t_{j+1}} - \mathcal{B}_{t_j}$ then

$$E\left[\left(\int_W^T \rho(t,w)d\mathcal{B}_t\right)^2\right] = E\left[\sum_{j=1}^{n_1-1} \rho_j(w)(\mathcal{B}_{t_{j+1}} - \mathcal{B}_{t_j})\right]^2 = E\left[\sum_{j=1}^{n_1-1} \rho_j(w)d\mathcal{B}_j\right]^2,$$

knowing that

$$E(\rho_j \rho_i d\mathcal{B}_j d\mathcal{B}_i) = \begin{cases} 0, & i \neq j \\ E(\rho_i)^2(t_{i+1} - t_i), & i = j. \end{cases}$$

Then

$$E\left[\left(\int_W^T \rho(t,w)d\mathcal{B}_t\right)^2\right] = \sum_{i,j=1}^{n_1-1} E(\rho_j \rho_i d\mathcal{B}_j d\mathcal{B}_i) = \sum_{i=1}^{n_1-1} E(\rho_i)^2(t_{i+1} - t_i)$$
$$= E\left[\int_W^T \rho^2(t,w)dt\right].$$

∎

Next, we define the Itô isometry for all functions in $\mathcal{G}$. The definition was an extension of the space of elementary functions.

Definition 1.10 *For $g \in \mathcal{G}(W, T)$, we define the Itô integral as*

$$\int_W^T g(t,w)d\mathcal{B}_t = \lim_{n\to\infty} \int_W^T \rho_n(t,w)d\mathcal{B}_t, \tag{1.14}$$

where the sequence of elementary functions $\{\rho_n\}$ verify

$$E\left[\int_W^T (g - \rho_n)^2 dt\right] \to 0 \qquad as \quad n \to \infty. \tag{1.15}$$

The Itô isometry plays a fundamental role in the analysis and application of Itô calculus, ensuring that the Itô integral behaves consistently with respect to its integrand and stochastic integration.

Theorem 1.2 *[66] (**The Itô isometry**)*

For all $g \in \mathcal{G}$, we have

$$E\left[\left(\int_W^T g(t,w)d\mathcal{B}_t\right)^2\right] = E\left[\int_W^T g^2(t,w)dt\right]. \tag{1.16}$$

Example 1.3 *We want to calculate the integral $\int_0^t \mathcal{B}_s d\mathcal{B}_s$, so we try to find a sequence of elementry functions $\{\rho_n\}$ which verify Eq.(1.15).*

For $\rho_n = \sum_{j=1}^{n-1} \mathcal{B}_{t_j}(w)\chi_{[t_j,t_{j+1}]}$ then

$$
\begin{aligned}
E\left[\int_0^t (\mathcal{B}_s - \rho_n)^2 ds\right] &= E\left[\sum_j \int_{t_j}^{t_{j+1}} (\mathcal{B}_s - \mathcal{B}_{t_j})^2 ds\right] = \sum_j \int_{t_j}^{t_{j+1}} E\left[(\mathcal{B}_s - \mathcal{B}_{t_j})^2\right] ds \\
&= \sum_j \int_{t_j}^{t_{j+1}} (s - t_j)ds = \sum_j \frac{1}{2}(t_{j+1} - t_j)^2 \\
&\leq \frac{K}{2}\sum_j (t_{j+1} - t_j) \leq \frac{K}{2}t \to 0 \quad \text{as} \quad n \to \infty,
\end{aligned}
$$

where $K = \max_j(t_{j+1} - t_j)$. Now we can define the Itô integral as follows

$$\int_0^t \mathcal{B}_s d\mathcal{B}_s = \lim_{n\to\infty} \int_0^t \rho_n(t,w)d\mathcal{B}_s, \tag{1.17}$$

thus

$$
\begin{aligned}
\int_0^t \rho_n(t,w)d\mathcal{B}_s &= \sum_{j=1}^{n-1} \mathcal{B}_{t_j}(\mathcal{B}_{t_{j+1}} - \mathcal{B}_{t_j}) = \frac{1}{2}\sum_{j=1}^{n-1} \mathcal{B}_{t_{j+1}}^2 - \mathcal{B}_{t_j}^2 - (\mathcal{B}_{t_{j+1}} - \mathcal{B}_{t_j})^2 \\
&= \frac{1}{2}\sum_{j=1}^{n-1} (\mathcal{B}_{t_{j+1}}^2 - \mathcal{B}_{t_j}^2) - \frac{1}{2}\sum_{j=1}^{n-1}(\mathcal{B}_{t_{j+1}} - \mathcal{B}_{t_j})^2 = \frac{1}{2}\sum_{j=1}^{n-1} d\mathcal{B}_{t_j}^2 - \frac{1}{2}\sum_{j=1}^{n-1}(d\mathcal{B}_{t_j})^2 \\
&= \frac{1}{2}\mathcal{B}_t^2 - \frac{1}{2}\sum_{j=1}^{n-1}(d\mathcal{B}_{t_j})^2.
\end{aligned}
$$

Then, we have

$$\lim_{n\to\infty} \int_0^t \rho_n(t,w)d\mathcal{B}_s = \lim_{n\to\infty}\left(\frac{1}{2}\mathcal{B}_t^2 - \frac{1}{2}\sum_{j=1}^{n-1}(d\mathcal{B}_{t_j})^2\right) = \frac{1}{2}\mathcal{B}_t^2 - \frac{t}{2}.$$

Now, we introduce some properties of the Itô integral.

Properties of Ito integral

Let $g, f \in \mathcal{G}(W,T), 0 \leq W < S < T$, and a is a constant.

Theorem 1.3 [66]

- $\int_W^T g d\mathcal{B}_t = \int_W^S g d\mathcal{B}_t + \int_S^T g d\mathcal{B}_t.$

- $\int_W^T (ag + f) d\mathcal{B}_t = a \int_W^T g d\mathcal{B}_t + \int_W^T f d\mathcal{B}_t.$

- $E\left[\int_W^T g d\mathcal{B}_t\right] = 0.$

- $\int_W^T g d\mathcal{B}_t$ is $\mathcal{A}_T$ measurable.

We can see from example 1.3, that the definition of the Ito integral is not very convenient when it comes to evaluating a stochastic integral. Ito introduce the Ito's formula which simplifies the evaluation of stochastic integrals.

For example we want to compute $f(\mathcal{B}_t)$, in classical calculus the following equation make sense

$$df = f'(\mathcal{B}_t) d\mathcal{B}_t, \tag{1.18}$$

but this equation is wrong. It seems logical, though, but let's prove why.

According to Taylor's formula, we have

$$f(t + x) = f(t) + f'(t)x + \frac{f^{(2)}(t)}{2} x^2 + \ldots,$$

so

$$f(t + x) - f(t) = f'(t)x + \frac{f^{(2)}(t)}{2} x^2 + \ldots,$$

then, if we take the Brownian motion, it become

$$f(\mathcal{B}_{t+x}) = f(\mathcal{B}_t) + f'(\mathcal{B}_t)(\mathcal{B}_{x+t} - \mathcal{B}_t) + \frac{f^{(2)}(\mathcal{B}_t)}{2} (\mathcal{B}_{x+t} - \mathcal{B}_t)^2 + \ldots$$

$$f(\mathcal{B}_{t+x}) - f(\mathcal{B}_t) = f'(\mathcal{B}_t) d\mathcal{B}_t + \frac{f^{(2)}(\mathcal{B}_t)}{2} (d\mathcal{B}_t)^2 + \ldots,$$

using the fact that $(d\mathcal{B}_t)^2 = dt$ (**from quadratic variation**), then

$$df \simeq f'(\mathcal{B}_t) d\mathcal{B}_t + \frac{f^{(2)}(d\mathcal{B}_t)}{2} dt. \tag{1.19}$$

Its clear now that the Eq. (1.18) is wrong. Now, let $f(t, X)$ be a function with two variables; we want to evaluate $f(t, \mathcal{B}_t)$, using Taylor formula, we have

$$f(t + \Delta t, X + \Delta X) = f(t, X) + \left(\frac{\partial f}{\partial t}(t, X)\Delta t + \frac{\partial f}{\partial X}(t, X)\Delta X\right)$$

$$+ \frac{1}{2}\left(\frac{\partial^2 f}{\partial t^2}(t, X)(\Delta t)^2 + \frac{\partial^2 f}{\partial X^2}(t, X)(\Delta X)^2 + 2\frac{\partial^2 f}{\partial t \partial X}(t, X)\Delta t \Delta X\right) + \ldots,$$

we can observe directly that

$$df = \frac{\partial f}{\partial t} dt + \frac{\partial f}{\partial X} dX_t + \frac{1}{2}(dX_t)^2.$$

Let's $X = \mathcal{B}_t$ then we obtain

$$f(t + dt, \mathcal{B}_t + d\mathcal{B}_t) - f(t, \mathcal{B}_t) \simeq \left(\frac{\partial f}{\partial t} + \frac{1}{2}\frac{\partial^2 f}{\partial X^2} \right) dt + \frac{\partial f}{\partial X} d\mathcal{B}_t, \tag{1.20}$$

and this is exactly what Itô's formula means. If we want to generalize the strongest lemma in one-dimensional case, then , we will introduce the following theorem.

Theorem 1.4 *[16] (**Itô's lemma**)*

Let f be a smooth function such that $f(t, x) \in \mathcal{C}^2([0, \infty] \times \mathbb{R}, \mathbb{R})$, and X_t is a stochastic process with $dX_t = \mu(t, X_t)dt + \sigma(t, X_t)d\mathcal{B}_t$, Then we have

$$df(t, X_t) = \left(\frac{\partial f}{\partial t} + \mu_t \frac{\partial f}{\partial X} + \frac{1}{2}\sigma_t^2 \frac{\partial^2 f}{\partial X^2} \right) dt + \sigma_t \frac{\partial f}{\partial X} d\mathcal{B}_t. \tag{1.21}$$

Example 1.4   • *Let $f(t, X) = X^2$, so we have*

$$df(t, X_t) = \left(2\mu_t X_t + \sigma_t^2 \right) dt + 2\sigma_t X_t d\mathcal{B}_t.$$

For $X_t = \mathcal{B}_t$, we get

$$df(\mathcal{B}_t) = 2\mathcal{B}_t d\mathcal{B}_t + dt.$$

• *If $f(t, \mathcal{B}_t) = e^{at + b\mathcal{B}_t}$, then*

$$df(t, \mathcal{B}_t) = (a + \frac{1}{2}b^2)f dt + bf d\mathcal{B}_t.$$

Now, let introduce the multi-dimensional Itô's lemma.

Theorem 1.5 *[66] (**Multi-dimensional Itô's lemma**)*

Let $f : [0, \infty[\times \mathbb{R}^n \mapsto \mathbb{R}$ have continuous partial derevatives $\frac{\partial f}{\partial t}, \frac{\partial f}{\partial x_k}, \frac{\partial^2 f}{\partial x_k \partial x_i}$ for $k, i = 1, 2, ..., n$, and define a scalar process $\{U_t, t \in [0, \infty[\}$ by $U_t = f(t, X_t) = f(t, X_t^1, X_t^2, ..., X_t^n)$, where X_t verifies the differential

$$dX_t = F_t dt + G_t d\mathcal{B}_t,$$

where $F : [0, \infty[\times \Omega \mapsto \mathbb{R}^n, G : [0, \infty[\times \Omega \mapsto \mathbb{R}^{n \times m}$, and $\mathcal{B}_t = (\mathcal{B}_t^1, \mathcal{B}_t^2, ..., \mathcal{B}_t^m)$ is an m-dimensional Wiener process. Then the stochastic differential equation for U_t is written as

$$dU_t = \left(\frac{\partial f}{\partial t} + \sum_{k=1}^{n} \frac{\partial f}{\partial x_k} F_t^k + \frac{1}{2} \sum_{j=1}^{m} \sum_{k=1}^{n} \frac{\partial^2 f}{\partial x_i \partial x_k} G_t^{i,j} G_t^{k,j} \right) dt + \sum_{j=1}^{m} \sum_{i=1}^{n} G_t^{i,j} \frac{\partial f}{\partial x_i} d\mathcal{B}_t^j. \tag{1.22}$$

1.3.3   Existence and uniqueness of solutions for SDEs

Many phenomena in life are modeled by SDEs with the form Eq. (1.9) or an integral form Eq. (1.10), our purpose is to solve this kind of equations if possible. Thus, the first theory that needs to be verified is when such equations have a solution, and when it is a unique solution.

We'll present the robust solution of SDE in the form

$$\begin{cases} dX_t = F(t, X_t)dt + G(t, X_t)d\mathcal{B}_t, & t \in [0, T] \\ X_0 = x_0 \end{cases} \tag{1.23}$$

where $F(.,.) : [0, T] \times \mathbb{R}^n \mapsto \mathbb{R}^n$ and $G(.,.) : [0, T] \times \mathbb{R}^n \mapsto \mathbb{R}^{n \times m}$ are measurable functions, $\{\mathcal{B}(t) = (\mathcal{B}_1, \mathcal{B}_2, .., \mathcal{B}_m)^T, \ t \geq 0\}$ be an m-dimensional Brownian motion on the provided probability space, and x_0 is a random variable. We called F the drift of SDE and G the diffusion of SDE. Because $\mathcal{B}(t)$ is an m-dimensional Brownian motion, then we define the σ-algebra generated by the random variable $\mathcal{B}(s)$, $s \leq t$ noted by $\mathcal{A}_t^m$ which is the smallest σ-algebra containing all sets of the form

$$\{w, \mathcal{B}(t_1, w) \in \mathcal{A}_1, ..., \mathcal{B}(t_j, w) \in \mathcal{A}_j\} \tag{1.24}$$

where $t_i \leq t, i \leq j = 1, 2, 3, ...$ and $\mathcal{A}_i \subset \mathbb{R}^m$ are Borel sets (We assume that all sets of measure zero are included in $\mathcal{A}_t$).

As long as F and G are reasonable functions, a solution exists, and it's unique if we hold it with a initial condition $X_0 = x_0$. Hence, the following theorem gives the existence and uniqueness of the solution for stochastic differential equation (1.23).

Theorem 1.6 *[98] Let $T > 0$ and $F(.,.) : [0, T] \times \mathbb{R}^n \mapsto \mathbb{R}^n$, $G(.,.) : [0, T] \times \mathbb{R}^n \mapsto \mathbb{R}^{n \times m}$ are measurable functions satisfying*

- **Linear growth condition**

$$|F(t, x)| + |G(t, x)| \leq D(1 + |x|), \ \ x \in \mathbb{R}^n, t \in [0, T] \tag{1.25}$$

  where D is a constant and $(|G|^2 = \sum |G_{ij}|^2)$.

- **Lipshitz condition**

$$|F(t, x) - F(t, y)| + |G(t, x) - G(t, y)| \leq K|x - y|, \ \ x, y \in \mathbb{R}^n, \ t \in [0, T] \tag{1.26}$$

  where K is a constant.

- *Consider x_0 a random variable independent of σ-algebra $\mathcal{A}_\infty^{(m)}$ generated by $\mathcal{B}_t(.), t \geq 0$ such that*

$$E|x_0|^2 < \infty. \tag{1.27}$$

Then the stochastic differential equation Eq.(1.23) has a unique solution $X_t(w)$ continious and adapted to the filtration $\mathcal{A}_t^{x_0}$ generated by x_0 and $\mathcal{B}_s(.), s \leq t$, and

$$E\left[\int_0^T |X_t|^2 dt\right] < \infty. \tag{1.28}$$

The proof of this theorem is based on two steps: proving the uniqueness using the Gronwalls lemma ([66] page 129), and proving the existence using the successive approximation method "Picard iteration method." [98].

Remark 1.3   • *A strong solution is identified when the Theorem 1.6 yields the solution X_t, since the Brownian motion version $\mathcal{B}(t)$ is predetermined, and the constructed solution X_t is $\mathcal{A}_t^{x_0}$-adapted. Conversely, if we are provided solely with the functions $F(t, X_t)$ and $G(t, X_t)$ and seek a pair of processes $((X'(t), \mathcal{B}'(t)), \mathcal{A}_t)$ on a probability space $(\Omega, \mathcal{A}, P)$ such that equation Eq.(1.23) holds, $X'(t)$ then is termed a weak solution.*

- *The strong uniqunesse means :*
  if X_1 and X_2 satisfy Eqs.(1.23) and (1.28), then

$$X_1(t, w) = X_2(t, w), \qquad \forall t \leq T, \text{ a.s.}$$

- *Weak uniqueness means that X_1 and X_2 have the same finite-dimensional distribution.*

Lemma 1.2 *[98] If F and G satisfy (1.25) and (1.26), then the solution of Eq.(1.23) X_t "weak or strong" is weakly unique.*

Example 1.5 *Consider the stochastic differential equation*

$$\begin{cases} dX(t) = \mu X(t)dt + \sigma X(t)d\mathcal{B}(t) \\ X(0) = X_0, \quad \mu \in \mathbb{R}, \ \sigma > 0. \end{cases} \tag{1.29}$$

Let $X(t) = f(t, \mathcal{B}(t))$, using Itô's lemma, then

$$dX(t) = \left(\frac{\partial f}{\partial t} + \frac{1}{2}\frac{\partial^2 f}{\partial \mathcal{B}^2}\right)dt + \frac{\partial f}{\partial \mathcal{B}}d\mathcal{B}_t, \tag{1.30}$$

according to Eq. (1.29), we have

$$
\begin{cases}
\dfrac{\partial f}{\partial t} + \dfrac{1}{2}\dfrac{\partial^2 f}{\partial \mathcal{B}^2} = \mu X(t) = \mu f \\[4mm]
\dfrac{\partial f}{\partial \mathcal{B}} = \sigma X(t) = \sigma f.
\end{cases}
\tag{1.31}
$$

It's clear that $f(t, \mathcal{B}(t)) = e^{\sigma \mathcal{B} + g(t)}$, then

$$
\begin{cases}
\dfrac{\partial f}{\partial t} = g'(t)f, \\[4mm]
\dfrac{\partial^2 f}{\partial \mathcal{B}^2} = \sigma^2 f,
\end{cases}
\tag{1.32}
$$

substituting equations (1.32) into (1.31), we obtain

$$
g'(t)f + \frac{1}{2}\sigma^2 f = \mu f \;\Rightarrow\; g'(t) = (\mu - \frac{1}{2}\sigma^2) \;\Rightarrow\; g(t) = (\mu - \frac{1}{2}\sigma^2)t + c.
$$

so

$$
f(t, \mathcal{B}(t)) = e^{\sigma \mathcal{B} + (\mu - \frac{1}{2}\sigma^2)t + c}.
\tag{1.33}
$$

Now, using the initial condition $f(0,0) = e^c = X_0$, then $f(t, \mathcal{B}(t)) = X_0 e^{\sigma \mathcal{B} + (\mu - \frac{1}{2}\sigma^2)t}$.

Example 1.6 *Consider the stochastic differential equation*

$$
\begin{cases}
dX(t) = -\alpha X(t)dt + \sigma d\mathcal{B}(t) \\[2mm]
X(0) = X_0, \quad \alpha > 0.
\end{cases}
\tag{1.34}
$$

The exact solution is given by

$$
X(t) = a(t)\left(X_0 + \int_0^t b(s)d\mathcal{B}(s) \right), \quad a(0) = 1,
\tag{1.35}
$$

where $a(t) = e^{-\alpha t}$, and $b(t) = \sigma e^{\alpha t}$, this process is called **Ornstein-Uhlenbeck process**.

Example 1.7 The importance of Lipshitz and Linear growth conditions

Consider the deterministic differential equations, it's mean $G(t, X_t) = 0$

- *Let*

$$
\begin{cases}
dX(t) = 3X_t^{2/3}dt \\[2mm]
X(0) = 0.
\end{cases}
\tag{1.36}
$$

Notice that $F(t, X_t) = 3X_t^{2/3}$, which is not Lipschitzian. The solutions of Eq.(1.36) for any $c > 0$ are written in the form

$$
X(t) =
\begin{cases}
0 & \text{if } t \le c \\[2mm]
(t - c)^3, & \text{if } t > c
\end{cases}
$$

- *Let*

$$\begin{cases} dX(t) = X_t^2 dt \\ X(0) = 1, \end{cases} \tag{1.37}$$

we have $F(t, X_t) = X_t^2$. This function does not satisfy the linear growth condition, so we don't have the existence of a global solution for all $t \in \mathbb{R}$, but we have a particular unique solution in the interval $[0, 1[$ given by

$$X(t) = \frac{1}{1 - t}. \tag{1.38}$$

1.4   Jumps differential model

Stochastic differential equations have greatly contributed to clarifying many ambiguous problems. These equations help to capture the random fluctuations observed in real-world processes. However, many phenomena may not be adequately captured by traditional continuous models. Therefore, it was necessary to address this type of phenomenon by introducing a model that provides more accurate representations of these scenarios, and from here jump-diffusion models have appeared which are essential because they allow for the incorporation of sudden, discontinuous changes (jumps) into stochastic differential equations. These models combine both continuous diffusion processes (modeled by stochastic differential equations) and discrete jump processes (modeled by jump terms). We can find this theory in various fields such as finance, ecology, biology, engineering, and physics. Among the common examples in real-world processes, are sudden changes in population sizes due to environmental factors, disease outbreaks, or other catastrophic events, sudden changes in asset prices in financial markets due to unexpected news or events, and sudden changes in network traffic, such as spikes in data transmission rates or sudden network congestion. Jump models occur according to various stochastic processes that capture the occurrence of sudden, discontinuous changes or "jumps" in a system. In the following, we define some of the common stochastic processes used to model jumps.

1.4.1   Poisson process

First, we need to know the exponential random variables so that we can construct a model (Poisson process) where an event (or jump) occurs from time to time.

Exponential random variables

An exponential random variables τ is defined by the probability density function

$$g(t) = \begin{cases} \lambda e^{-\lambda t}, & t \geq 0, \\ 0 & t < 0, \end{cases} \tag{1.39}$$

where $\lambda > 0$ is the rate parameter. The expected value of τ is $\frac{1}{\lambda}$.

Definition 1.11 *Let $\{\tau_i\}_{i \geq 1}$ be a series of independent exponential random variables each having the same mean $\frac{1}{\lambda}$. Suppose the first jump occure at time τ_1, and the second happens at time $\tau_1 + \tau_2$ and ect. The arrival time are $S_n = \sum_{i=1}^{n} \tau_i$ where τ_i called the interarrival times and S_n is the time of the nth jump. Then the Poisson process N_t which represent the number of jumps at or before time t is defined as*

$$N_t = \sum_{n \geq 1} 1_{t \geq S_n}. \tag{1.40}$$

The paramater λ is called the intensity of Poisson process.

Lemma 1.3 *[122] For a Poisson process N, the random variable N_t has a Poisson distribution with parameter λt, where λ is constant so*

$$P(N_t = n) = \frac{(\lambda t)^n}{n!} e^{-\lambda t}, \quad n \in \mathbb{N} \tag{1.41}$$

The expected value of Poisson distributed $dN_t = N_{t+dt} - N_t$ is λdt it's mean $P(dN_t = n) = \frac{(\lambda dt)^n}{n!} e^{-\lambda dt}, \quad n \in \mathbb{N}$.

Figure 1.5 shows a path of Poisson process with intensity $\lambda = 20$ in the interval $[0, 1]$, we registered the total count of jumps that have happened up to time points dt_i and so on, up to 1 where $dt_i = i/1000$.

1.4.2   Compound Poisson process

A Compound Poisson process is a stochastic process that combines the jumps that occur from time to time with random sizes (or amplitudes) associated with each event. These random variables are often independent and identically distributed. Merton Jump diffusion is considered as one of the models that used the compound Poisson process because in this model the jump times and also the jump heights both of them are random.
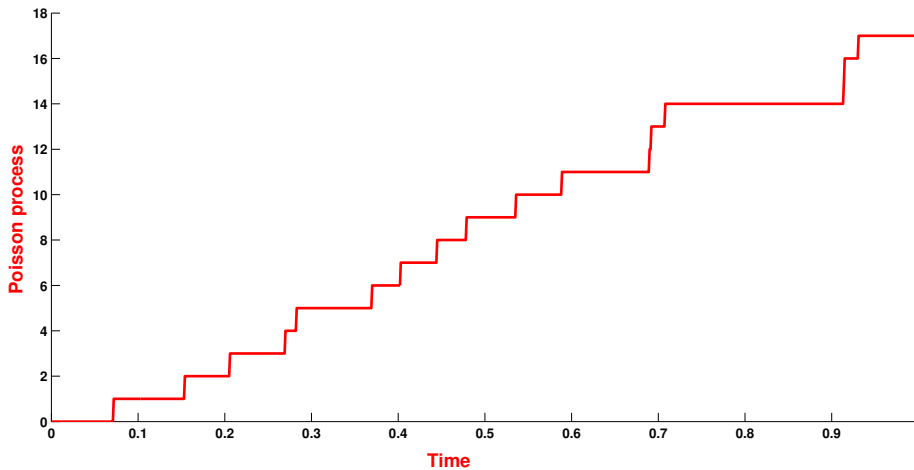
Figure 1.5: A path of Poisson process with intensity $\lambda = 20$.

Definition 1.12 *Let $\{N_t\}_{t\geq 0}$ be a Poisson process with intensity λ, and $\{Y_i\}_{i\geq 1}$ is a sequence of identically distributed random variables. A compound Poisson process $\{\mathcal{J}_t\}_{t\geq 0}$ with jump intensity λ is defined as*

$$\mathcal{J}_t = \sum_{i=1}^{N_t} Y_i. \tag{1.42}$$

If $N_t = 0$, so $\mathcal{J}_t = 0$.

Figure 1.6 represent a compound Poisson process with intensity $\lambda = 20$, and normal distributed jumps $\mathcal{N}(0.3, 1)$.

1.4.3   Lévy processes

Lévy processes are stochastic processes named after the French mathematician Paul Lévy. They are defined as follows

Definition 1.13 *If a process X_t satisfy*

- *The independent increasing process: $\forall t > s \geq 0, X_{s+t} - X_s$ independent of $\{X_u, u \leq s\}$.*

- *The stationary increment*

  $$\forall u > 0, \{X_t, t \geq 0\} \text{ have the same distribution with } \{X_{t+u}, t \geq 0\}$$

so X_t is called a Lévy process.
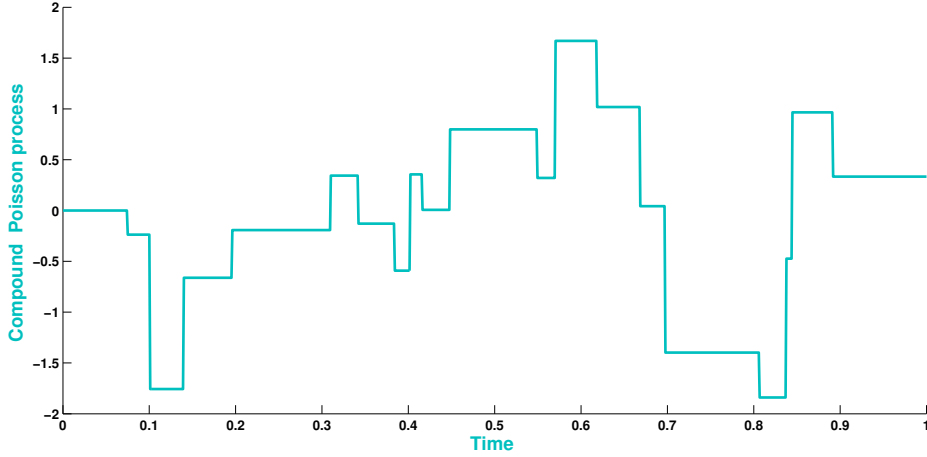
Figure 1.6: A path of compound Poisson process with intensity $\lambda = 20$ and normal distributed jumps $\mathcal{N}(0.3, 1)$.

One of the examples of Lévy process is the Poisson process, compound Poisson process, also, the Brownian motion is a Lévy process but with continuous paths.

Now, we will present the jump-diffusion stochastic differential Equation, which effectively captures the interplay between continuous random fluctuations and sudden, discontinuous jumps within stochastic processes.

In a filtrated probability space $(\Omega, \mathcal{A}, (\mathcal{A}_t)_{t \geq 0}, P)$, we call the following equation a Jump-Diffusion SDE for $t \geq 0$

$$
\begin{cases}
dX_t = F(X_t, t)dt + G(X_t, t)d\mathcal{B}_t + \underbrace{H(X_t, t)d\mathcal{J}_t}_{(I)} \\
X_0 = x_0,
\end{cases}
\tag{1.43}
$$

where x_0 is a given initial value at t_0 and $\{\mathcal{B}_t = (\mathcal{B}_t^1, \mathcal{B}_t^2, ..., \mathcal{B}_t^m)^T, t \geq 0\}$ is a standard independant vector of Brownian motion $\mathcal{A}_t$-Adapted, $F(X_t, t)$ is the drift coefficient, $G(X_t, t)$ the diffusion coefficient and the part (I) called magnitude of the jump where $\{\mathcal{J}_t = (\mathcal{J}_t^1, \mathcal{J}_t^2, ..., \mathcal{J}_t^l)^T, t \geq 0\}$ is $\mathcal{A}_t$-Adapted compound Poisson process, such that each scalar $\mathcal{J}_t^k$ are defined as

$$
\mathcal{J}_t^k = \sum_{j=1}^{N_t^k} Y_j^k,
\tag{1.44}
$$

where $\{N_t = (N_t^1, N_t^2, ..., N_t^l)^T, t \geq 0\}$ are standard Poisson process $\mathcal{A}_t$-Adapted with intensity λ^k respectively and $\{Y_j^k : \Omega \mapsto \mathbb{R}, j \in \{1, 2, .., N_t^k\}\}$ is an independent identically distribution random variables represents the jump sizes.

SDEJs have been widely used in various fields for modeling different physical and natural problems. Their applications span physics, ecology, biology, chemistry, astronomy, and more. Particularly in modeling events in the finance or insurance industries, unpredictability is the most important factor to consider, leading to the use of SDEJs.

2

Numerical methods for solving stochastic differential equations

In this chapter, we will explore two overarching approaches for solving stochastic differential equations (SDEs). The initial section delves into the construction of Itô-Taylor schemes and presents several numerical methods derived from this framework. The second section discusses spectral methods as an alternative strategy for solving SDEs.

2.1 Itô-Taylor expansion

Before discussing the Itô-Taylor expansion, the Ito-Taylor formula for stochastic differential equations will be briefly discussed in the next subsection.

2.1.1 Itô-Taylor formula

First, our focus will be on the construction of the deterministic Itô formula, which will be of great importance in explaining its stochastic counterparts. To start, we will study the solution X_t of a one-dimensional ordinary differential equation

$$\frac{dX_t}{dt} = F(X_t), \;\; X(t_0) = X_0, \;\; t \in [t_0, T], \tag{2.1}$$

where $t \in [t_0, T]$ and F is a function sufficiently smooth and have a linear growth. The Eq.(2.1) is equivalent to the following integral equation

$$X_t = X_0 + \int_{t_0}^{t} F(X_s) ds. \tag{2.2}$$

29

Let $g : \mathbb{R} \mapsto \mathbb{R}$ be a continuously differentiable function. Then, applying the chain rule, we have

$$\frac{dg(X_t)}{dt} = F(X_t)\frac{\partial g(X_t)}{\partial x}, \tag{2.3}$$

let $S = F\dfrac{\partial}{\partial x}$, so from Eq.(2.3), and for $t \in [t_0, T]$ we can write

$$g(X_t) = g(X_0) + \int_{t_0}^{t} Sg(X_s)ds. \tag{2.4}$$

For $g = F$, we get

$$F(X_t) = F(X_0) + \int_{t_0}^{t} SF(X_s)ds, \tag{2.5}$$

substituting Eq.(2.5) into Eq.(2.2), leads us to the simplest non-trivial Taylor expansion

$$X_t = X_0 + \int_{t_0}^{t} \left(F(X_0) + \int_{t_0}^{s} SF(X_k)dk \right) ds,$$
$$= X_0 + F(X_0)\int_{t_0}^{t} ds + \int_{t_0}^{t}\int_{t_0}^{s} SF(X_k)dkds. \tag{2.6}$$

Continuing in the same way, let's now consider $g = SF$, so we will have

$$X_t = X_0 + F(X_0)\int_{t_0}^{t} ds + SF(X_0)\int_{t_0}^{t}\int_{t_0}^{s} dkds + L_1, \tag{2.7}$$

where

$$L_1 = \int_{t_0}^{t}\int_{t_0}^{s}\int_{t_0}^{l} S^2 F(X_z)dzdlds. \tag{2.8}$$

For the general form, this approach yields to the classical deterministic Taylor formula given by

$$g(X_t) = g(X_0) + \sum_{j=1}^{i} \frac{(t-t_0)^j}{j!}S^j g(X_0) + \int_{t_0}^{t}...\int_{t_0}^{s_2} S^{i+1}g(X_{s_1})ds_1...ds_{i+1}, \quad i = 1, 2, ... \tag{2.9}$$

Now, we will examine the solution X_t of a one-dimensional Ito stochastic differential equation written in the following way

$$X_t = X_0 + \int_{t_0}^{t} F(X_s)ds + \int_{t_0}^{t} G(X_s)d\mathcal{B}_s. \tag{2.10}$$

Let $g : \mathbb{R} \mapsto \mathbb{R}$ be a twice continuously differentiable function. Then, applying the Ito formula, we get

$$g(X_t) = g(X_0) + \int_{t_0}^{t} \left(F(X_s)\frac{\partial g(X_s)}{\partial x} + \frac{1}{2}G^2(X_s)\frac{\partial^2 g(X_s)}{\partial x^2} \right) ds + \int_{t_0}^{t} G(X_s)\frac{\partial g(X_s)}{\partial x}d\mathcal{B}_s.$$

Using the operators

$$S^0 = F\frac{\partial}{\partial x} + \frac{1}{2}G^2\frac{\partial^2}{\partial x^2}, \quad S^1 = G\frac{\partial}{\partial x}, \tag{2.11}$$

and applying the Ito formula to $F(X_t)$ and $G(X_t)$, then, substitute it into equation (2.10), we obtain the approximation

$$
\begin{aligned}
X_t = X_0 &+ \int_{t_0}^t \left(F(X_0) + \int_{t_0}^s S^0 F(X_k)dk + \int_{t_0}^s S^1 F(X_k)d\mathcal{B}_k \right) ds \\
&+ \int_{t_0}^t \left(G(X_0) + \int_{t_0}^s S^0 G(X_k)dk + \int_{t_0}^s S^1 G(X_k)d\mathcal{B}_k \right) d\mathcal{B}_s,
\end{aligned}
\tag{2.12}
$$

so it can be written as follows

$$X_t = X_0 + F(X_0)(t - t_0) + G(X_0)(\mathcal{B}_t - \mathcal{B}_{t_0}) + L, \tag{2.13}$$

where

$$
\begin{aligned}
L = &\int_{t_0}^t \int_{t_0}^s S^0 F(X_k)dkds + \int_{t_0}^t \int_{t_0}^s S^1 F(X_k)d\mathcal{B}_kds + \int_{t_0}^t \int_{t_0}^s S^0 G(X_k)dkd\mathcal{B}_s \\
&+ \int_{t_0}^t \int_{t_0}^s S^1 G(X_k)d\mathcal{B}_kd\mathcal{B}_s.
\end{aligned}
\tag{2.14}
$$

This is the remainder of the Ito Taylor expansion.

2.1.2   Multiple integral

The following concept introduce certain notations to formulate the Ito-Taylor expansion.

Multiple index

A row vector $\beta = (i_1, i_2, ..., i_n)$, where $i_j \in \{0, 1, ..., m\}$ for $j \in \{1, 2, ..., n\}$, $m = 1, 2, ...$, is called a multi-index of length $l := l(\beta) \in \{1, 2, ...\}$. Notice that m denote the number of components of the Wiener process. We define the set of all multi-indices by

$$\mathcal{Z} = \{(i_1, i_2, ..., i_n) : i_j \in \{1, 2, ..., m\}, j \in \{1, 2, ..., n\} \quad \text{for } n = 1, 2, ... \text{ and } m = 1, 2, ..\} \cup \{u\},$$

where u is the multi index of length zero ($l(u) = 0$). For $\beta \in \mathcal{Z}$, we denote by $n(\beta)$ the number of components of a multi-index β which are equal to 0.

Example 2.1 *We have*

1. *If* $\beta = (0, 0, 1)$ *then* $l(\beta) = 3$ *and* $n(\beta) = 2$.

2. *For $\beta = (3, 4, 0, 0)$, we have $l(\beta) = 4$ and $n(\beta) = 2$.*

3. *For $\beta = (0, 1)$, we have $l(\beta) = 2$ and $n(\beta) = 1$.*

For a given $\beta \in \mathcal{Z}$ with $l(\beta) \geq 1$, we denoted $-\beta$ and $\beta-$ for the multi-index in $\mathcal{Z}$, obtained by deleting the first and the last component respectively. For two multi-indices $\beta_1 = (i_1, i_2, ..., i_n)$ and $\beta_2 = (i'_1, i'_2, ..., i'_n)$, we define the operator $*$ on $\mathcal{Z}$ by

$$\beta_1 * \beta_2 = (i_1, i_2, ..., i_n, i'_1, i'_2, ..., i'_n).$$

Example 2.2 *Suppose that $\beta_1 = (2, 3, 4)$ and $\beta_2 = (0, 1)$, then $\beta_1 * \beta_2 = (2, 3, 4, 0, 1)$.*

Multiple Itô integral

First of all, let define the three sets $\mathcal{H}$ of adapted right continuous stochastic processes $g = \{g(t), \ t \geq 0\}$ with left hand limite

- if $g \in \mathcal{H}_u$ then $|g(t, w)| < \infty$,

- if $g \in \mathcal{H}_{(0)}$ then $\int_0^t |g(s, w)|ds < \infty$,

- if $g \in \mathcal{H}_{(1)}$ then $\int_0^t |g(s, w)|^2 ds < \infty$.

For all integer $j \geq 2$, we have $\mathcal{H}_{(j)} = \mathcal{H}_{(1)}$. Now, we will define the sets $\mathcal{H}_\beta$, for multi-indices $\beta \in \mathcal{Z}$ with length $l(\beta) > 1$.

Definition 2.1 *Let τ_1 and τ_2 be two stopping times (A stopping time τ is a random variable which for each $t \geq 0$, the event $\{\tau \leq t\}$ belongs to the sigma-algebra $\mathcal{A}_t$) with $0 \leq \tau_1 \leq \tau_2 \leq T$, for a multi-index $\beta = (i_1, i_2, ..., i_n) \in \mathcal{Z}$ and a stochastic process $g \in \mathcal{H}_\beta$, we define the multiple Ito integral noted by $I_\beta[g(.)]_{\tau_1, \tau_2}$ by*

$$I_\beta[g(.)]_{\tau_1, \tau_2} = \begin{cases} g(\tau_2) & l(\beta) = 0 \\ \int_{\tau_1}^{\tau_2} I_{\beta-}[g(.)]_{\tau_1, s} ds, & l(\beta) \geq 1 \text{ and } i_n = 0 \\ \int_{\tau_1}^{\tau_2} I_{\beta-}[g(.)]_{\tau_1, s} d\mathcal{B}_s^{i_n}, & l(\beta) \geq 1 \text{ and } i_n \geq 1. \end{cases} \tag{2.15}$$

So $\mathcal{H}_\beta$ is the set of adapted right continuous stochastic processes $g = \{g(t), \ t \geq 0\}$ with left hand limite such that the integral process $\{I_\beta[g(.)]_{\tau_1, t}, t \geq 0\}$ viewed as a function of t satisfy

$$I_{\beta-}[g(.)]_{\tau_1, .} \in \mathcal{H}_{(i_n)}. \tag{2.16}$$

Example 2.3   • $I_u[g(.)]_{0,t} = g(t)$.

  • *For more details, let's consider the following*

$$I_{(0,1,2)}[g(.)]_{0,t} = \int_0^t I_{(0,1)}[g(.)]_{0,s} d\mathcal{B}_s^2 = \int_0^t \int_0^s \int_0^k g(l) dl d\mathcal{B}_k^1 d\mathcal{B}_s^2. \tag{2.17}$$

2.1.3   Itô coefficient function

We introduce the diffusion operator by

$$S^0 = \frac{\partial}{\partial t} + \sum_{k=1}^d F_k \frac{\partial}{\partial x^k} + \frac{1}{2} \sum_{k,n=1}^d \sum_{i=1}^m G_{k,i} G_{n,i} \frac{\partial^2}{\partial x^k \partial x^n}, \tag{2.18}$$

  and

$$S^i = \sum_{k=1}^d G_{k,i} \frac{\partial}{\partial x^k}, \quad \forall i \in \{1, 2, ..., m\}. \tag{2.19}$$

We define the Itô coefficient function as

$$g_\beta = \begin{cases} g & n = 0, \\ S^{i_1} g_{-\beta} & n \geq 1, \end{cases} \tag{2.20}$$

where $\beta = (i_1, i_2, ..., i_n)$ and $g \in \mathcal{C}^h(\mathbb{R}^+ \times \mathbb{R}^d, \mathbb{R})$, with $h = l(\beta) + n(\beta)$.

Example 2.4 *Consider the identity function $g(t, x) = x$, in the one-dimensional case $d = m = 1$, we have*

  • $g_{(0)} = S^0 g_u = S^0 g = F$,

  • $g_{(1,1)} = S^1 g_{(1)} = S^1 S^1 g_u = S^1 S^1 g = S^1 G = G \frac{\partial G}{\partial x}$,

  • $g_{(0,1)} = F \frac{\partial G}{\partial x} + \frac{1}{2} G^2 \frac{\partial^2 G}{\partial x^2}$.

2.1.4   Hierarchical and remainder sets

The next definition is indispensable for the definition of the stochastic Taylor expansion and indicates that the multiple stochastic integrals appearing in the Taylor expansion cannot be chosen arbitrarily. If a subset $A \subset \mathcal{Z}$ satisfy

  • $A \neq \emptyset$

  • $\sup_{\beta \in A} l(\beta) < \infty$

- $-\beta \in A$ for each $\beta \in A \backslash \{u\}$,

then A is called an hierarchical set. For example $A = \{u\}$ or $A = \{u, (1,1), (0), (1)\}$ are hierarchical sets. Now for all hierarchical set A, we define a remaider set $B(A)$ of A by $B(A) = \{\beta \in \mathcal{Z} \backslash A : -\beta \in A\}$.

Example 2.5 *If $A = \{u, (0), (1)\}$ then $B(A) = \{(0,0), (1,1), (1,0), (0,1)\}$.*

2.1.5   Itô-Taylor schemes

The following theorem gives the Itô Taylor shemes for a d-dimensional Itô process solution of the following SDE,

$$\begin{cases} dX_t & = F(t, X_t)dt + \sum_{j=1}^{m} G^j(t, X_t)d\mathcal{B}_t^j, \quad t \in [t_0, T], \\ X_{t_0} & = X_0. \end{cases} \tag{2.21}$$

Theorem 2.1 *[66] Consider τ_1 and τ_2 be two stopping times with $0 \leq \tau_1 \leq \tau_2 \leq T$, and $A \subset \mathcal{Z}$ be an hierarchical set. Let $g : \mathbb{R}^+ \times \mathbb{R}^d \mapsto \mathbb{R}$, then the Itô Taylor scheme is given by*

$$g(\tau_2, X_{\tau_2}) = \sum_{\beta \in A} I_\beta[g_\beta(\tau_1, X_{\tau_1})]_{\tau_1, \tau_2} + \sum_{\beta \in B(A)} I_\beta[g_\beta(., X.)]_{\tau_1, \tau_2}, \tag{2.22}$$

provided that all of the multiple Itô integrals exists.

Example 2.6 *In the one-dimensional $d = m = 1$, $g(t, x) = x$, $\tau_1 = t_0$ and $\tau_2 = t$ where $0 \leq t_0 \leq t \leq T$ and the hierarchical set $A = \{\beta \in \mathcal{Z} : l(\beta) \leq 1\} = \{u, (0), (1)\}$. We have the coefficient function*

- $g_u(t_0, X_0) = X_0$

- $g_{(0)}(t_0, X_0) = S^0 g_u = S^0 X_0 = F(t_0, X_0)$

- $g_{(1)}(t_0, X_0) = S^1 g_u = S^1 X_0 = G(t_0, X_0)$.

Then

$$X_t = X_0 + F(t_0, X_0)I_{(0)} + G(t_0, X_0)I_{(1)} + L. \tag{2.23}$$

where

- $I_{(0)} = \int_{t_0}^{t} ds = t - t_0,$

- $I_{(1)} = \int_{t_0}^t d\mathcal{B}_s = \mathcal{B}_t - \mathcal{B}_{t_0}.$

Now for the case $l(\beta) \leq 2$, we add the following terms:

- $g_{(1,0)} = S^1 g_{(0)}(t_0, X_0) = S^1 S^0 g_u = G(t_0, X_0)\frac{\partial F}{\partial X_t}(t_0, X_0),$

- $g_{(1,1)} = S^1 g_{(1)}(t_0, X_0) = S^1 S^1 g_u = G(t_0, X_0)\frac{\partial G}{\partial X_t}(t_0, X_0),$

- $g_{(0,0)} = \frac{\partial F}{\partial t}(t_0, X_0) + F(t_0, X_{t_0})\frac{\partial F}{\partial X_t}(t_0, X_0) + \frac{1}{2}G^2(t_0, X_0)\frac{\partial^2 F}{\partial X_t^2}(t_0, X_0),$

- $g_{(0,1)} = \frac{\partial G}{\partial t}(t_0, X_0) + F(t_0, X_{t_0})\frac{\partial G}{\partial X_t}(t_0, X_0) + \frac{1}{2}G^2(t_0, X_0)\frac{\partial^2 G}{\partial X_t^2}(t_0, X_0).$

Then we have

$$X_t = X_0 + F(t_0, X_0)I_{(0)} + G(t_0, X_0)I_{(1)} + g_{(1,1)}I_{(1,1)} + g_{(0,1)}I_{(0,1)} + g_{(1,0)}I_{(1,0)} + g_{(0,0)}I_{(0,0)} + L.$$

where L is the remaider of the Itô expansion and

- $I_{(1,0)} = \int_{t_0}^t I_{(1)}ds = \int_{t_0}^t (\mathcal{B}_s - \mathcal{B}_{t_0})ds.$

- $I_{(0,1)} = \int_{t_0}^t I_{(0)}ds = \int_{t_0}^t (s - t_0)d\mathcal{B}_s.$

- $I_{(0,0)} = \int_{t_0}^t \int_{t_0}^s dk ds = \frac{(t-t_0)^2}{2}.$

- $I_{(1,1)} = \int_{t_0}^t \int_{t_0}^s d\mathcal{B}_k d\mathcal{B}_s = \frac{1}{2}[(\mathcal{B}_t - \mathcal{B}_{t_0})^2 - (t - t_0)].$

2.2 Approximation by Itô-Taylor schemes

In this section, we will present the numerical schemes derived from the Itô-Taylor expansion. They fall into two categories, explicit and implicit schemes.

Let consider an Itô process $\{X_t\}_{t_0 \leq t \leq T}$ satisfying Eq.(2.21), in the interval $[t_0, T]$. Taking a discretization of the interval $[t_0, T]$, for some integer N as $t_0 < t_1 < t_2 < ... < t_i < ... < t_N = T$, we denote $\Delta_i = t_{i+1} - t_i$, and $\delta = \max_i \Delta_i$.

The step size Δ_i play an important role for computational efficiency, when applying the Itô-Taylor approximation over an interval $[t_0, T]$. The approximation process obtained through an iterative schemes is denoted by $Z_t = \{Z(t), t_0 \leq t \leq T\}$ where $Z_0 = X_0$.

Convergence and error estimate

Typically, the lack of an explicit solution to a stochastic differential equation necessitates the use of a numerical simulations. However, if the problem has an analytical solution, then we can calculate the estimated error between the Itô process and its approximation at time T as

$$\epsilon_{strong} = E(|X_T - Z_T|). \tag{2.24}$$

The absolute error is estimated by running N diverse simulations of simple paths for the Itô process and its approximations Z. These simulations are based on the same sample trajectories of the Brownian motion. We will use the following estimate

$$\bar{\epsilon} = \frac{1}{N} \sum_{j=1}^{N} |X_T - Z_T|. \tag{2.25}$$

Definition 2.2 *(**Strong convergence**)*

A time-discrete approximation Z^δ with maximum step size δ converge strongly to X at time T if

$$\lim_{\delta \to 0} E(|X_T - Z_T^\delta|) = 0. \tag{2.26}$$

We say that Z^δ converges strongly with order $\lambda > 0$ at time T if there exists a constant M such that

$$E(|X_T - Z_T^\delta|) \leq M\delta^\lambda. \tag{2.27}$$

Definition 2.3 *(**Weak convergence**)*

A time-discrete approximation Z^δ converges weakly to X at time T, if for all $h : \mathbb{R}^d \mapsto \mathbb{R}$ in class C of test functions

$$\lim_{\Delta_i \to 0} \left| E(h(X_T)) - E(h(Z_T^\delta)) \right| = 0. \tag{2.28}$$

If the set C encompasses all polynomials, this definition suggests the convergence of all moments. Therefore, any theoretical inquiry involving it necessitates the presence of all moments. Let $C^l(\mathbb{R}^d, \mathbb{R})$ represent the space of functions $h : \mathbb{R}^d \mapsto \mathbb{R}$ that are l times continuously differentiable, and let $C_P^l(\mathbb{R}^d, \mathbb{R})$ denote the subspace of functions $h \in C^l(\mathbb{R}^d, \mathbb{R})$ for which all partial derivatives up to order l possess polynomial growth, it means that there exist constants $M > 0$ and $i \in \{1, 2, ...\}$, depending on h such that

$$|\partial_x^j h(x)| \leq M(1 + |x|^{2i}), \tag{2.29}$$

for all $x \in \mathbb{R}^d$ and any partial derivative $\partial_x^j h$ of order $j \leq l$.

Definition 2.4 *(Weak order of convergence)*

We say that the approximation Z^δ converges weakly with order $\lambda_1 > 0$ at time T if there exists a constant M_1 such that

$$\left| E(h(X_T)) - E(h(Z_T^\delta)) \right| \leq M_1 \delta^{\lambda_1}. \tag{2.30}$$

Therfore, in all of the following we assume $\Delta_i = \frac{T-t_0}{N}$ and $t_i = i\Delta_i = i\frac{(T-t_0)}{N}$ for $i \in \{0, 1, ..., N\}$.

2.2.1 Strong explicit approximations

Strong Euler-Maruyama method

The Euler method is one of the simplest approaches to finding approximation to solutions of ordinary differential equations. This method can be generalized to find approximate solutions of SDE.

To construct the Euler scheme from Eq.(2.21), let write the integral stochastic form

$$X(T) = X_0 + \int_{t_0}^{T} F(t, X_t)dt + \int_{t_0}^{T} G(t, X_t)d\mathcal{B}_t, \tag{2.31}$$

for $T = t_{i+1}$ and $T = t_i$, we have

$$X(t_{i+1}) = X_0 + \int_{t_0}^{t_{i+1}} F(t, X_t)dt + \int_{t_0}^{t_{i+1}} G(t, X_t)d\mathcal{B}_t, \tag{2.32}$$

and

$$X(t_i) = X_0 + \int_{t_0}^{t_i} F(t, X_t)dt + \int_{t_0}^{t_i} G(t, X_t)d\mathcal{B}_t, \tag{2.33}$$

by subtracting the Eqs.(2.32) and (2.33), we get the following stochastic equation

$$X(t_{i+1}) = X(t_i) + \int_{t_i}^{t_{i+1}} F(t, X_t)dt + \int_{t_i}^{t_{i+1}} G(t, X_t)d\mathcal{B}_t. \tag{2.34}$$

Let denoted by $X_i = X(t_i)$ and $X_{i+1} = X(t_{i+1})$ for $i = 0, .., N$, approximating the integrals in Eq.(2.34) gives

$$\int_{t_i}^{t_{i+1}} F(t, X_t)dt \simeq F(t_i, X_i)(t_{i+1} - t_i) = F(t_i, X_i)\Delta_i \tag{2.35}$$

and

$$\int_{t_i}^{t_{i+1}} G(t, X_t)d\mathcal{B}_t \simeq G(t_i, X_i)(\mathcal{B}_{i+1} - \mathcal{B}_i) = G(t_i, X_i)\Delta\mathcal{B}_i. \tag{2.36}$$

Now, substitute (2.35) and (2.36) into (2.34) gives

$$X(t_{i+1}) = X(t_i) + F(t_i, X_i)\Delta_i + G(t_i, X_i)\Delta\mathcal{B}_i. \tag{2.37}$$

Eq.(2.37) represents the Euler-Maruyama formula for the stochastic differential equation (2.21).

In the multi-dimensional case where $d = 1, 2, ...$ and $m = 1$, the kth component of Euler scheme is given by

$$X_{i+1}^k = X_i^k + F^k(t_i, X_i)\Delta_i + G^k(t_i, X_i)\Delta\mathcal{B}_i, \tag{2.38}$$

where $k = 1, 2, ..., d$, $F^k = (F^1, F^2, ..., F^d)$ and $G^k = (G^1, G^2, ..., G^d)$ are d-dimensional vector. For the general multi-dimensional case with $d, m = 1, 2, ...$, the kth component of Euler scheme is given by

$$X_{i+1}^k = X_i^k + F^k(t_i, X_i)\Delta_i + \sum_{j=1}^m G^{k,j}(t_i, X_i)\Delta\mathcal{B}_i^j, \tag{2.39}$$

where $[G^{k,\cdot}]$ is a $d \times m$ matrix and $\Delta\mathcal{B}_i^j = \mathcal{B}_{t_{i+1}}^j - \mathcal{B}_{t_i}^j$, noting that $\mathcal{B}^j \sim \mathcal{N}(0, \Delta_i)$ and $\Delta\mathcal{B}^{j_1}$ and $\Delta\mathcal{B}^{j_2}$ are independent for $j_1 \neq j_2$.

Theorem 2.2 *[66] Suppose that F and G satisfy the Lipschitz and linear growth conditions given in Eqs.(1.26)-(1.25). For all $s, t \in [t_0, T]$ and $x \in \mathbb{R}^d$ if*

$$E(|X_0|^2) < \infty, \tag{2.40}$$

$$E(|X_0 - Z_0^\delta|^2)^{1/2} \leq L_1\delta^{1/2}, \tag{2.41}$$

$$|F(s, x) - F(t, x)| + |G(s, x) - G(t, x)| \leq L_2(1 + |x|)|s - t|^{1/2}, \tag{2.42}$$

where L_1, L_2 do not depend on δ, then the estimate error of Euler approximation Z^δ is given by

$$E(|X_T - Z_T^\delta|) \leq L_3\delta^{1/2}, \tag{2.43}$$

where the constant L_3 does not depend on δ.

Remark 2.1 *From Theorem 2.2, it's clear that the Euler-Maruyama method has strong order $\lambda = 0.5$.*

Strong Milstien scheme

This scheme is proposed by Milstien with strong order 1.0. For the one-dimensional case where $m = d = 1$, we add to the Euler-Maruyama scheme the term

$$G(t_i, X_i)\frac{\partial}{\partial X_t}G(t_i, X_i)I_{(1,1)} = \frac{1}{2}G(t_i, X_i)\frac{\partial}{\partial X_t}G(t_i, X_i)\{(\Delta\mathcal{B}_i)^2 - \Delta_i\}, \tag{2.44}$$

we get Milstien scheme as follows

$$X_{i+1} = X_i + F(t_i, X_i)\Delta_i + G(t_i, X_i)\Delta\mathcal{B}_i + \frac{1}{2}G(t_i, X_i)\frac{\partial}{\partial X_t}G(t_i, X_i)\{(\Delta\mathcal{B}_i)^2 - \Delta_i\}. \quad (2.45)$$

In the multi-dimensional case with $d = 1, 2, ...$ and $m = 1$, the kth component of Milstien scheme is

$$X_{i+1}^k = X_i^k + F^k(t_i, X_i)\Delta_i + G^k(t_i, X_i)\Delta\mathcal{B}_i + \frac{1}{2}\left(\sum_{j=1}^{d} G^j(t_i, X_i)\frac{\partial}{\partial X_t^j}G^k(t_i, X_i)\right)\{(\Delta\mathcal{B}_i)^2 - \Delta_i\},$$
$$(2.46)$$

where $k = 1, 2, ..., d$, $F^k = (F^1, F^2, ..., F^d)$ and $G^k = (G^1, G^2, ..., G^d)$ are d-dimensional vector.

Example 2.7 *Consider the linear stochastic differential equation*

$$dX_t = \lambda X_t dt + \mu X_t d\mathcal{B}_t, \quad t \in [0, T], \quad (2.47)$$

where the exact solution is given by

$$X(t) = X_0 e^{(\lambda - \frac{1}{2}\mu^2)t + \mu\mathcal{B}(t)}. \quad (2.48)$$

Let $T = 1$, with a discretization step size $\Delta_i = 1/N$, and for $X_0 = 1$, $\lambda = 1.5$ and $\mu = 1$, the Euler-Maruyama scheme of this example is

$$X(t_{i+1}) = X(t_i) + \lambda X_{t_i}\Delta_i + \mu X_{t_i}\Delta\mathcal{B}_i. \quad (2.49)$$

Now for the Milstien scheme, we have

$$X(t_{i+1}) = X(t_i) + \lambda X_{t_i}\Delta_i + \mu X_{t_i}\Delta\mathcal{B}_i + \frac{1}{2}\mu^2\{(\Delta\mathcal{B}_i)^2 - \Delta_i\}. \quad (2.50)$$

Figure 2.1 represents the exact and approximate solutions obtained by Euler and Milstien schemes for one trajectory of Brownian motion and $N = 100$. Figure 2.2 represents the exact and approximate solutions obtained by Euler and Milstien schemes with the absolute error with 10^2 different sample paths of Brownian motion and $N = 100$.

Example 2.8 *We examine the nonlinear SDE*

$$dX_t = -a^2 X_t(1 - X_t^2)dt + a(1 - X_t^2)d\mathcal{B}_t, \quad 0 \le t \le 1, \quad (2.51)$$

where the analytical solution is given by

$$X(t) = \tanh(a\mathcal{B}(t) + \arctan(X_0)). \quad (2.52)$$
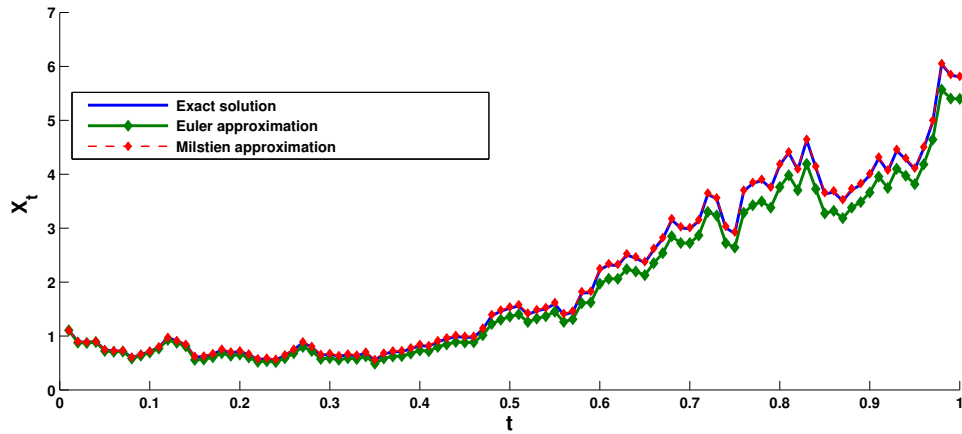
Figure 2.1: Exact solution, Euler and Milstien approximate solutions with one trajectory for Example 2.7.
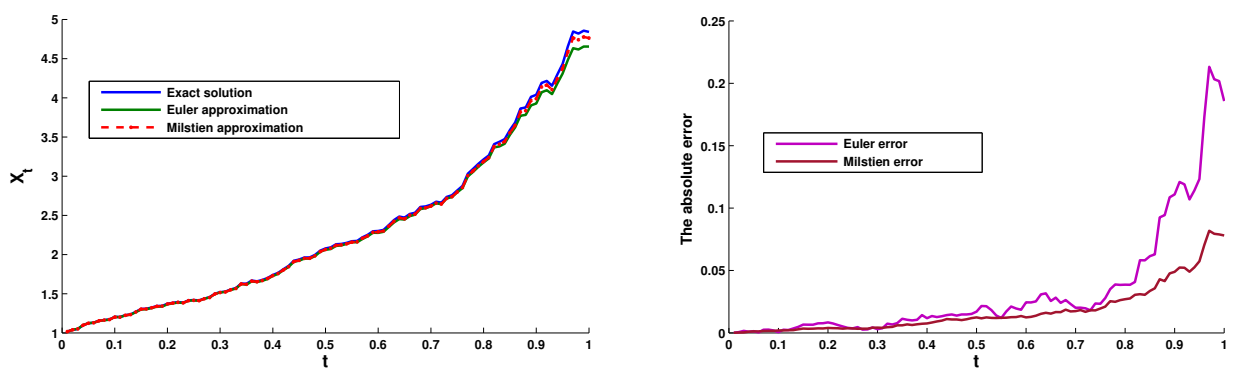
Figure 2.2: Exact solution, Euler and Milstien approximate solutions with the absolute error for Example 2.7.
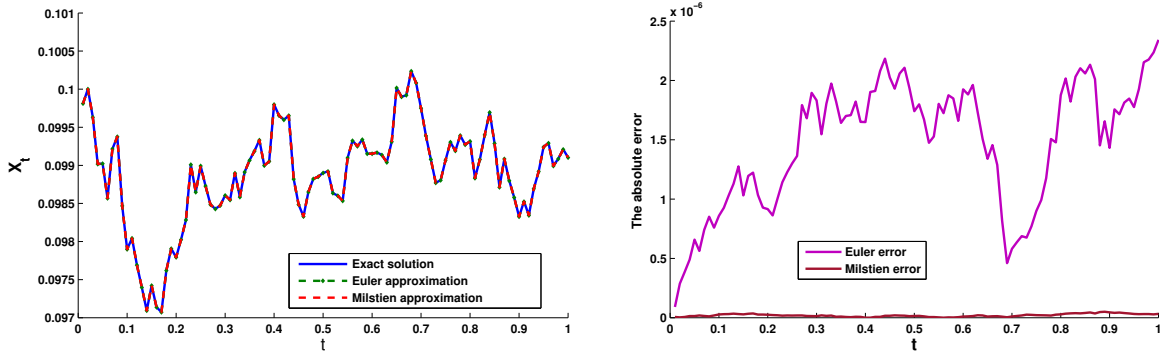
Figure 2.3: Exact solution, Euler and Milstien approximate solutions with the absolute error for Example 2.8.

Let $a = 1/30$ and $X_0 = 1/10$. The explicit Euler scheme of this example, is given by

$$X(t_{i+1}) = X(t_i) + \left[-a^2 X_{t_i}(1 - X_{t_i}^2)\right]\Delta_i + a(1 - X_{t_i}^2)\Delta\mathcal{B}_i. \tag{2.53}$$

The Milstein scheme is

$$X(t_{i+1}) = X(t_i) + \left[-a^2 X_{t_i}(1 - X_{t_i}^2)\right]\Delta_i + a(1 - X_{t_i}^2)\Delta\mathcal{B}_i + \left[-a^2 X_{t_i}(1 - X_{t_i}^2)\right]\left\{(\Delta\mathcal{B}_i)^2 - \Delta_i\right\}.$$

Figure 2.3 illustrates the exact and approximate solutions generated by Euler and Milstein schemes, accompanied by the absolute error, across 10^2 distinct sample paths of Brownian motion, all with $N = 100$.

Example 2.9 *Consider the problem*

$$dX_t = a^2 \cos(X(t))\sin^3(X(t))dt + a\sin^2(X(t))d\mathcal{B}_t, \qquad 0 \le t \le 1. \tag{2.54}$$

The analytical solution of this problem is as follows

$$X(t) = arccot(a\mathcal{B}(t) + cot(X_0)). \tag{2.55}$$

Let $a = 1/20$ and $X_0 = 1/20$, so the explicit Euler scheme of this example is

$$X(t_{i+1}) = X(t_i) + \left[a^2 \cos(X_{t_i})\sin^3(X_{t_i})\right]\Delta_i + (a\sin^2(X_{t_i}))\Delta\mathcal{B}_i. \tag{2.56}$$

For the Milstien scheme, we have

$$X(t_{i+1}) = X(t_i) + \left[a^2 \cos(X_{t_i})\sin^3(X_{t_i})\right]\Delta_i + (a\sin^2(X_{t_i}))\Delta\mathcal{B}_i$$
$$+ a^2 \sin^2(X_{t_i})\cos(X_{t_i})\sin(X_{t_i})\{(\Delta\mathcal{B}_i)^2 - \Delta_i\}. \tag{2.57}$$

Figure 2.4 presents the precise and approximate solutions produced by Euler and Milstein schemes, with the associated absolute error, for 10^2 sample paths of Brownian motion, all obtained by taking $N = 100$.
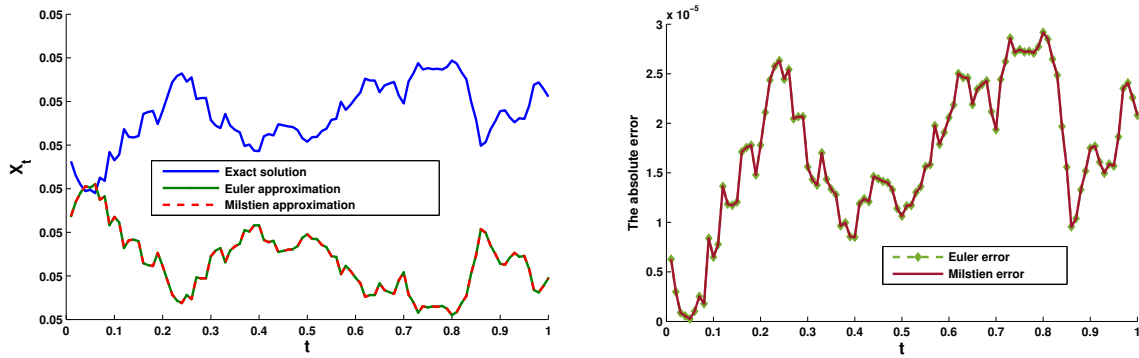
Figure 2.4: Exact solution, Euler and Milstien approximate solutions and the absolute error for Example 2.9.

Figure 2.5-2.6 illustrates the approximate solution obtained by explicit Euler and Milstien schemes, with the absolute error , in the interval $[0, 10]$ for 10^2 sample paths of Brownian motion, obtained with $N = 10000$ and $N = 100$ respectively.
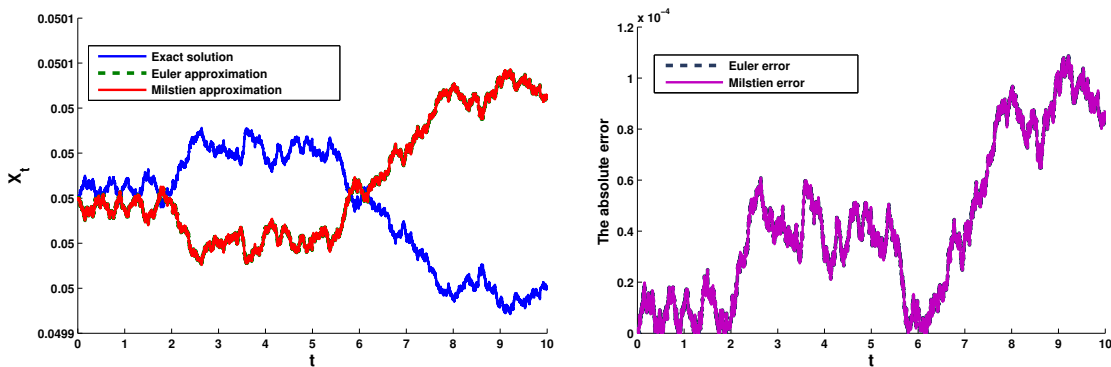
Figure 2.5: Exact solution, Euler and Milstien approximate solutions with the absolute error with $N = 10000$ for Example 2.9.

Example 2.10 *Consider the problem*

$$X(t) = X_0 + \int_0^t (\frac{1}{3}X(s)^{\frac{1}{3}} + 6X(s)^{\frac{2}{3}})ds + \int_0^t X(s)^{\frac{2}{3}} d\mathcal{B}(s), \quad 0 \le t \le 1, \qquad (2.58)$$
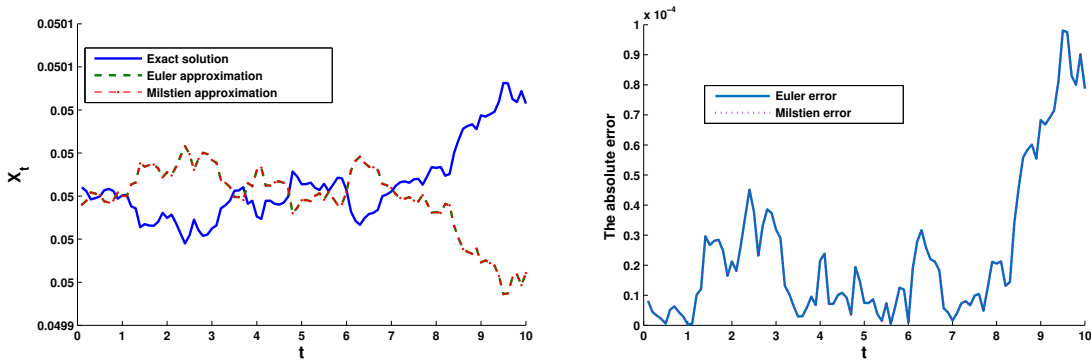
Figure 2.6: Exact solution, Euler and Milstien approximate solutions with the absolute error with $N = 100$ for Example 2.9.

the exact solution is given by

$$X(t) = (2t + 1 + \frac{1}{3}\mathcal{B}(t))^3,$$

(2.59)

where $X_0 = 1$. Figures 2.7-2.9 illustrate the exact and approximate solutions using strong Euler and Milstien schemes for $\Delta = 1/1000$, $\Delta = 1/100$ and $\Delta = 1/10000$ respectively for 100 simulations.
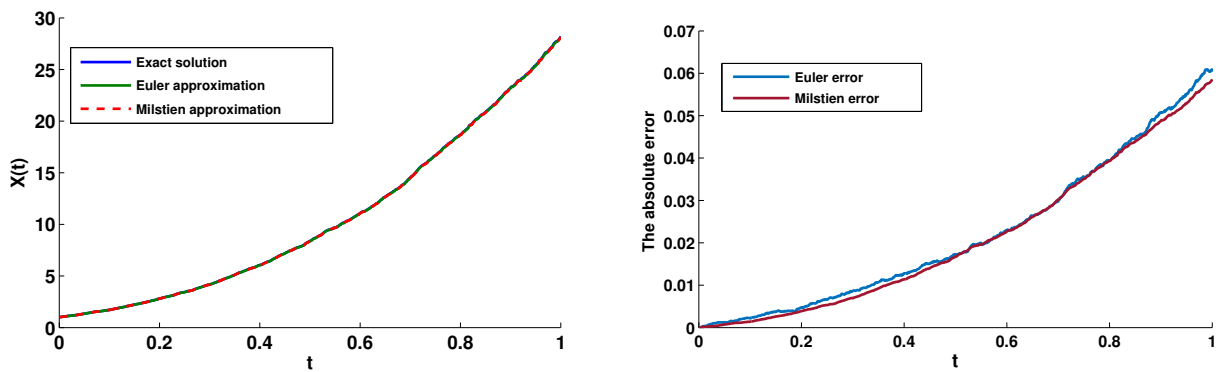
Figure 2.7: Exact solution compared with Euler and Milstein approximations and the absolute error for Example 2.10 for $N = 1000$.
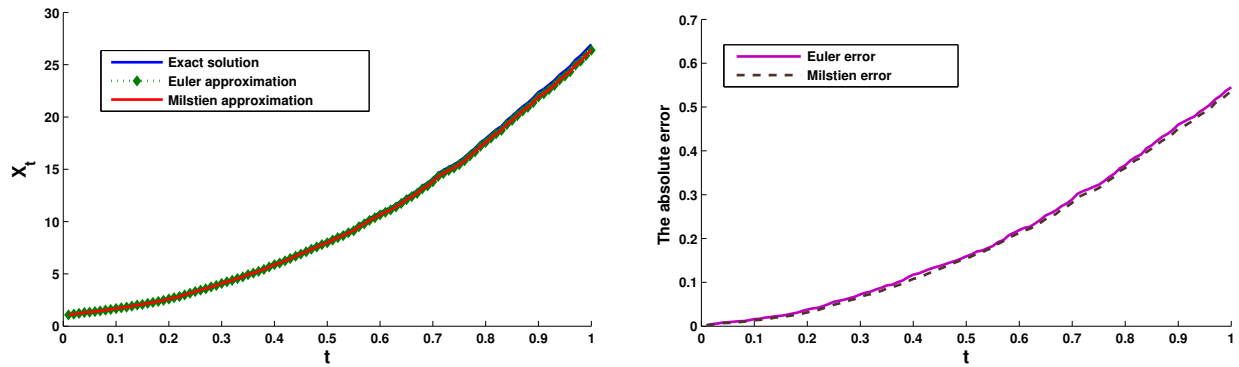
Figure 2.8: Exact solution compared with Euler and Milstein approximations with the absolute error for Example 2.10 for $N = 100$.
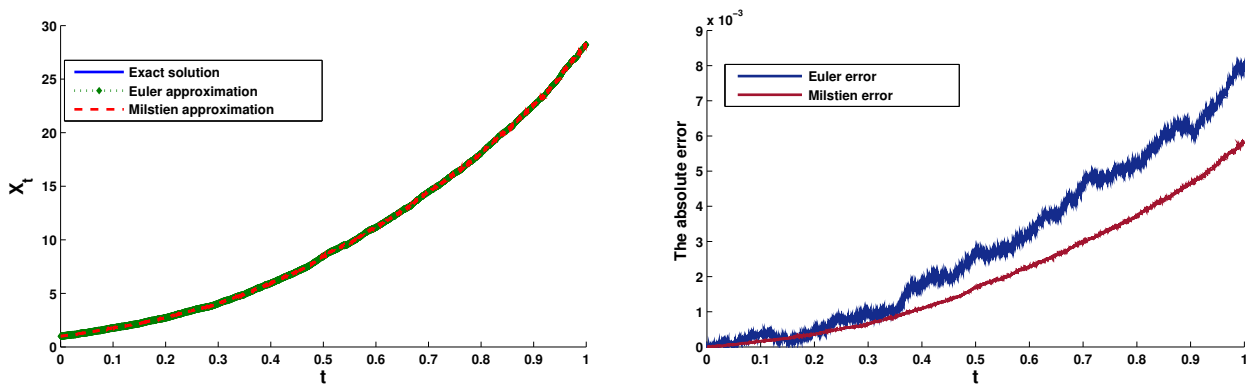
Figure 2.9: Exact solution compared with Euler and Milstein approximations with the absolute error for Example 2.10 for $N = 10000$.

The order 1.5 strong Taylor scheme

This scheme is obtaining by adding some termes from the Itô-Taylor expansion into the Milstien scheme, in the one-dimensional case where $m = d = 1$, the resulting 1.5 strong Itô-Taylor scheme is outlined as follows

$$
\begin{aligned}
X_{i+1} = {} & X_i + F\Delta_i + G\Delta\mathcal{B}_i + \frac{1}{2}G\left(\frac{\partial}{\partial X_t}G\right)\{(\Delta\mathcal{B}_i)^2 - \Delta_i\} + \left(\frac{\partial}{\partial X_t}F\right)G\Delta Z \\
& + \frac{1}{2}\Delta_i^2\left(F\frac{\partial}{\partial X_t}F + \frac{1}{2}G^2\frac{\partial^2}{\partial X_t^2}F\right) + \left(F\frac{\partial}{\partial X_t}G + \frac{1}{2}G^2\frac{\partial^2}{\partial X_t^2}G\right)\{\Delta\mathcal{B}_i\Delta_i - \Delta Z\} \\
& + \frac{1}{2}G\left(G\frac{\partial^2}{\partial X_t^2}G + \left(\frac{\partial}{\partial X_t}G\right)^2\right)\{\frac{1}{3}(\Delta\mathcal{B}_i)^2 - \Delta_i\}\Delta\mathcal{B}_i,
\end{aligned}
\tag{2.60}
$$

where the random variable ΔZ is defined as

$$
\Delta Z = I_{(1,0)} = \int_{\tau_1}^{\tau_2}\int_{\tau_1}^{s} d\mathcal{B}_k ds
\tag{2.61}
$$

with $\Delta Z \sim \mathcal{N}(0, \frac{1}{3}\Delta_i^3)$, and covariance $E(\Delta Z\Delta\mathcal{B}) = \frac{1}{2}\Delta^2$.

Example 2.11 *Consider the linear SDE as presented in example 2.7. The exact and approximate solutions generated by the explicit Euler, Milstein and the order 1.5 Taylor schemes with the absolute error, across 10^2 different sample paths of Brownian motion, all with $N = 10$, $N = 100$ and $N = 1000$ are presented in Figures 2.10-2.12 respectively.*
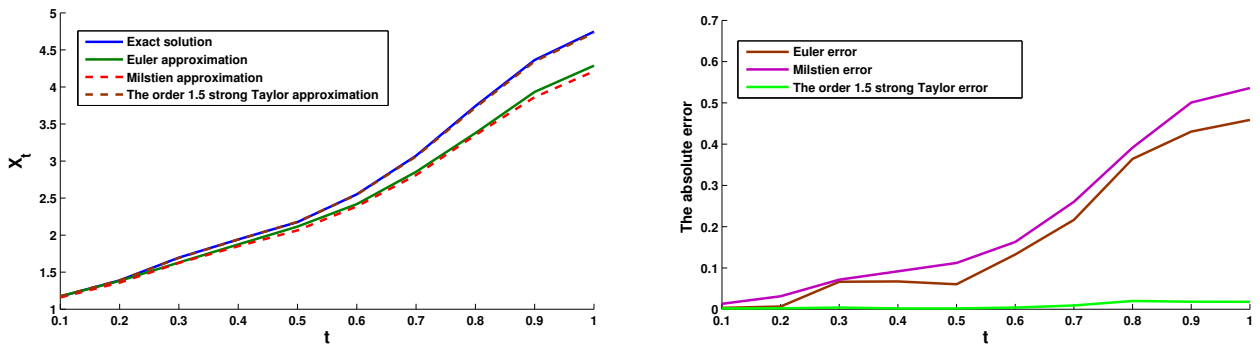
Figure 2.10: Exact solution compared with three approximations with the absolute error for Example 2.11 for $N = 10$.
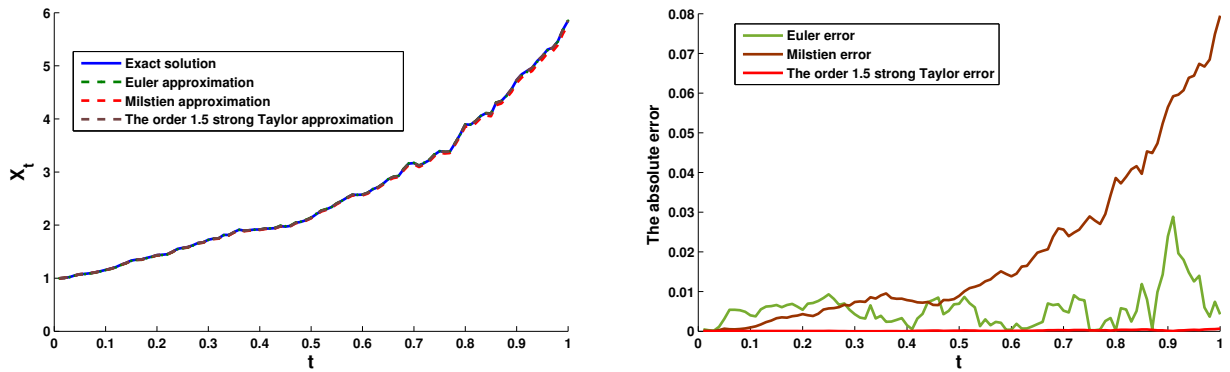
Figure 2.11: Exact solution compared with three approximations with the absolute error for Example 2.11 for $N = 100$.
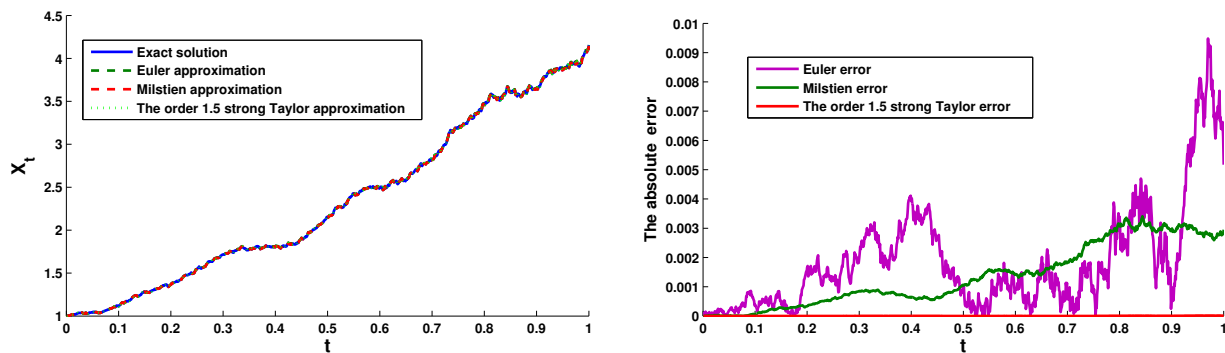
Figure 2.12: Exact solution compared with three approximations with the absolute error for Example 2.11 for $N = 1000$.

Remark 2.2 *We can also get the higher-order approximations by incorporating additional terms from the Itô-Taylor expansion, the issue in this kind of approximation is the existence of certain multiple integrals which can be challenging to compute and demand more numerical approximations and increased computation time. Some information on how to obtain high- order approximations can be found in [66].*

2.2.2 Strong implicit approximations

Strong implicit Euler-Maruyama scheme

Let consider an Itô process $\{X_t\}_{t_0 \leq t \leq T}$ satisfying Eq.(2.21) in the interval $[t_0, T]$. By following the same steps as in the strong explicit Euler scheme, the implicit scheme differs from it in the approximation of the integral (2.35). This leads to

$$\int_{t_i}^{t_{i+1}} F(t, X_t)dt \simeq F(t_{i+1}, X_{i+1})(t_{i+1} - t_i) = F(t_{i+1}, X_{i+1})\Delta_i, \tag{2.62}$$

so in the one-dimensional cases $d = m = 1$, the implicit Euler-Maruyama scheme is given by

$$X(t_{i+1}) = X(t_i) + F(t_{i+1}, X_{i+1})\Delta_i + G(t_i, X_i)\Delta\mathcal{B}_i. \tag{2.63}$$

We can construct a familly of implicit Euler scheme by

$$X(t_{i+1}) = X(t_i) + \{\lambda F(t_{i+1}, X_{i+1}) + (1 - \lambda)F(t_i, X_i)\}\Delta_i + G(t_i, X_i)\Delta\mathcal{B}_i, \tag{2.64}$$

where $\lambda \in [0, 1]$. If $\lambda = 0$, we get the explicit Euler-Maruyama scheme, and if $\lambda = 1$ we obtain the implicit Euler scheme Eq.(2.63).

In the general case where $d, m = 1, 2, ...$, the kth component familly of Euler scheme is written as

$$X^k(t_{i+1}) = X^k(t_i) + \{\lambda_k F^k(t_{i+1}, X_{i+1}) + (1 - \lambda_k)F^k(t_i, X_i)\}\Delta_i + \sum_{j=1}^{m} G^{k,j}(t_i, X_i)\Delta\mathcal{B}_i^j, \tag{2.65}$$

where $k \in \{1, 2, ..., d\}$ and $\lambda_k \in [0, 1]$.

Strong implicit Milstien scheme

This scheme has a strong order 1.0, in the one-dimensional case where $m = d = 1$, we add to the implicit Euler Maruyama scheme the term

$$\frac{1}{2}G(t_i, X_i)\frac{\partial}{\partial X_t}G(t_i, X_i)\{(\Delta\mathcal{B}_i)^2 - \Delta_i\}. \tag{2.66}$$

Example 2.12 *Consider the same nonlinear SDE as presented in example 2.8.*

The implicite Euler scheme of problem (2.51) is given by

$$X(t_{i+1}) = X(t_i) + \left[-a^2 X_{t_{i+1}}(1 - X_{t_{i+1}}^2) \right] \Delta_i + a(1 - X_{t_i}^2)\Delta\mathcal{B}_i. \tag{2.67}$$

For the implicit Milstien scheme, we have

$$X(t_{i+1}) = X(t_i) + \left[-a^2 X_{t_{i+1}}(1 - X_{t_{i+1}}^2) \right] \Delta_i + a(1 - X_{t_i}^2)\Delta\mathcal{B}_i + \left[-a^2 X_{t_i}(1 - X_{t_i}^2) \right] \{(\Delta\mathcal{B}_i)^2 - \Delta_i\}.$$

The exact and approximate solutions generated by the implicit Euler scheme and implicit Milstien scheme, accompanied by the absolute error, across 10^2 distinct sample paths of Brownian motion, all with $N = 100$ are presented in Figure 2.13. Figure 2.14 shows the approximate solution obtained by the explicit and implicit Euler, Milstien schemes with the absolute error for $N = 100$ and 10^2 distinct sample paths of Brownian motion.
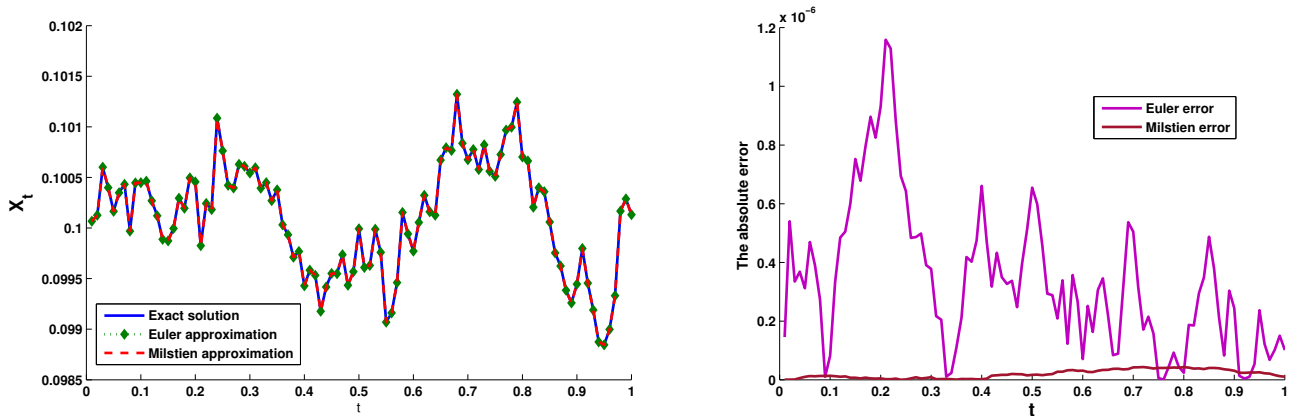
Figure 2.13: Exact solution, the implicit Euler and Milstien approximate solutions with the absolute error for Example 2.12.
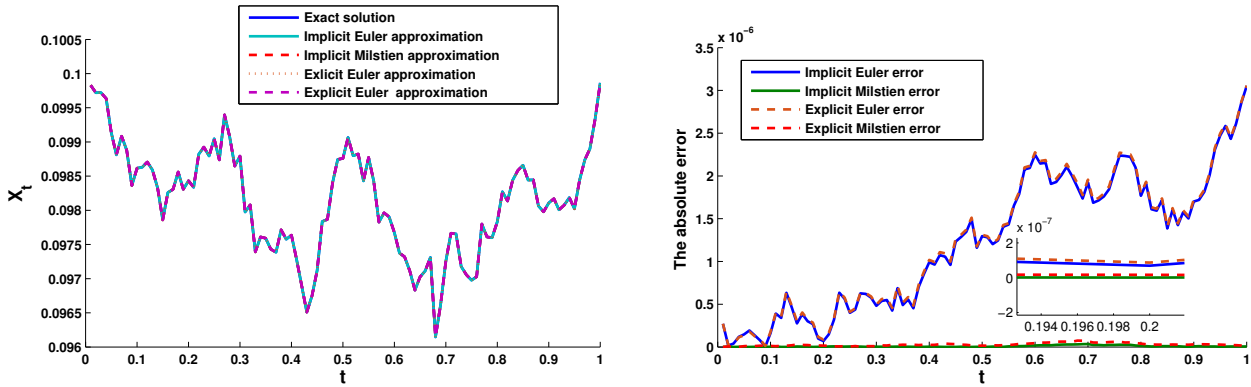
Figure 2.14: Exact solution, Euler and Milstien approximate solutions with the absolute error for Example 2.12.

Example 2.13 *Let's consider the problem*

$$dX_t = -0.015625X_t(1 - X_t^2)ds + 0.125(1 - X_t^2)d\mathcal{B}(s), \quad 0 \le t \le 1, \tag{2.68}$$

with the exact solution

$$X(t) = \frac{\frac{9}{8}e^{0.25\mathcal{B}(t)} - \frac{7}{8}}{\frac{9}{8}e^{0.125\mathcal{B}(t)} + \frac{7}{8}}. \tag{2.69}$$

For $X_0 = 1/8$, the implicit Euler scheme of Eq(2.68) is written as follows

$$X(t_{i+1}) = X(t_i) + \left[-0.015625X_{t_{i+1}}(1 - X_{t_{i+1}}^2)\right]\Delta_i + 0.125(1 - X_{t_i}^2)\Delta\mathcal{B}_i. \tag{2.70}$$

The corresponding Milstein scheme is reformulated in the following way

$$
\begin{aligned}
X(t_{i+1}) = X(t_i) + &\left[-0.015625X_{t_{i+1}}(1 - X_{t_{i+1}}^2)\right]\Delta_i \\
&+ 0.125(1 - X_{t_i}^2)\Delta\mathcal{B}_i + \left[-0.015625X_{t_i}(1 - X_{t_i}^2)\right]\{(\Delta\mathcal{B}_i)^2 - \Delta_i\}.
\end{aligned} \tag{2.71}
$$

Figure 2.15 illustrates the exact and approximate solutions generated by the implicit Euler and Milstein schemes, accompanied by the absolute error, across 10^2 distinct sample paths of Brownian motion, all with $N = 100$ simulations. Figure 2.16 shows the explicit and implicit Euler and Milstein schemes with their respective absolute errors for $N = 100$ and 10^2 distinct sample paths of Brownian motion.

The approximate solutions obtained by implicit Euler and Milstein schemes compared with exact solution are presented in Figure 2.17 for the linear stochastic differential equation (2.47).
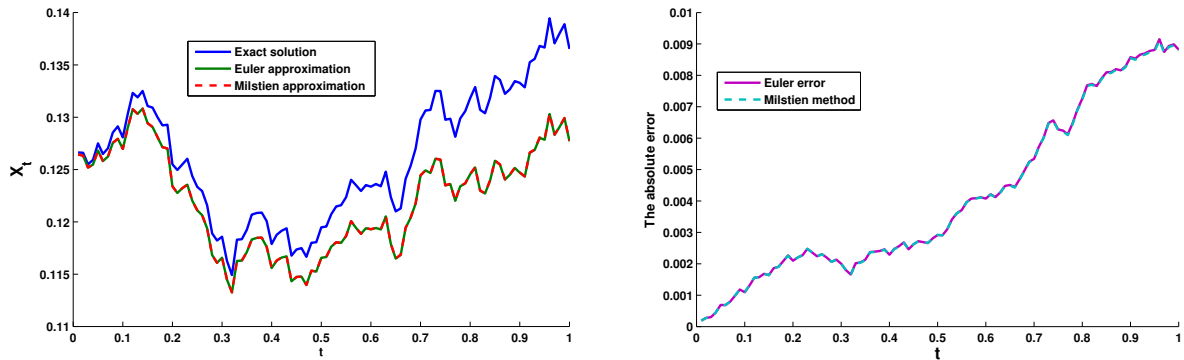
Figure 2.15: Exact solution, the implicit Euler and Milstien approximate solutions with the absolute error for Example 2.13.
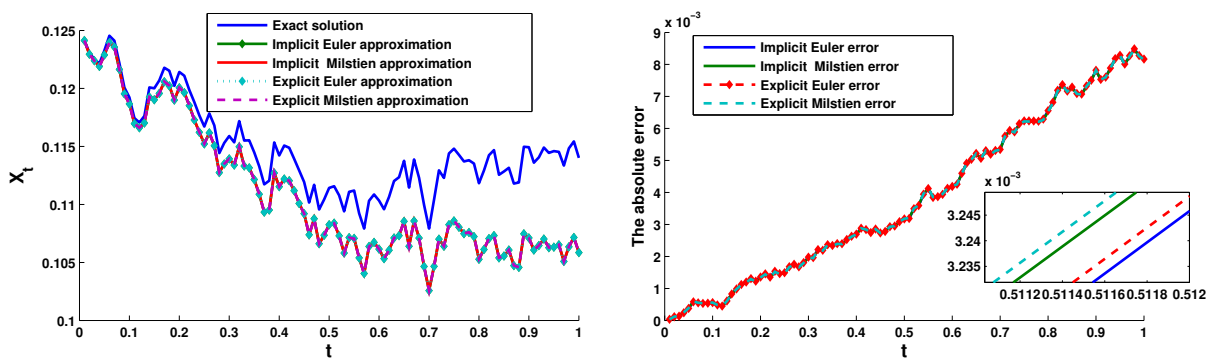
Figure 2.16: Exact solution, Euler and Milstien approximate solutions with the absolute error for Example 2.13.
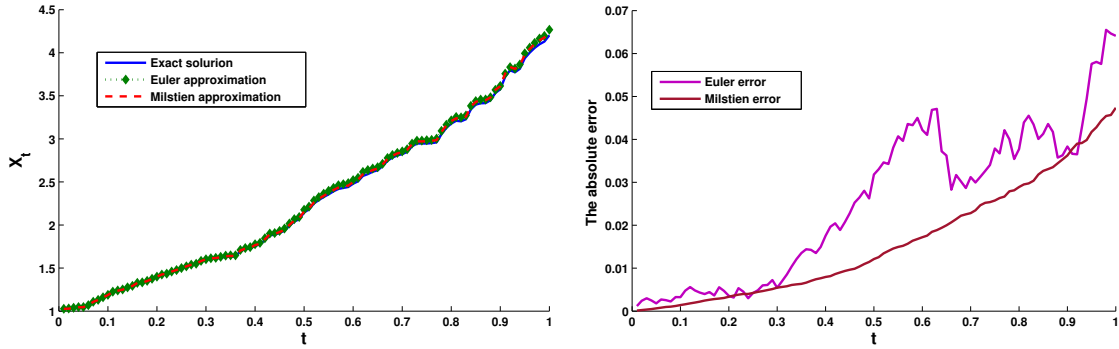
Figure 2.17: Exact solution, implicit Euler and Milstien approximate solutions with the absolute error for Example 2.7.

Implicit order 1.5 strong Taylor scheme

In the one-dimensional case where $m = d = 1$, the implicit order 1.5 strong Taylor scheme has the following form

$$
\begin{aligned}
X_{i+1} = X_i &+ \frac{1}{2}\left(F(t_{i+1}, X_{i+1}) - F(t_i, X_i)\right)\Delta_i + \frac{1}{2}G\left(\frac{\partial}{\partial X_t}G\right)\{(\Delta\mathcal{B}_i)^2 - \Delta_i\} \\
&+ G\frac{\partial}{\partial X_t}F\{\Delta Z - \frac{1}{2}\Delta\mathcal{B}_i\Delta_i\} + \left(F\frac{\partial}{\partial X_t}G + \frac{1}{2}G^2\frac{\partial^2}{\partial X_t^2}G\right)\{\Delta\mathcal{B}_i\Delta_i - \Delta Z\} \\
&+ \frac{1}{2}G\left[\frac{\partial}{\partial X_t}\left(G\frac{\partial G}{\partial X_t}\right)\right]\{\frac{1}{3}(\Delta\mathcal{B}_i)^2 - \Delta_i\}\Delta\mathcal{B}_i,
\end{aligned} \tag{2.72}
$$

where $\Delta Z \sim \mathcal{N}(0, \frac{1}{3}\Delta_i^3)$, and $\Delta\mathcal{B}_i \sim \mathcal{N}(0, \Delta_i)$. For more information and details, see [66].

2.2.3   Weak expilicit approximations

Weak Euler schemes

In subsection (2.2.1), we examined different Euler schemes. The form of the k-th component in Euler schemes in Eq. (2.39) implies robust multidimensional schemes with strong convergence. Now we will consider weak approximations to Itô processes. In this approach, we replace the Brownian increments with other increments that have similar moments to a certain degree. These approximations lead to the first scheme, called the simplified Euler weak scheme, as shown below

$$
X_{i+1}^k = X_i^k + F^k(t_i, X_i)\Delta_i + \sum_{j=1}^{m} G^{k,j}(t_i, X_i)\Delta\tilde{\mathcal{B}}_i^j, \tag{2.73}
$$

where $\Delta\tilde{\mathcal{B}}^j$ are independent $\mathcal{A}_{t_{i+1}}$-measurable satisfying

$$\left| E(\Delta\tilde{\mathcal{B}}^j) \right| + \left| E\left((\Delta\tilde{\mathcal{B}}^j)^3\right) \right| + \left| E\left((\Delta\tilde{\mathcal{B}}^j)^2\right) - \Delta_i \right| \leq A\Delta_i^2, \tag{2.74}$$

and A is a constant. We can take $\tilde{\mathcal{B}}^j$ as a two point distributed random variabes with

$$P(\Delta\tilde{\mathcal{B}}^j = \pm\sqrt{\Delta_i}) = \frac{1}{2}. \tag{2.75}$$

According to Theorem (14.5.2) in Kloden's book [66]. The simplified Euler scheme is of order 1.0.

Order 2.0 weak schemes

The order 2.0 weak Taylor scheme is constructed by incorporating all the double stochastic integrals from the Itô-Taylor expansion into the Euler scheme. For the one dimensional case $(d = m = 1)$, The simplified weak order 2.0 is given by

$$\begin{aligned}
X_{i+1} = {}& X_i + F\Delta_i + G\Delta\mathcal{B}_i + \frac{1}{2}G\left(\frac{\partial}{\partial X_t}G\right)\{(\Delta\mathcal{B}_i)^2 - \Delta_i\} \\
& + \left(\frac{\partial}{\partial X_t}F\right)G\Delta Z + \frac{1}{2}\Delta_i^2\left(F\frac{\partial}{\partial X_t}F + \frac{1}{2}G^2\frac{\partial^2}{\partial X_t^2}F\right) \\
& + \left(F\frac{\partial}{\partial X_t}G + \frac{1}{2}G^2\frac{\partial^2}{\partial X_t^2}G\right)\{\Delta\mathcal{B}_i\Delta_i - \Delta Z\}.
\end{aligned} \tag{2.76}$$

From the scheme (2.76), an adapted scheme can be obtained by replacing the Gaussian increment $\Delta\mathcal{B}$ with $\Delta\tilde{\mathcal{B}}$ with similar moment properties, and avoiding the second random variable ΔZ, by replacing it with the random variable $\frac{1}{2}\Delta\tilde{\mathcal{B}}\Delta_i$. Then, we get the simplified order 2.0 weak Taylor scheme as follows

$$\begin{aligned}
X_{i+1} = {}& X_i + F\Delta_i + G\Delta\tilde{\mathcal{B}}_i + \frac{1}{2}G\left(\frac{\partial}{\partial X_t}G\right)\{(\Delta\tilde{\mathcal{B}}_i)^2 - \Delta_i\} \\
& + \frac{1}{2}\Delta\tilde{\mathcal{B}}\Delta_i\left(G\frac{\partial}{\partial X_t}F + F\frac{\partial}{\partial X_t}G + \frac{1}{2}G^2\frac{\partial^2}{\partial X_t^2}G\right) \\
& + \frac{1}{2}\Delta_i^2\left(F\frac{\partial}{\partial X_t}F + \frac{1}{2}G^2\frac{\partial^2}{\partial X_t^2}F\right),
\end{aligned} \tag{2.77}$$

where $\Delta\tilde{\mathcal{B}}^j$ are independent $\mathcal{A}_{t_{i+1}}$-measurable satisfying

$$\begin{aligned}
\left| E(\Delta\tilde{\mathcal{B}}) \right| + {}& \left| E\left((\Delta\tilde{\mathcal{B}})^3\right) \right| + \left| E\left((\Delta\tilde{\mathcal{B}})^5\right) \right| \\
& + \left| E\left((\Delta\tilde{\mathcal{B}})^2\right) - \Delta_i \right| + \left| E\left((\Delta\tilde{\mathcal{B}})^4\right) - 3\Delta_i^2 \right| \leq A\Delta_i^3,
\end{aligned} \tag{2.78}$$

we can take $\Delta\tilde{\mathcal{B}}$ is $\mathcal{N}(0, \Delta_i)$ that satisfies Eq. (2.78), or satifiy the following conditions

$$P(\Delta\tilde{\mathcal{B}} = \pm\sqrt{3\Delta_i}) = \frac{1}{6}, \qquad P(\Delta\tilde{\mathcal{B}} = 0) = \frac{2}{3}. \tag{2.79}$$

Now, for $d = 1, 2, 3...$ and $m = 1$, the explicit order 2.0 weak scheme is given by

$$\begin{aligned}
X_{i+1} = X_i &+ \frac{1}{2}\left(F(\Upsilon) + F\right)\Delta_i \\
&+ \frac{1}{4}\left(G(\Upsilon^+) + G(\Upsilon^-) + 2G\right)\Delta\tilde{\mathcal{B}} \\
&+ \frac{1}{4}\left(G(\Upsilon^+) - G(\Upsilon^-)\right)\{(\Delta\tilde{\mathcal{B}})^2 - \Delta_i\}\Delta_i^{-\frac{1}{2}},
\end{aligned} \tag{2.80}$$

with $\Upsilon = X_i + F\Delta_i + G\Delta\tilde{\mathcal{B}}$, $\Upsilon^\pm = X_i + F\Delta_i \pm G\sqrt{\Delta}$, and $\Delta\tilde{\mathcal{B}}$ are independent $\mathcal{A}_{t_{i+1}}$-measurable satisfying Eq.(2.78) and could be a three point distributed random variable meets the Eq. (2.79).

Example 2.14 *Consider the linear stochastic differential equation*

$$dX_t = -2X_t dt + X_t d\mathcal{B}_t, \quad 0 \leq t \leq 1, \tag{2.81}$$

where X(0)=1 and the exact solution is given by $X(t) = e^{\frac{-5}{2}t + \mathcal{B}(t)}$. By taking $\Delta_i = 1/N$, and $N = 100$, across 10^2 distinct sample paths of Brownian motion, the mean error between the expectation of the approximation using Euler and the order 2.0 schemes at time t with the expectation of the exact solution is summarized in Figure 2.18.
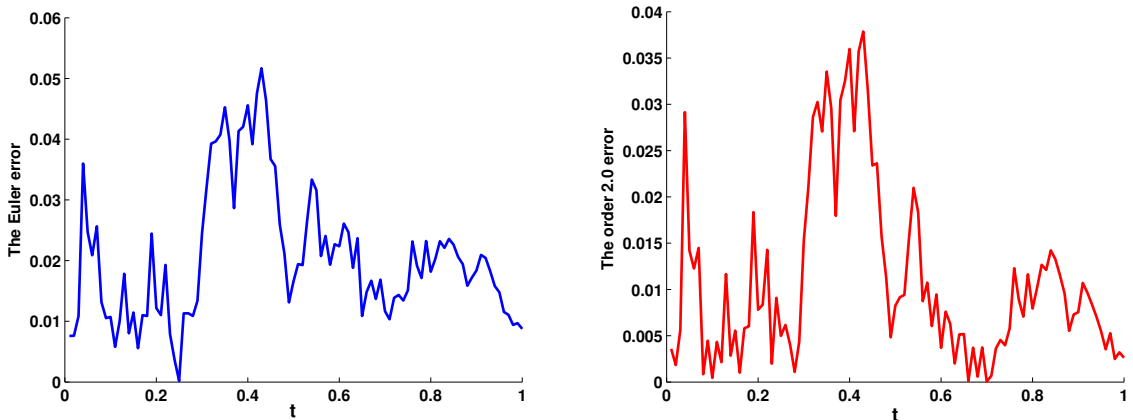
Figure 2.18: Computed error using Euler (left) and the order 2.0 (right) schemes for Example 2.14.

In the following example, we will examine the effect of the step size on the approximation of the mean error expectation between the exact and approximate solutions at the end point $T = 1$.

Example 2.15 *Consider the same problem in Example 2.10, the exact value of $E(X(1)) = 28$. $E(X(1))$ was estimated using weak Euler and order 2.0 methods, by taking 100 independent sample paths of Brownian motion. The results are summarized in Table 2.1 where st.d represents the standard deviation, in different step size Δ.*

Table 2.1: Error and standard deviation for the approximation of $E(X(1))$ for Example 2.15.

Δ	Euler Error	St.d	Order 2.0 Error	St.d
2^{-1}	16.0495	2.4534	4.1948	6.71183
2^{-2}	10.4861	4.7590	2.6116	7.3183
2^{-3}	5.3733	6.6968	1.9127	7.9136
2^{-4}	2.1239	8.2614	1.3046	9.5940
2^{-5}	1.7698	7.5461	0.9942	9.1804
2^{-8}	0.6623	8.0569	0.3415	9.8649
2^{-10}	0.2669	8.7128	0.2934	9.3069

2.2.4   Weak implicit approximations

Weak implicit Euler schemes

This scheme is considered as the simplest implicit weak scheme, it is written as follows

$$X_{i+1} = X_i + F(t_{i+1}, X_{i+1})\Delta_i + \sum_{j=1}^{m} G^j(t_i, X_i)\Delta\tilde{\mathcal{B}}_i^j, \quad i = 1, 2, ... \tag{2.82}$$

where $d, m = 1, 2, 3, ...$ For $j \in \{1, 2, ..., m\}$, the $\Delta\tilde{\mathcal{B}}^j$ are independent random variables satisfying Eq.(2.75). Also, we can construct a familly of implicit Euler schemes as

$$X(t_{i+1}) = X(t_i) + \{\lambda F(t_{i+1}, X_{i+1}) + (1 - \lambda)F(t_i, X_i)\}\Delta_i + \sum_{j=1}^{m} G^{k,j}(t_i, X_i)\Delta\mathcal{B}_i^j, \tag{2.83}$$

where λ is the degree of implicitness. If $\lambda = 0$, we get the explicit Euler scheme, and for $\lambda = 1$ we get Eq.(2.82).

The implicit order 2.0 weak Taylor scheme

In the one-dimensional case $d = m = 1$, the implicit order 2.0 weak Taylor scheme is given by

$$
\begin{aligned}
X_{i+1} = {} & X_i + F(X_{i+1})\Delta_i + G\Delta\tilde{\mathcal{B}}_i + \frac{1}{2}G\left(\frac{\partial}{\partial X_t}G\right)\{(\Delta\tilde{\mathcal{B}}_i)^2 - \Delta_i\} \\
& - \frac{1}{2}\Delta_i^2\left(F(X_{i+1})\frac{\partial}{\partial X_t}F(X_{i+1}) + \frac{1}{2}G^2(X_{i+1})\frac{\partial^2}{\partial X_t^2}F(X_{i+1})\right) \\
& + \frac{1}{2}\Delta\tilde{\mathcal{B}}\Delta_i\left(-G\frac{\partial}{\partial X_t}F + F\frac{\partial}{\partial X_t}G + \frac{1}{2}G^2\frac{\partial^2}{\partial X_t^2}G\right)
\end{aligned}
\tag{2.84}
$$

where $\Delta\tilde{\mathcal{B}} \sim \mathcal{N}(0, \Delta_i)$ or $P(\Delta\tilde{\mathcal{B}} = \pm\sqrt{3\Delta_i}) = \frac{1}{6}$, and $P(\Delta\tilde{\mathcal{B}} = 0) = \frac{2}{3}$.

Consider the Example 2.14, Figure 2.19 represents the mean error between the expectation of the approximation using implicit Euler and the order 2.0 schemes at different time t, and the expectation of the exact solution with $N = 100$ and 10^2 distinct sample paths of Brownian motion.
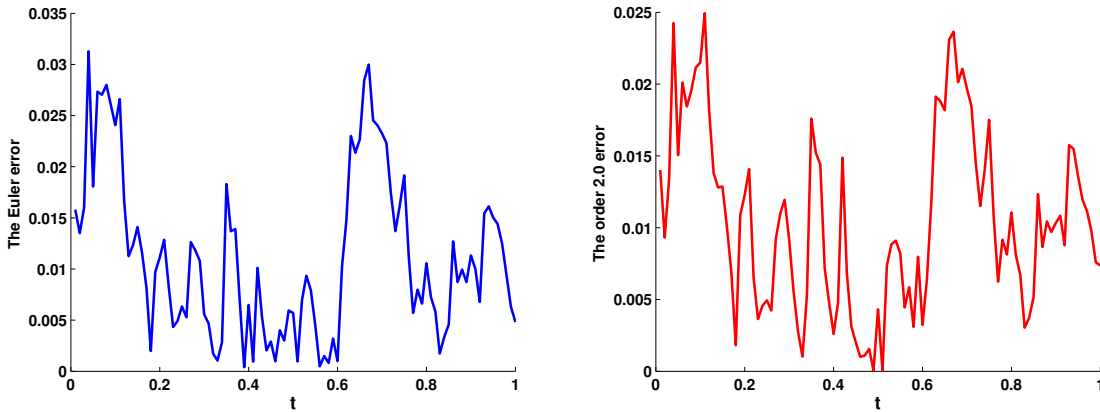
Figure 2.19: Computed errors using implicit Euler and the order 2.0 schemes for Example 2.14.

Additional details for weak approximations can be found in [66].

2.2.5   Analysis of numerical experiments

The convergence of approximate solution using Taylor shemes is based on two strategies, strong approximation or weak approximation, each strategy has its characteristics.

- From the above computation we can see that small discretization steps give better results in both convergence modes. This is the case in Examples 2.9 and 2.10.

- As can be seen in Examples 2.7- 2.8, 2.10 and 2.12, when the SDE contains a diffusion term that is not constant, or in both the scalar and multiplicative cases, one can use either the Euler-Maruyama method or the Milstein method, where the Milstein method has superior accuracy.

- In Example 2.11, the order 1.5 strong Taylor scheme shows a very accurate results compared with Euler and Milstein schemes in a different step size discretization.

- The use of the higher order Ito-Taylor methods produces a better results in both cases when compared to the Euler and Milstein schemes for small step size. Again, this depends on the respective stability domain of these schemes.

- The stability of the approximate solution and its convergence to the exact solution are confirmed in Example 2.15.

- In addition, implicit schemes have been shown to be superior to explicit schemes. (See Examples 2.12-2.14).

- We experimentally test the numerical stability of the explicit Euler-Maruyama and Milstein schemes using a linear test equation. The choice of the parameters λ and μ affects the stability of the numerical solution.

- In Example 2.9, the Ito-Taylor schemes still give good results even for a large scale interval. However, the error decreases over a small scale interval for large N.

- In the previous tests, we have already seen that the Euler-Maruyama scheme and the Milstein scheme perform similarly in the sense of a weak convergence. However, Milstein usually produces slightly better results.

2.3   Applications

In this section we will look at some of the applications of the Ito-Taylor schemes, for simplicity we will use only the Euler scheme to describe the behavior of the Lorenz system, the Duffing equation and the Merton jump diffusion model.

2.3.1   Lorenz system

Lorenz system named after the meteorologist Edward Lorenz describes a simplified model of atmospheric convection. This system shows its chaotic behavior which is characterized by sensitive dependence on initial conditions, so the behavior of the system appears random and unpredictable over a long time scales. The system is

$$
\begin{cases}
\dfrac{dX}{dt} = \delta(Y - X) \\[2em]
\dfrac{dY}{dt} = \beta X - Y - XZ \\[2em]
\dfrac{dZ}{dt} = XY - \gamma Z,
\end{cases}
\tag{2.85}
$$

where X represents the rate of convective overturning in the system, related to temperature differences, Y represents the horizontal temperature variation in the system also influenced by convective motion, and Z the vertical temperature gradient in the system related to the stability of the atmosphere. The parameters δ, β, and γ are positive real numbers that control the dynamics of the system. Lorenz system is often used as a prototype for studying chaotic dynamics and nonlinear phenomena in various fields including mathematics, physics, and meteorology. Moreover, it's useful in the study of turbulence and climate modeling. In the Lorenz's paper, he studied the particular case $\delta = 10$, $\beta = 28$ and $\gamma = \frac{8}{3}$, so we will take this case also. Applying the Euler scheme to the system by taking $T = 50$ and $\Delta = \frac{50}{10^6}$, the Figure 2.20 illustrates the Lorenz attractor. Figure 2.21 represents the solution of Lorenz equations by taking the initial condition $X(0) = 0$, $Y(0) = 1$ and $Z(0) = 0$. We notice that the trajectory appears an irregular oscillation, so how it's gonna be if we add a random noise to the system.

The stochastic Lorenz system is given as follows

$$
\begin{cases}
\dfrac{dX_t}{dt} = \delta(Y_t - X_t) \\[2em]
\dfrac{dY_t}{dt} = \beta X_t - Y_t - X_t Z_t + \alpha_1 Y_t \dfrac{d\mathcal{B}_1}{dt} \\[2em]
\dfrac{dZ_t}{dt} = X_t Y_t - \gamma Z_t + \alpha_2 Z_t \dfrac{d\mathcal{B}_2}{dt},
\end{cases}
\tag{2.86}
$$

where α_1 and α_2 are positive constants and $\mathcal{B}_1$, $\mathcal{B}_2$ are one-dimensional Brownian motion. Lets keep the same value of parameters and initial condition, using the Euler scheme to the system (2.86) by taking $T = 50$ and $\Delta = \frac{50}{10^6}$, we obtain some intersting plot where Figure 2.22 represents Lorenz attractor for $\alpha_1 = 0.3, \alpha_2 = 0.8$, the solutions are shown in Figure 2.23. Figures 2.24-2.25 illustrate the stochastic Lorenz attractor and solutions respectively with $\alpha_1 = \alpha_2 = 0.9$. We notice that if we add a small random noise, the result is still has irregular oscillations but trajectories are jagged due to the chaotic behavior on each direction and its different compared to the deterministic case.

Now if we take a large random noise by taking $\alpha_1 = \alpha_2 = 5$. The results will be completely different from the deterministic ones, we can see that in Figures 2.26-2.27, where Figure 2.26 represents the stochastic Lorenz attractor with $\alpha_1 = \alpha_2 = 5$ by using the Euler scheme with $T = 50$ and $\Delta = \frac{50}{10^6}$. Figure 2.27 illustrate the solutions $X(t)$, $Y(t)$ and $Z(t)$ of stochastic Lorenz equations. We notice that the solution moves around the value 0, so for a large random noise, the system is forced to go to zero.

2.3.2   Duffing equation

The deterministic Duffing equation describes the motion of a damped driven oscillation, it is expressed as

$$\ddot{x} + \delta\dot{x} + \alpha x + \beta x^3 = \gamma\cos(\omega t), \tag{2.87}$$

where x represents the displacement of the oscillator from its equilibrium position, δ is the damping coefficient, α is the linear stifness coefficient, β is the nonlinear stiffness coefficient, γ is the amplitude of the external forcing, ω is the frequency of the external forcing and t represents time. The Duffing equation is used to model various systems such that electrical circuits, biological systems and mechanical systems like spring-mass-damper systems. If $x = X$ and $\dot{X} = Y$, we get the following system

$$\begin{cases} \dot{X} = Y \\ \dot{Y} = \gamma\cos(\omega t) - \delta Y - \alpha X - \beta X^3, \end{cases} \tag{2.88}$$

where $t \in [0, T]$. Let take for example $\delta = 0.02$, $\alpha = 1$, $\beta = 5$, $\gamma = 8, \omega = 0.5$, $X(0) = 0$ and $Y(0) = 1$, applying Euler scheme for the particular case with $T = 40$ and $\Delta = \frac{40}{10^6}$. Figure 2.28 represents one trajectory of damped deterministic Duffing equation. Now lets take the
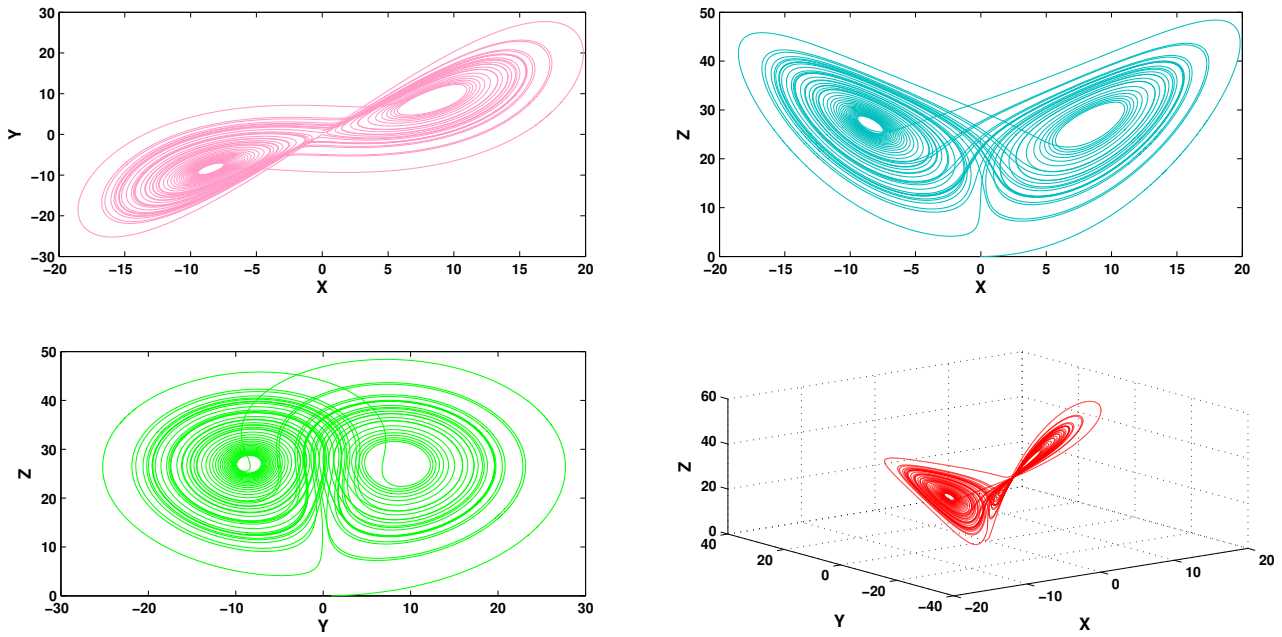
Figure 2.20: Lorenz attractor (2.85).
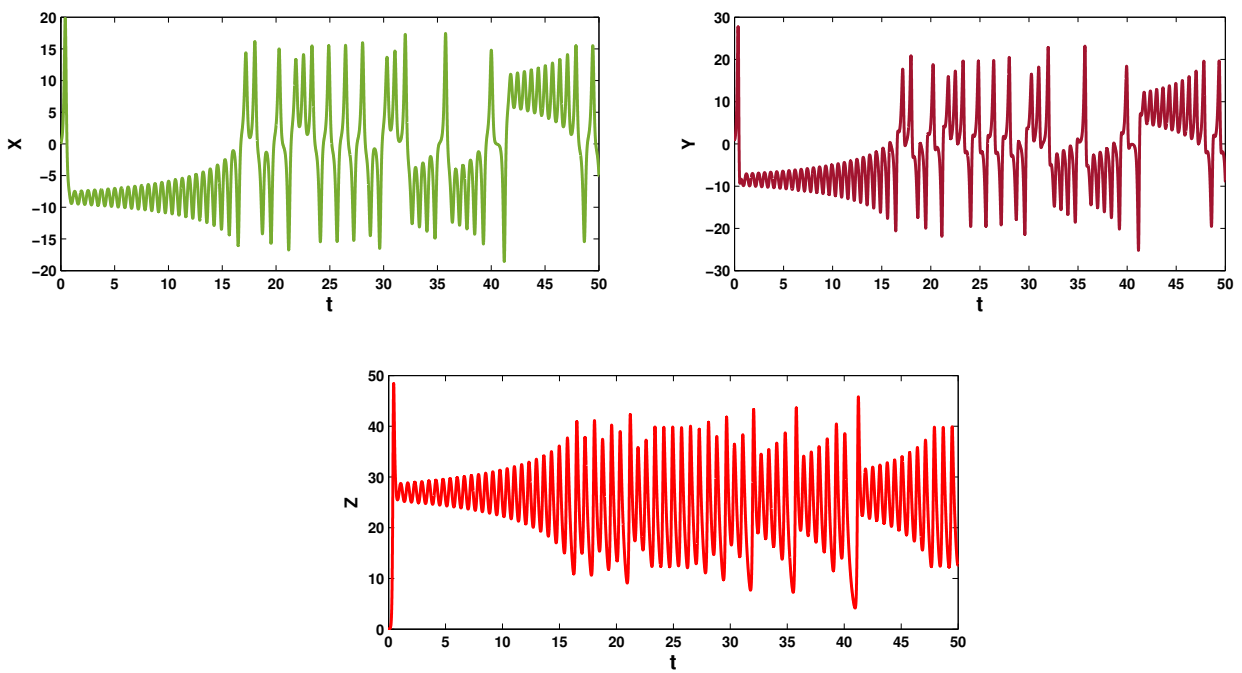
Figure 2.21: Solution of Lorenz equations (2.85).
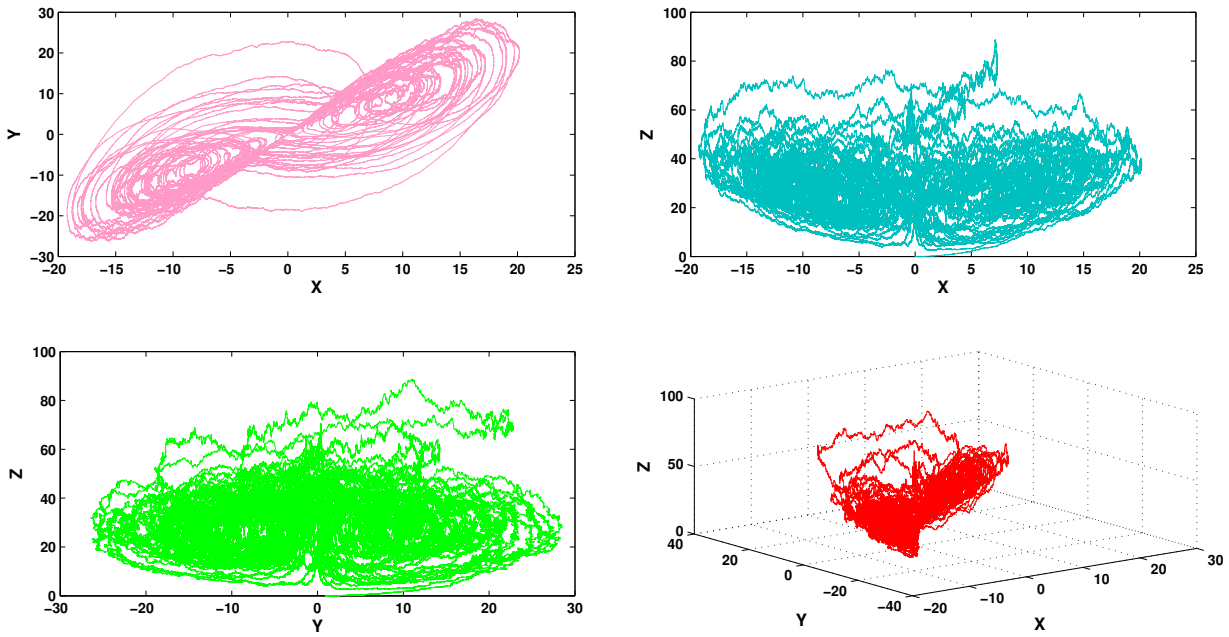
Figure 2.22: Stochastic Lorenz attractor with $\alpha_1 = 0.3, \alpha_2 = 0.8$.
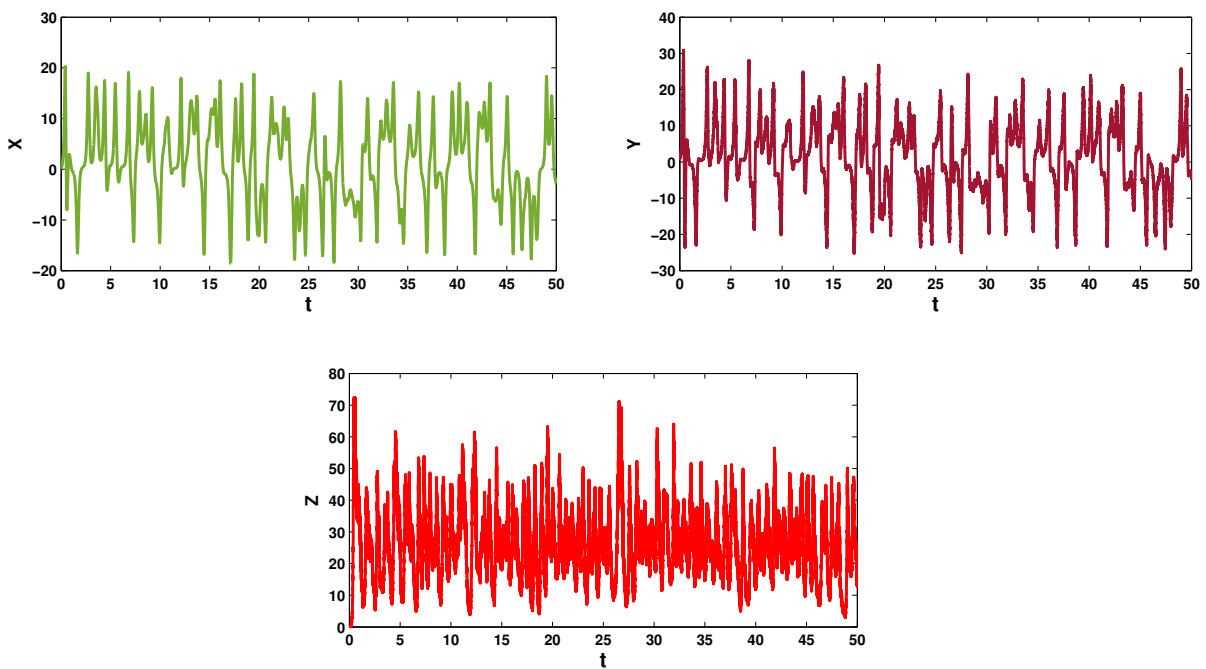
Figure 2.23: Solution of stochastic Lorenz equations with $\alpha_1 = 0.3, \alpha_2 = 0.8$.
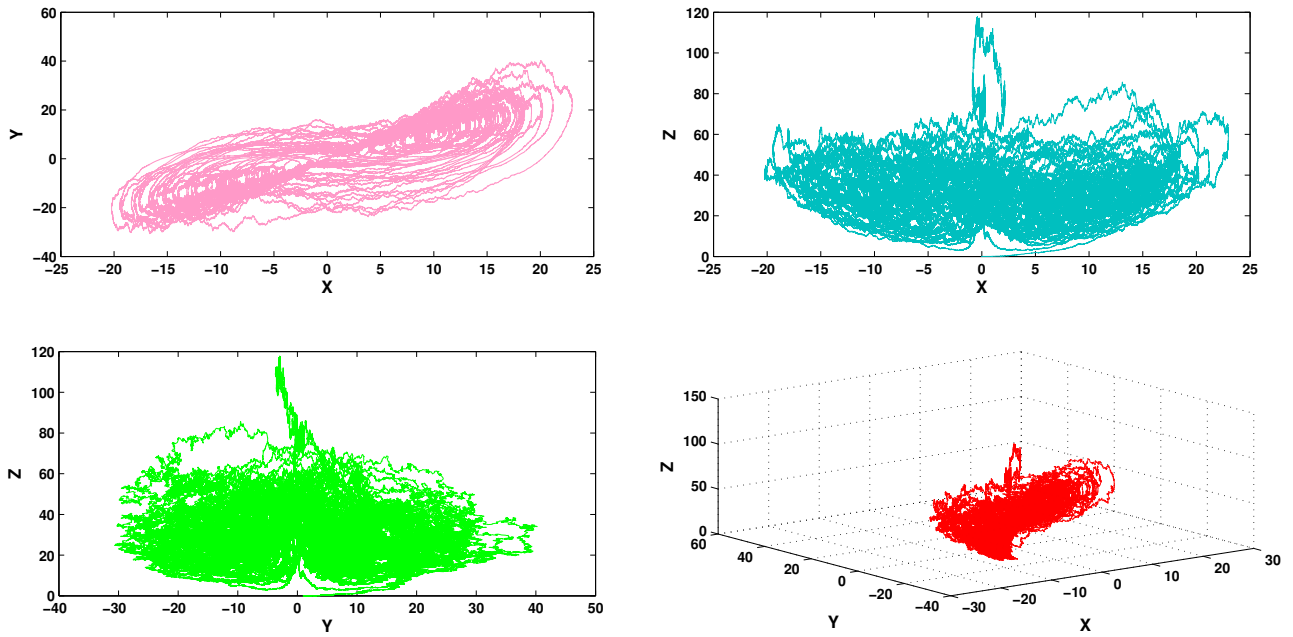
Figure 2.24: Stochastic Lorenz attractor with $\alpha_1 = 0.9, \alpha_2 = 0.9$.
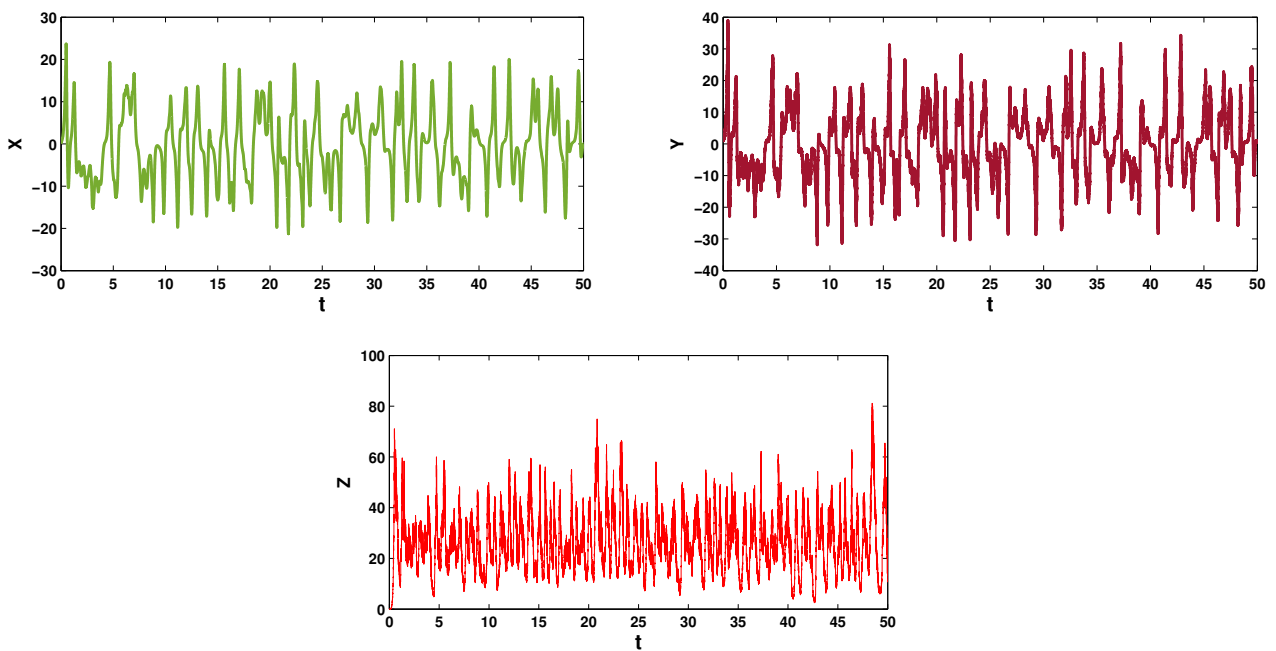
Figure 2.25: Solution of stochastic Lorenz equations with $\alpha_1 = 0.9, \alpha_2 = 0.9$.
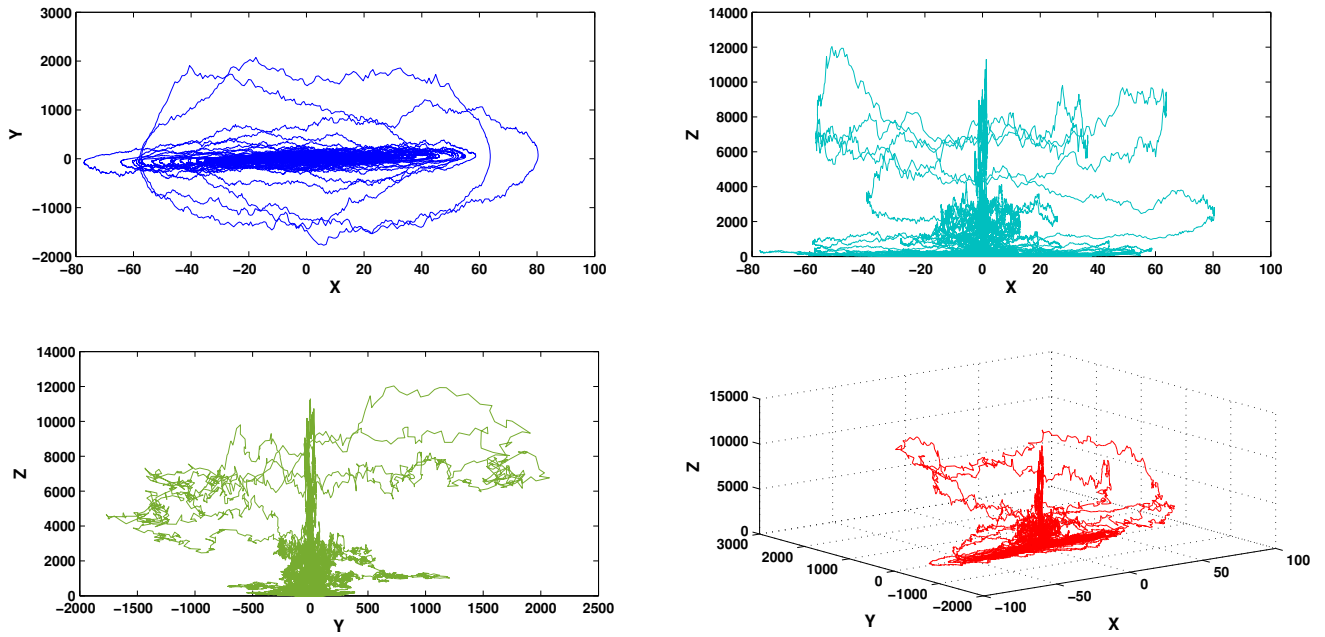
Figure 2.26: Stochastic Lorenz attractor with $\alpha_1 = 5, \alpha_2 = 5$.
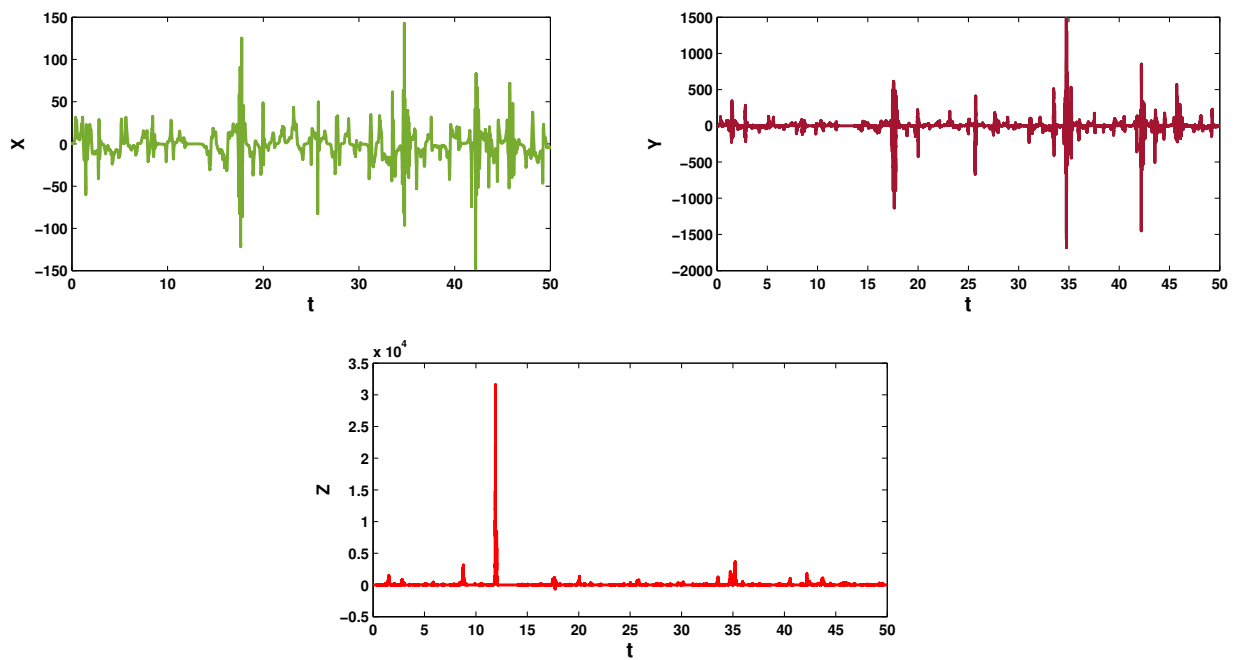
Figure 2.27: Solution of stochastic Lorenz equations with $\alpha_1 = 5, \alpha_2 = 5$.
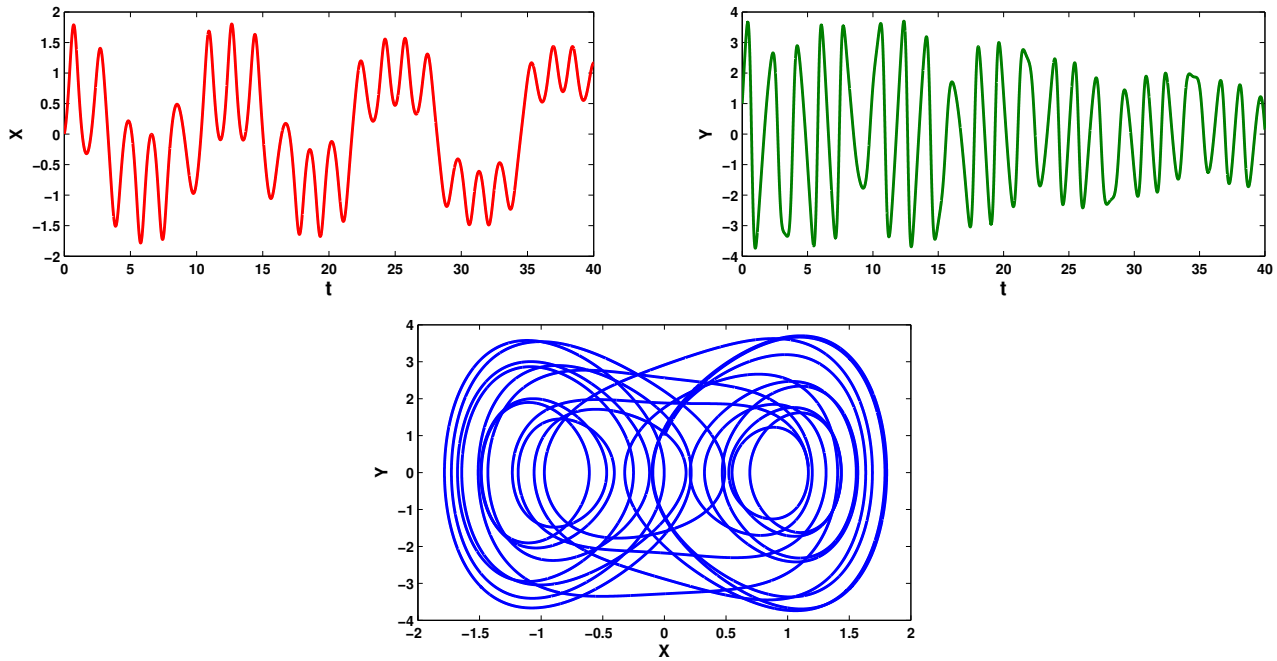
Figure 2.28: Trajectories of deterministic Duffing equation with force.

simplest Duffing system with no forcing

$$\begin{cases} \dot{X} = Y \\ \dot{Y} = -\delta Y + X - X^3. \end{cases} \tag{2.89}$$

Figure 2.29 shows the trajectories of system (2.89) via the Euler method by taking $\delta = 0$, $X(0) = 0.5$ and $Y(0) = 0.6$. By adding a random noise to the system (2.89), we obtain the stochastic Duffing equation

$$\begin{cases} \dot{X} = Y \\ \dot{Y} = -\delta Y + X - X^3 + \sigma X \dot{\mathcal{B}}. \end{cases} \tag{2.90}$$

So let's see: What happens when we add a random noise? by taking the same example shown in the Figure 2.29, for $\delta = 0$, $X(0) = 0.5$, $Y(0) = 0.6$ and $\sigma = 0.5$ using Euler and Milstien schemes with step size $\Delta = \frac{40}{10^6}$. Figure 2.30 represents the trajectories of stochastic Duffing equation with no force. Notice that if we add the random noise, the solution is not periodic any more.

2.3.3   Merton jump diffusion

Many risks appear in finance, including random fluctuation in financial market prices that negatively affect companies, businesses, or organizations associated with them. Therefore
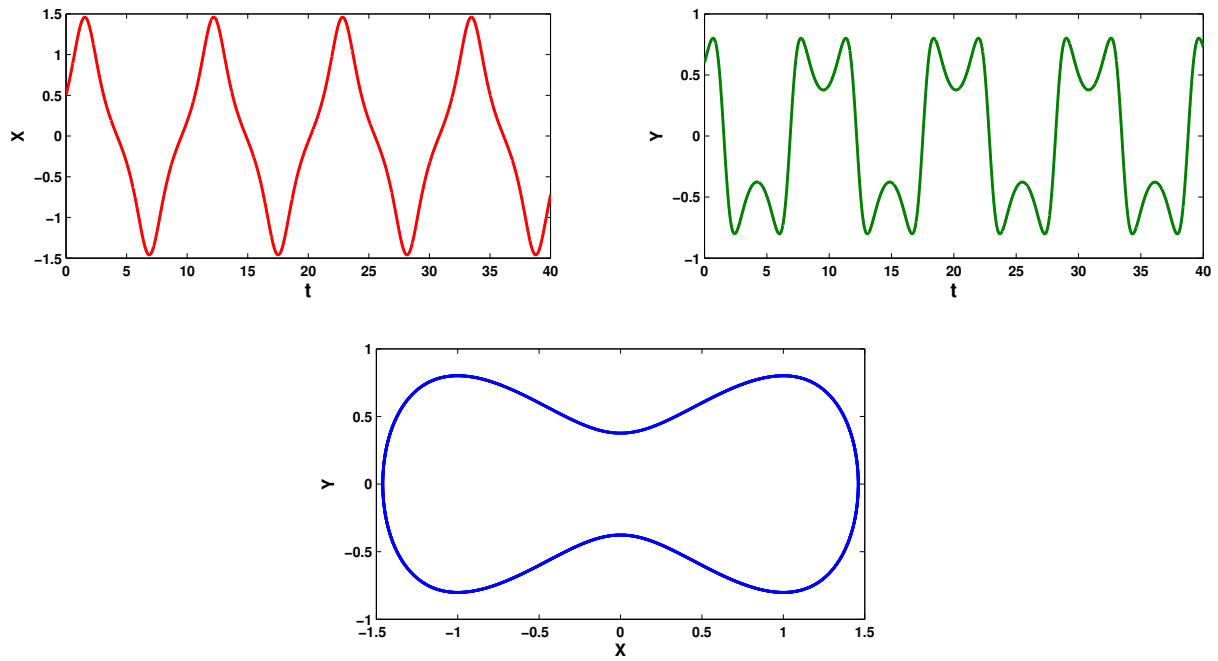
Figure 2.29: Trajectories of deterministic Duffing equation with no force for $\delta = 0$.
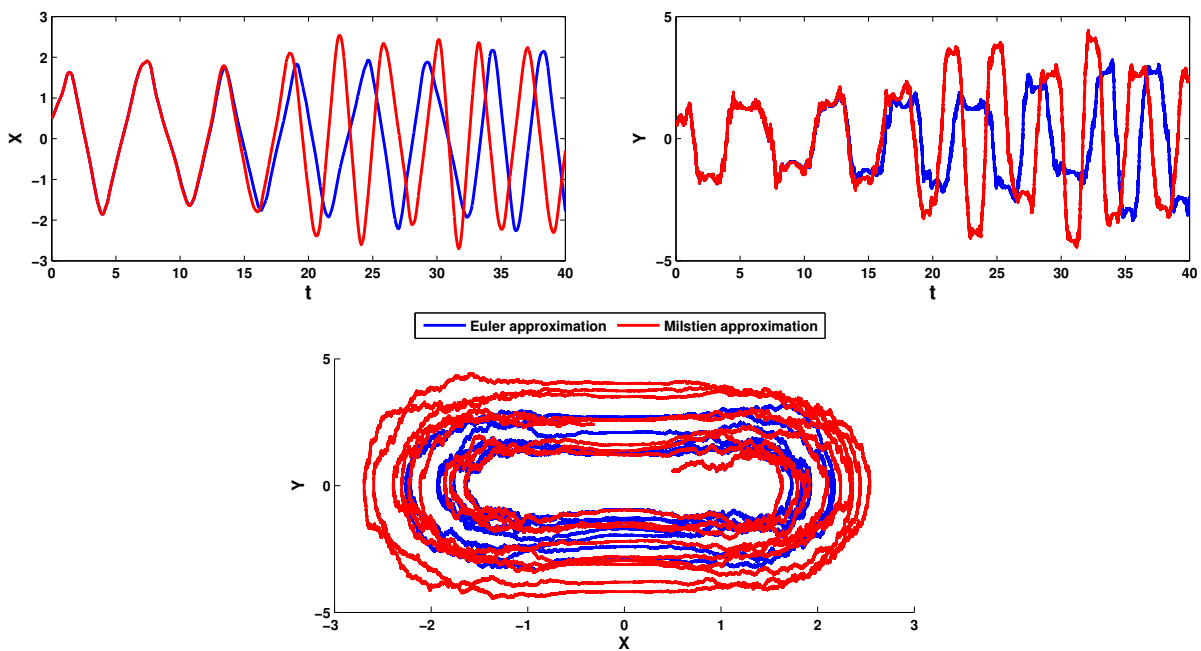
Figure 2.30: Trajectories of undamped stochastic Duffing equation with no force for $\sigma = 0.5$.

modeling this type of problem greatly helps investors and traders to analyse real-world data. These models aim to predict the future movements of the asset price financial market, thereby mitigating associated risks.

   The Black Scholes model was effective in many situations, however it assumed that asset prices follow a smooth continuous pattern described by geometric Brownian motion. This assumption works in many cases but it has limitations, one significant limitation is its assumption of continuous price movements which doesn't fully capture the sudden changes observed in financial markets. To address this limitation and provide a more accurate representation of real-world market dynamics, Robert Merton developed a model called the Merton Jump diffusion model. It is a generalization of the Black Scholes model by incorporating the jumps in asset price, this addition is very important because financial asset prices often exhibit discontinuous movements, which cannot be adequately explained by continuous diffusion process alone.

   To define Merton's jump-diffusion model mathematically, we incorporate both the continuous Brownian motion and the occasional jumps in the asset price. The model is described by the following stochastic differential equation

$$\frac{dX_t}{X_t} = \mu dt + \sigma d\mathcal{B}_t + \text{Jump},   \tag{2.91}$$

where X_t represent the price of the asset at time t, μ is the expected return rate of the asset, σ is the volatility of the asset's return. Now if we talk about the jump part, two things come to our mind, the jump arrival according to Poisson process with intensity λ, and the size of the jump is log normal ditribution.

Let Y_i represent the absolute price jump size in which the asset price X_t jumps to $Y_t X_t$ in a small time interval dt where $Y_t > 0$, so

$$dX_t = Y_t X_t - X_t   \Rightarrow \frac{dX_t}{X_t} = Y_t - 1.$$

Now if we talk about the jump arrivals which assumed to follow a Poisson process $N(t)$, so the likelihood that an asset price jumps within a short time interval can be expressed as

$$\begin{cases} P(dN_t = 1) = \lambda dt \\ P(dN_t = 0) = 1 - \lambda dt. \end{cases}$$

So Eq.(2.91) become

$$\frac{dX_t}{X_t} = \mu dt + \sigma d\mathcal{B}_t + (Y_t - 1)dN_t.   \tag{2.92}$$

Merton assumes that $\ln(Y_t) \sim N(\mu_1, \sigma_1^2)$ and Y_t, $\mathcal{B}_t$ and N_t are independent. Now, if we left the drift term unadjusted (μdt), it would imply that the expected return on the asset already accounts for the expected impact of jumps.

Merton in this step adjusting the drift term by subtracting a term $k\lambda dt$ which represents the expected impact of jumps during the time interval dt. Note that $E((Y_t - 1)dN_t) = E(Y_t - 1)E(dN_t) = k\lambda dt$, where $k = E(Y_t - 1)$.

Merton did this to treat jumps as unpredictable events in the model. This adjustment helps maintain the realism of the model, so Eq.(2.92) become

$$\frac{dX_t}{X_t} = (\mu - \lambda k)dt + \sigma d\mathcal{B}_t + (Y_t - 1)dN_t. \tag{2.93}$$

If the time interval is not too small, then more than one jump can occur, so the price X_t after a random jumps is $X_t \prod_{j=1}^{dN_t} Y_j$, so we obtain

$$\frac{dX_t}{X_t} = (\mu - \lambda k)dt + \sigma d\mathcal{B}_t + (\prod_{j=1}^{dN_t} Y_j - 1). \tag{2.94}$$

Now, applying the Itô's lemma for the jump model

$$df = \frac{df}{dX}dX + \frac{1}{2}\frac{d^2 f}{dX^2}dX^2 + f(X \prod_{j=1}^{dN_t} Y_j) - f(X),$$

with $f(t, X) = ln(X)$, we obtain

$$X_t = X_0 e^{(\mu - \lambda k - \frac{1}{2}\sigma^2)t + \sigma\mathcal{B}_t + \sum_{j=1}^{N_t} ln(Y_j)}. \tag{2.95}$$
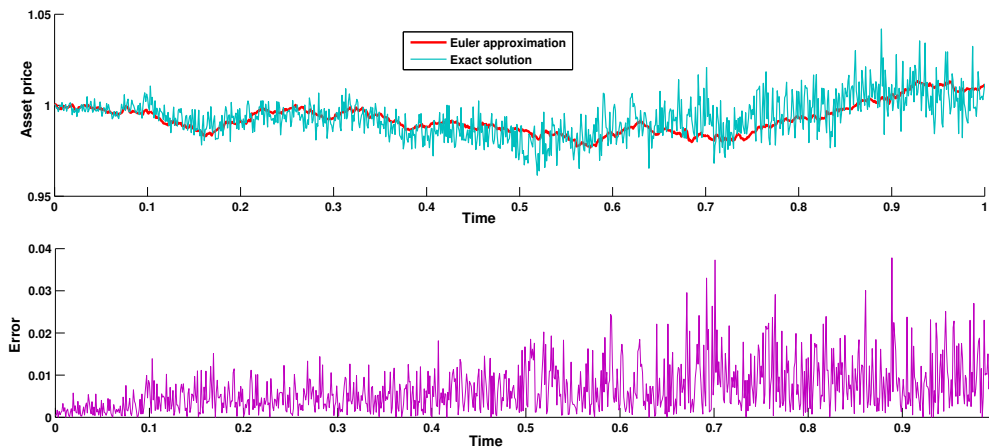
Figure 2.31: Exact solution and Euler approximation for MJD with the absolute error for $\mu = 0.005, \sigma = 0.2, \mu_1 = 0.01, \sigma_1 = 0.1$ and $\lambda = 1$.

Figure 2.31 represents the exact asset price and the approximate solution by Euler scheme with the absolute error for $\mu = 0.005, \sigma = 0.2, \mu_1 = 0.01, \sigma_1 = 0.1$, $\lambda = 1$, $X_0 = 1$ and $\Delta_i = i/1000$, by taking 100 simulations.
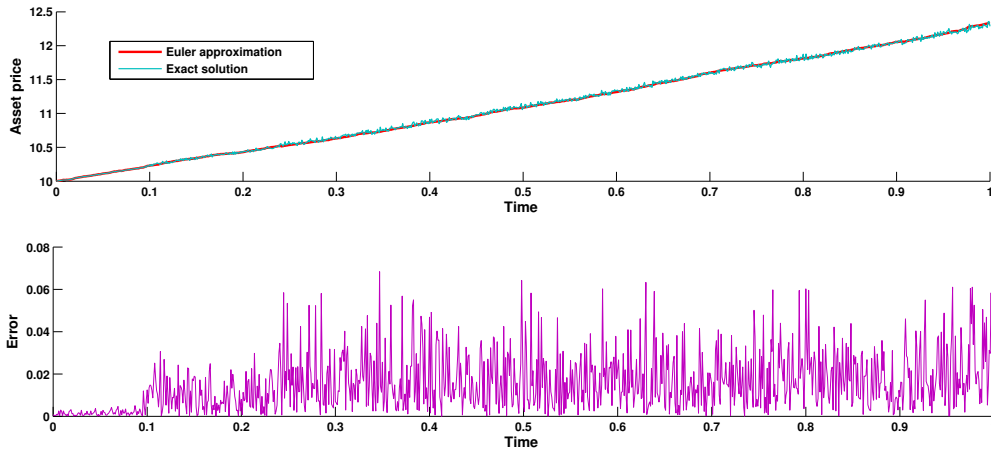
Figure 2.32: Exact solution and Euler approximation for MJD with the absolute error for $\mu = 0.21, \sigma = 0.056, \mu_1 = 0.056, \sigma_1 = 0.097$ and $\lambda = 0.1$.

Figure 2.32 illustrates the exact asset price and the approximate solution by Euler scheme with the absolute error for $\mu = 0.21, \sigma = 0.056, \mu_1 = 0.056, \sigma_1 = 0.097, \lambda = 0.1, X_0 = 10$ and $\Delta_i = i/1000$, through 100 simulations.
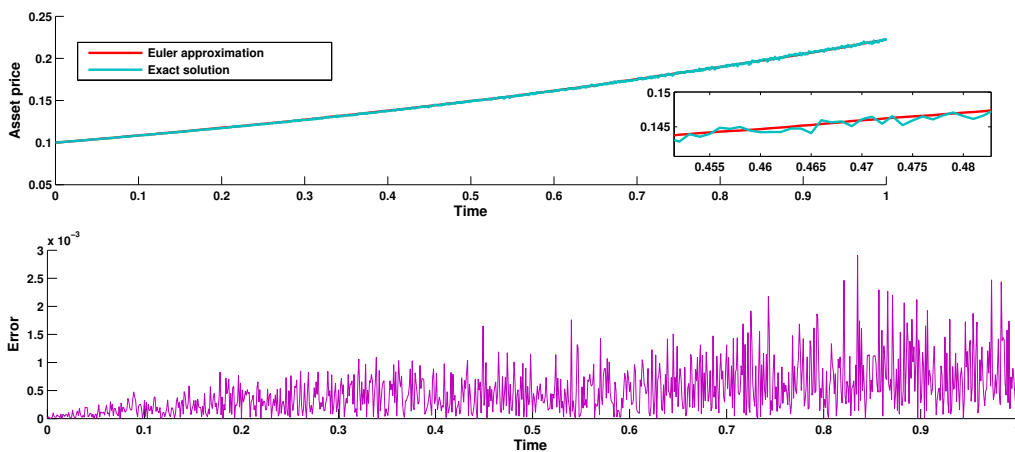
Figure 2.33: Exact solution and Euler approximation for MJD with the absolute error for $\mu = 0.8, \sigma = 0.03, \mu_1 = 0.02, \sigma_1 = 0.05$ and $\lambda = 10$.

Figure 2.33 shows the exact asset price and its approximate solution using the Euler

scheme, with absolute error, in the case $\mu = 0.8, \sigma = 0.03, \mu_1 = 0.02, \sigma_1 = 0.05, \lambda = 10$, $X_0 = 0.1$, and $\Delta_i = i/1000$, with 100 simulations.

2.4   Spectral methods

We do not deny that the Itô-Taylor schemes are a valuable numerical methods for approximating the solutions of stochastic differential equations. But for some complex problems, traditional numerical methods for solving these equations are often challenged by the complex interplay between deterministic dynamics and stochastic fluctuations. In this context, the emergence of spectral methods over time has helped to provide a powerful and flexible approach to the challenges posed by the randomness and complexity in many real-world systems. The spectral method is a powerful numerical technique used for solving differential equations by representing the solution as a combination of basis functions. Essentially, it transforms complex mathematical problems into a series of more simple algebraic equations, allowing for efficient computation and accurate approximation of the solution. In 1970s-1980s, the spectral method gained popularity in the scientific community for solving deterministic partial differential equations (PDEs). The concept of stochastic Galerkin methods gained attention. Researchers extended deterministic Galerkin and Monte Carlo methods [43, 106] to handle stochastic differential equations. In the early 2000s, researchers explored chaos functions, which are eigenfunctions of the Wiener process, as a basis for approximating solutions. This approach gained traction due to its convergence properties and efficiency [40, 74, 138]. The mid-2000s witnessed an increasing interest in hybrid methods [1, 44, 69], combining spectral techniques with other numerical approaches to address specific challenges associated with stochastic processes. Researchers continue to explore new mathematical tools and computational strategies [12, 83, 86, 110, 119]. It's important to note that the development of spectral methods for solving stochastic differential equations is a collaborative effort, with numerous researchers contributing to different aspects of the field.

2.4.1   Galerkin method

The Galerkin method was named after the mathematician Boris Galerkin in 1915 and has evolved from its origins in integral equations to become a versatile and widely adopted numerical technique for solving differential equations in diverse fields, it allows to transform a

continuous problem into a discrete problem. The Galerkin method is widely applied in various fields, including fluid dynamics [53], structural mechanics [15], and quantum mechanics [11], making it a versatile and powerful tool for solving a range of mathematical problems. It is also used effectively in solving stochastic differential equations (SDEs) [13, 139, 31]. For more details about this spectral method see the references [132, 137, 141, 95, 140, 123].

2.4.2   Collocation method

The collocation method is a numerical technique used to solve differential equations within the problem domain. The concept of solving stochastic differential equations (SDEs) using the collocation method is an extension of the collocation method for ordinary differential equations (ODEs), which is adapted to deal with the randomness introduced by stochastic terms. Spectral collocation methods force the approximate solution to satisfy the original problem at a given number of points, or in other words, let the residuals be zero at selected collocation points.

   The traditional stochastic collocation method is based on the full-tensor product of one-dimensional interpolation functions, but it becomes impractical for high-dimensional problems as the number of nodes grows exponentially with the stochastic dimension. However, there are several variations of the stochastic collocation method, such as sparse grid stochastic collocation and multilevel stochastic collocation, that can overcome the curse of dimensionality and provide accurate results.

2.5   Spectral computational method for solving SDE

On a filtrated probability space $(\Omega, \mathcal{F}, \mathcal{F}_t, P)$, we will focus on solving the nonlinear stochastic integral equation

$$X(t) = p(t) + \int_0^t W_1(t,s)\psi_1(X(s))ds + \int_0^t W_2(t,s)\psi_2(X(s))d\mathcal{B}(s), \ t \in [0,T]. \qquad (2.96)$$

where the kernels W_1, W_2 and ψ_1, ψ_2 are smooth functions on a filtrated space $(\Omega, \mathcal{F}, \mathcal{F}_t, P)$, and $\{\mathcal{B}(t), t \geq 0\}$ is the Brownian process $\mathcal{F}_t$-measurable. $X(t)$ is the unknown process that we need to find, and $p(t)$ is a random function.

2.5.1   The proposed computation method

Our algorithm is based on the spectral method using the Jacobi polynomials [36], and it is dividing in 4 steps. Let's start with the first one

Step 1

Collocating Eq.(2.96) at t_i points (**Collocation points**), $i = 1, 2, ..., M$. So Eq.(2.96) become

$$X(t_i) = p(t_i) + \underbrace{\int_0^{t_i} W_1(t_i, s)\psi_1(X(s))ds}_{(I)} + \underbrace{\int_0^{t_i} W_2(t_i, s)\psi_2(X(s))d\mathcal{B}(s)}_{(II)}, \qquad (2.97)$$

Step 2

Approximate the state variable with Jacobi polynomials noted by $\mathcal{J}^{\alpha,\beta}$ as follow

$$X(t) \simeq \sum_{j=1}^{M} X(t_j)\mathcal{J}_j^{\alpha,\beta}(t) = X'\mathcal{J}^{\alpha,\beta}(t), \qquad (2.98)$$

where X' is the unknown vecteur and $\mathcal{J}^{\alpha,\beta}(t) = (\mathcal{J}_1^{\alpha,\beta}(t), \mathcal{J}_2^{\alpha,\beta}(t), ..., \mathcal{J}_M^{\alpha,\beta}(t))$. The integrals (I) and (II) can be approximated by Gauss quadrature, so the integral (I) will be

$$\int_0^{t_i} W_1(t_i, s)\psi_1(X(s))ds \simeq \frac{t_i}{2} \sum_{j=1}^{n1} A_j W_1\left(t_i, \frac{t_i}{2}s_j + \frac{t_i}{2}\right) \psi_1\left(X\left(\frac{t_i}{2}s_j + \frac{t_i}{2}\right)\right)$$

$$= \frac{t_i}{2} \sum_{j=1}^{n_1} A_j W_1\left(t_i, \frac{t_i}{2}s_j + \frac{t_i}{2}\right) \psi_1\left(X'\mathcal{J}^{\alpha,\beta}\left(\frac{t_i}{2}s_j + \frac{t_i}{2}\right)\right), \qquad (2.99)$$

where s_j are the Gauss Legendre roots on $[-1, 1]$.

Step 3: Approximating the stochastic integral (II) as

$$\int_0^{t_i} W_2(t_i, s)\psi_2(X(s))d\mathcal{B}(s) = \sum_{j=1}^{n_2+1} W_2\left(t_i, \frac{1}{n_2}(j-1)t_i\right)\psi_2\left(X'\mathcal{J}^{\alpha,\beta}\left(\frac{1}{n_2}(j-1)t_i\right)\right)$$

$$\left[\mathcal{B}\left(\frac{j}{n_2}t_i\right) - \mathcal{B}\left(\frac{1}{n_2}(j-1)t_i\right)\right].$$

So the nonlinear stochastic integral Eq.(2.97) can be traced back to this algebraic system

$$X'\mathcal{J}^{\alpha,\beta}(t_i) = p(t_i) + \frac{t_i}{2} \sum_{j=1}^{n_1} A_j W_1\left(t_i, \frac{t_i}{2}s_j + \frac{t_i}{2}\right) \psi_1\left(X'\mathcal{J}^{\alpha,\beta}\left(\frac{t_i}{2}s_j + \frac{t_i}{2}\right)\right)$$

$$+ \sum_{j=1}^{n_2+1} W_2\left(t_i, \frac{1}{n_2}(j-1)t_i\right) \psi_2\left(X'\mathcal{J}^{\alpha,\beta}\left(\frac{1}{n_2}(j-1)t_i\right)\right)\left[\mathcal{B}\left(\frac{j}{n_2}t_i\right) - \mathcal{B}\left(\frac{1}{n_2}(j-1)t_i\right)\right]$$

$$(2.100)$$

Step 4

Solving the nonlinear algebraic system (2.100), where the unknown vector is X'. The above-mentioned steps can be given in the following Algorithm 1

Algorithm 1 Jacobi spectral method for solving SIVIE

Input: The interval $[0, T]$, the number of collocation points M, the number of simulation K, Jacobi polynomials $\mathcal{J}_M^{\alpha,\beta}(t)$, where the parameters α, $\beta \geq -1$, the functions $W_1(t, s)$, $\psi_1(X(s))$, $W_2(t, s)$, $\psi_2(X(s))$ and $p(t)$.

- Compute the roots of $\mathcal{J}_{M+1}^{\alpha,\beta}(t)$ and collocate the Eq.(2.96).

- Approximate the state variable with Jacobi polynomials.

- Compute the approximation of the integrals (I), and (II) in Eq.(2.97).

- Solve the algebraic system (2.100).

- Substitue the value achieved for X' into Eq. (2.98).

Output : The approximate solution $X(t) = X' \mathcal{J}_M^{\alpha,\beta}(t)$.

2.5.2   Convergence analysis

Theorem 2.3 *Assume that $X(t)$ is the exact solution of Eq.(2.96) and $X_M(t)$ is the approximate solution by the proposed method. We also assume that ψ_1 and ψ_2 are Lipschitzian with constants Q_1 and Q_2 respectively, and that the functions W_i satisfies the following constraints*

$$|W_i(t, s)| \leq V_i, \quad i = 1, 2, \quad (t, s) \in [0, T]^2, \tag{2.101}$$

where V_i, $i = 1, 2$ are a constants. So we have

$$\|X(t) - X_M(t)\|_{L^2(0,T)}^2 = E|X(t) - X_M(t)|^2 \to 0 \ \text{ as } M \to \infty \tag{2.102}$$

Proof. Let X and X_M be the exact and approximate solutions of Eq.(2.96) where

$$X(t_i) = p(t_i) + \int_0^{t_i} W_1(t_i, s)\psi_1(X(s))ds + \int_0^{t_i} W_2(t_i, s)\psi_2(X(s))d\mathcal{B}(s), \tag{2.103}$$

and

$$X_M(t_i) = p_M(t_i) + \int_0^{t_i} W_1(t_i, s)\psi_1(X_M(s))ds + \int_0^{t_i} W_2(t_i, s)\psi_2(X_M(s))d\mathcal{B}(s) - er_1^i - er_2^i, \tag{2.104}$$

---

er_1^i and er_2^i are the errors of the two integrals (I) and (II) in equation (2.97), and we can giving it as follows

$$er_1^i = \int_0^{t_i} W_1(t_i, s)\psi_1(X_M(s))ds - \frac{t_i}{2}\sum_{j=1}^{n1} A_j W_1\left(t_i, \frac{t_i}{2}s_j + \frac{t_i}{2}\right)\psi_1\left(X'\mathcal{J}^{\alpha,\beta}\left(\frac{t_i}{2}s_j + \frac{t_i}{2}\right)\right)$$

and

$$er_2^i = \int_0^{t_i} W_2(t_i, s)\psi_2(X_M(s))d\mathcal{B}(s) - \sum_{j=1}^{n_2+1} W_2\left(t_i, \frac{1}{n_2}(j-1)t_i\right)\psi_2\left(X'\mathcal{J}^{\alpha,\beta}\left(\frac{1}{n_2}(j-1)t_i\right)\right)$$

$$\left[\mathcal{B}\left(\frac{j}{n_2}t_i\right) - \mathcal{B}\left(\frac{1}{n_2}(j-1)t_i\right)\right].$$

Then we have the following

$$E|X(t) - X_M(t)|^2 \le E\left[\left|(p(t) - p_M(t)) + \int_0^{t_i} W_1(t,s)(\psi_1(X(s)) - \psi_1(X_M(s)))ds\right.\right.$$

$$\left.\left. + \int_0^t W_2(t,s)(\psi_2(X(s)) - \psi_2(X_M(s)))d\mathcal{B}(s) + er_1 + er_2\right|^2\right],$$

using $(k_1 + k_2 + k_3)^2 \le 4k_1^2 + 4k_2^2 + 4k_3^2$, we get

$$E|X(t) - X_M(t)|^2 \le 4E|p(t) - p_M(t)|^2 + 4E\left[\left|\int_0^t W_1(t,s)(\psi_1(X(s)) - \psi_1(X_M(s)))ds\right.\right.$$

$$\left.\left. + \int_0^t W_2(t,s)(\psi_2(X(s)) - \psi_2(X_M(s)))d\mathcal{B}(s)\right|^2\right] + 4E|er_1 + er_2|^2,$$

$$\le 4E|p(t) - p_M(t)|^2 + 8E\left|\int_0^t W_1(t,s)(\psi_1(X(s)) - \psi_1(X_M(s)))ds\right|^2$$

$$+ 8E\left|\int_0^t W_2(t,s)(\psi_2(X(s)) - \psi_2(X_M(s)))d\mathcal{B}(s)\right|^2 + 4E|er_1 + er_2|^2.$$

Using the boundedness of W_1 and W_2, Holder's inequality, Itô isometry and Lipschitz condition, we obtain

$$E|X(t) - X_M(t)|^2 \le 4E|p(t) - p_M(t)|^2 + 8tE\int_0^t |W_1(t,s)|^2|\psi_1(X(s)) - \psi_1(X_M(s))|^2 ds$$

$$+ 8E\int_0^t W_2^2(t,s)|\psi_2(X(s)) - \psi_2(X_M(s))|^2 ds + 4E|er_1 + er_2|^2,$$

$$\le 4E|p(t) - p_M(t)|^2 + 8Q_1^2 V_1^2\int_0^t E|X(s) - X_M(s)|^2 ds$$

$$+ 8Q_2^2 V_2^2\int_0^t E|X(s) - X_M(s)|^2 ds + 8E|er_1|^2 + 8E|er_2|^2$$

$$\le (8Q_1^2 V_1^2 + 8Q_2^2 V_2^2)\int_0^t E|X(s) - X_M(s)|^2 ds$$

$$+ 4E|p(t) - p_M(t)|^2 + 8E|er_1|^2 + 8E|er_2|^2.$$

By Gronwall's lemma we have $E|X(t) - X_M(t)|^2 \to 0$ as $M \to +\infty$. ∎

In the following, we will present some test examples in order to confirm the applicability of the proposed method.

2.5.3   Numerical tests

Example 2.16 [66] *Consider the nonlinear stochastic Itô integral equation*

$$X(t) = X_0 + a^2 \int_0^t \cos(X(s)) \sin^3(X(s)) ds + a \int_0^t \sin^2(X(s)) d\mathcal{B}(s), \quad 0 \le t \le 1,$$

The analytical solution is given by

$$X(t) = arccot(a\mathcal{B}(t) + cot(X_0)). \tag{2.105}$$

Let $X_0 = \frac{1}{20}$ and $a = \frac{1}{20}$. By taking $n_1 = 10$, $n_2 = 100$, $K = 20$ and $M = 6$, the numerical results of this example are presented in Table 2.2 and Figure 2.34. Table 2.2 shows the absolute error between the exact solution and various approaches using Jacobi collocation nodes and equidistant collocation points. Figure 2.34 illustrates the exact and approximate solutions using the Jacobi collocation nodes and equidistant collocation points with different values of α and β.

Table 2.2: The absolute errors for Example 2.16.

t	Jacobi collocation			Equidistant collocation		
	$\alpha = 0$ $\beta = 0$	$\alpha = 1/2$ $\beta = 1/2$	$\alpha = -3/4$ $\beta = -1/2$	$\alpha = 0$ $\beta = 0$	$\alpha = 1/2$ $\beta = 1/2$	$\alpha = -3/4$ $\beta = -1/2$
0	$9.58e^{-7}$	$1.95e^{-5}$	$5.32e^{-6}$	$1.76e^{-15}$	$1.76e^{-15}$	$1.76e^{-15}$
0.1	$3.56e^{-6}$	$4.82e^{-6}$	$6.15e^{-6}$	$1.37e^{-5}$	$8.53e^{-6}$	$6.21e^{-6}$
0.2	$3.93e^{-6}$	$9.67e^{-6}$	$1.08e^{-6}$	$1.97e^{-5}$	$1.98e^{-7}$	$9.23e^{-7}$
0.3	$5.83e^{-6}$	$1.85e^{-5}$	$1.00e^{-5}$	$9.01e^{-6}$	$6.79e^{-6}$	$8.83e^{-6}$
0.4	$2.07e^{-5}$	$9.46e^{-6}$	$1.08e^{-5}$	$9.00e^{-6}$	$7.69e^{-6}$	$1.08e^{-5}$
0.5	$3.00e^{-5}$	$1.08e^{-5}$	$2.40e^{-6}$	$2.49e^{-5}$	$6.04e^{-6}$	$1.18e^{-5}$
0.6	$2.65e^{-5}$	$2.12e^{-5}$	$1.15e^{-5}$	$2.61e^{-5}$	$4.80e^{-6}$	$1.49e^{-5}$
0.7	$7.24e^{-6}$	$1.17e^{-5}$	$2.33e^{-5}$	$1.13e^{-5}$	$7.67e^{-6}$	$2.05e^{-5}$
0.8	$1.61e^{-5}$	$1.23e^{-5}$	$4.67e^{-5}$	$7.96e^{-6}$	$1.54e^{-5}$	$1.74e^{-5}$
0.9	$1.02e^{-5}$	$1.20e^{-5}$	$6.94e^{-6}$	$2.83e^{-6}$	$1.63e^{-5}$	$2.12e^{-5}$
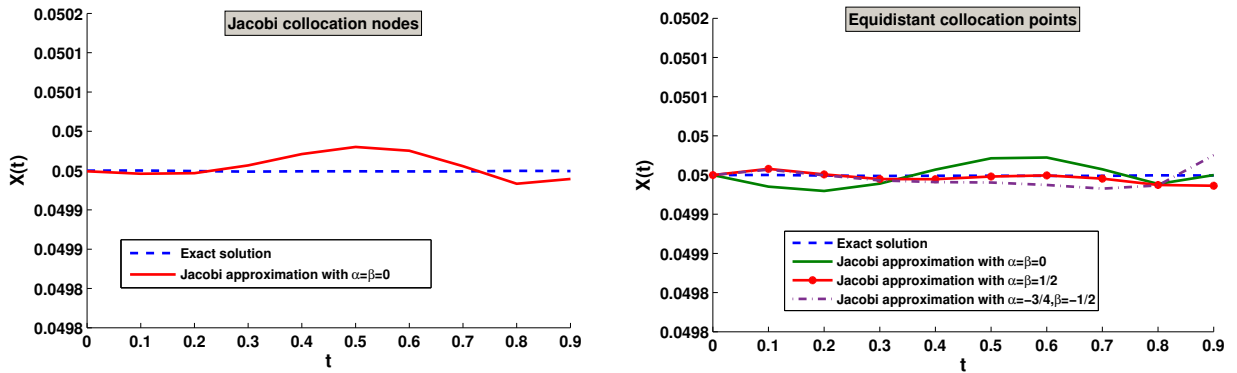
Figure 2.34: Exact solution compared with different Jacobi approaches using equidistant collocation points and Jacobi collocation nodes for Example 2.16.

Example 2.17 *[66] Let's given the nonlinear SIVIE*

$$X(t) = \frac{1}{8} - 0.015625 \int_0^t X(s)(1 - X^2(s))ds + 0.125 \int_0^t (1 - X^2(s))d\mathcal{B}(s), \quad 0 \le t \le 1,$$

with the exact solution

$$X(t) = \frac{\frac{9}{8}e^{0.25\mathcal{B}(t)} - \frac{7}{8}}{\frac{9}{8}e^{0.125\mathcal{B}(t)} + \frac{7}{8}}. \tag{2.106}$$

Table 2.3 represents the absolute error using the proposed technique with Jacobi collocation nodes and equidistant points respectively for $n_1 = 10$, $n_2 = 100$, $K = 20$ and $M = 8$. Figure 2.35 illustrates the exact and approximate solutions using the Jacobi collocation nodes and equidistant collocation points with different values of α and β.
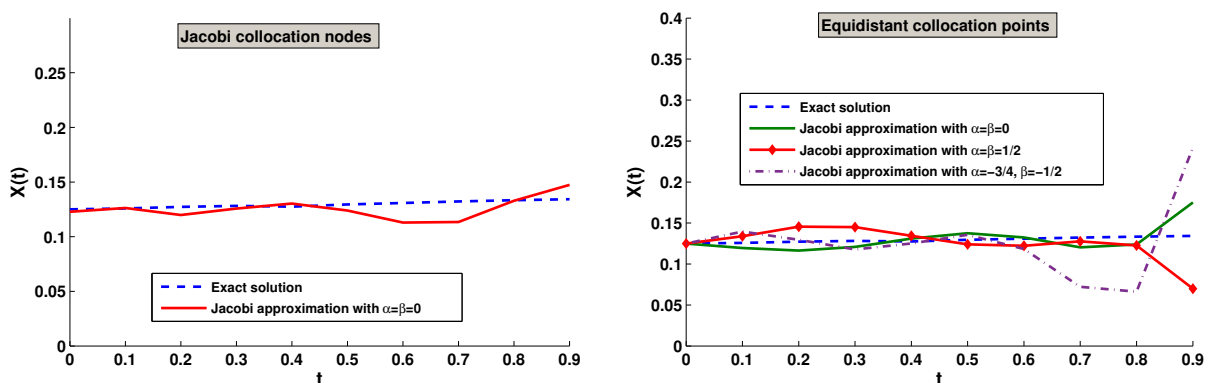
Figure 2.35: Exact solution compared to various Jacobi approaches using equidistant collocation points and Jacobi collocation nodes for Example 2.17.

Table 2.3: The absolute errors for Example 2.17.

	Jacobi collocation			Equidistant collocation		
t	$\alpha = 0$ $\beta = 0$	$\alpha = 1/2$ $\beta = 1/2$	$\alpha = -3/4$ $\beta = -1/2$	$\alpha = 0$ $\beta = 0$	$\alpha = 1/2$ $\beta = 1/2$	$\alpha = -3/4$ $\beta = -1/2$
0	$2.18e^{-3}$	$6.69e^{-3}$	$9.22e^{-3}$	$6.88e^{-41}$	$6.88e^{-41}$	$4.59e^{-41}$
0.1	$9.97e^{-4}$	$6.55e^{-3}$	$3.17e^{-3}$	$6.92e^{-3}$	$9.10e^{-3}$	$1.61e^{-2}$
0.2	$5.60e^{-3}$	$1.27e^{-2}$	$8.92e^{-3}$	$1.06e^{-2}$	$1.95e^{-2}$	$5.89e^{-3}$
0.3	$1.08e^{-3}$	$3.65e^{-3}$	$1.83e^{-2}$	$7.54e^{-3}$	$2.00e^{-2}$	$7.41e^{-3}$
0.4	$2.45e^{-3}$	$5.76e^{-3}$	$1.25e^{-2}$	$2.53e^{-3}$	$1.04e^{-2}$	$1.54e^{-3}$
0.5	$6.13e^{-3}$	$1.83e^{-2}$	$3.37e^{-3}$	$7.68e^{-3}$	$1.12e^{-3}$	$7.31e^{-3}$
0.6	$1.79e^{-2}$	$2.48e^{-2}$	$3.36e^{-3}$	$2.03e^{-3}$	$3.38e^{-3}$	$9.10e^{-3}$
0.7	$1.80e^{-2}$	$1.55e^{-2}$	$1.80e^{-2}$	$1.14e^{-2}$	$3.23e^{-4}$	$5.45e^{-2}$
0.8	$2.58e^{-3}$	$7.64e^{-3}$	$2.70e^{-2}$	$8.79e^{-3}$	$5.98e^{-3}$	$6.18e^{-2}$
0.9	$1.62e^{-2}$	$2.21e^{-2}$	$3.41e^{-3}$	$4.12e^{-2}$	$6.05e^{-2}$	$1.14e^{-1}$

Example 2.18 *Consider the problem*

$$X(t) = X_0 + \int_0^t e^s ds + \int_0^t d\mathcal{B}(s), \quad 0 \le t \le 4, \tag{2.107}$$

the exact solution is given by

$$X(t) = e^t - 1 + \mathcal{B}(t), \tag{2.108}$$

where $X_0 = 0$. Figure 2.36 illustrates the exact and approximate solutions using strong Euler scheme for $\Delta_i = 4/1000$, and 100 simulations. The Jacobi approximation and exact solutions with the absolute error when $M = 5, T = 4, n_1 = 10$ and $n_2 = 100$, are presented in Figures 2.37 and 2.38 with 50 trajectories, and when $M = 7, T = 4, n_1 = 10$ and $n_2 = 100$, are presented in Figures 2.39 and 2.40 with 50 trajectories. Table 2.4 represents different approaches of $X(t)$ using Jacobi approximation for $M = 7, T = 4, n_1 = 10$ and $n_2 = 100$, with 50 trajectories, and using strong Euler scheme for $\Delta = 4/10$ with 100 simulations. We conclude from this example that discretization step size also plays an important role when comparing Taylor approximations and spectral techniques.
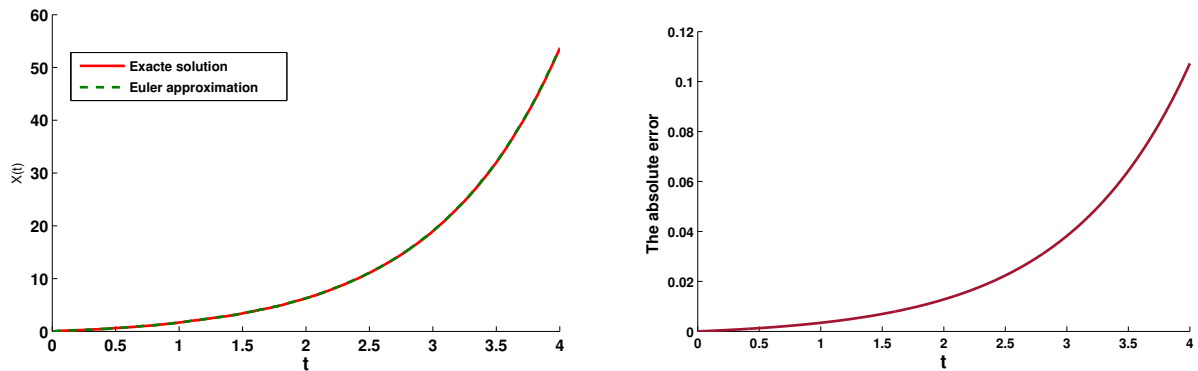
Figure 2.36: Exact solution compared with Euler approximation with the absolute error for Example 2.18.

Table 2.4: Different approximations of $X(t)$ for Example 2.18.

| t | Exact solution | Jacobi approximation | | Euler |
| | | $\alpha = 0$ | $\alpha = -3/4$ | |
		$\beta = 0$	$\beta = -1/2$	approximation
0	0	-0.0659	-0.0523	0
0.4	0.4794	0.5523	0.5472	0.5805
0.8	1.2434	1.3508	1.2646	1.4232
1.2	2.4308	2.5397	2.3091	2.7243
1.6	4.1410	4.1512	3.9078	4.6795
2.0	6.5239	6.3562	6.3223	7.6171
2.4	10.1469	9.6459	9.9084	11.9583
2.8	15.4318	14.880	15.2198	18.4789
3.2	23.6028	23.2037	23.1550	28.2787
3.6	35.6711	35.8231	35.1489	43.0029
4	53.5978	53.6575	53.4067	64.8241
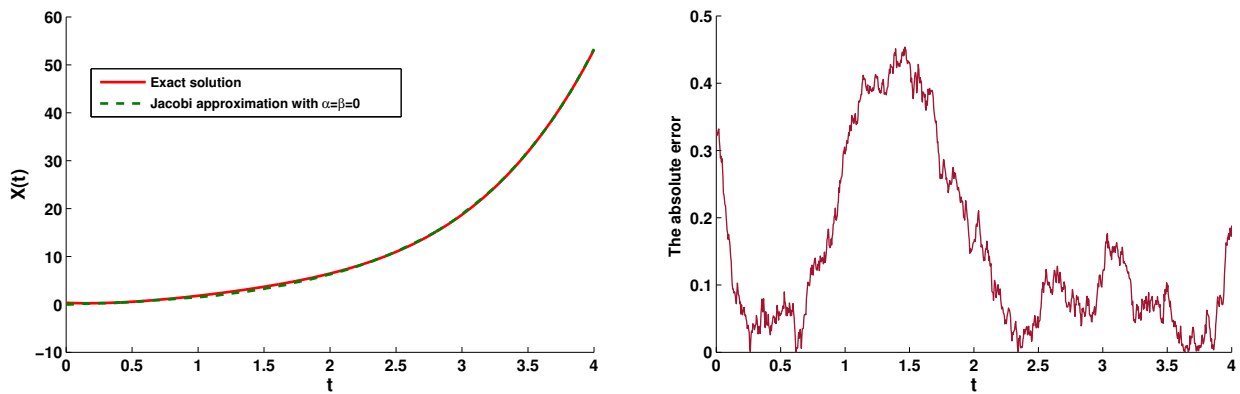
Figure 2.37: Exact solution, Jacobi approximation with the absolute error for $M = 5$ for Example 2.18.
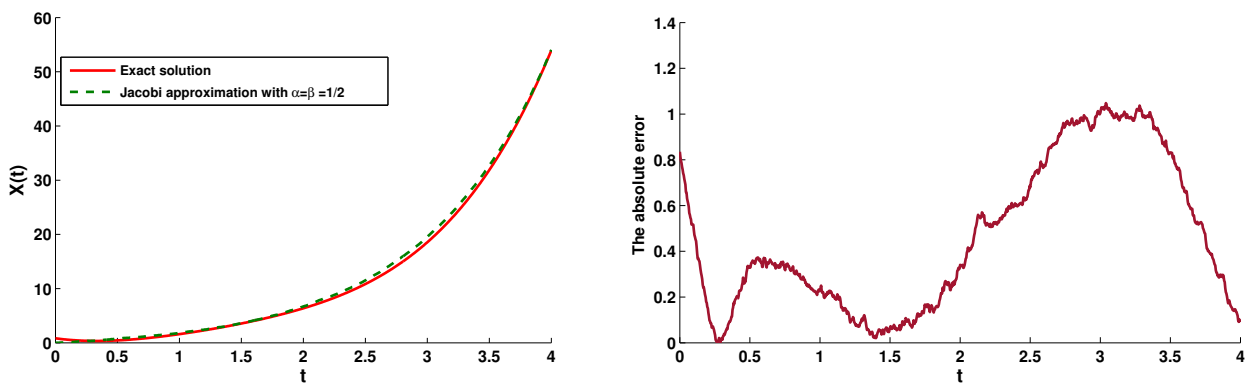
Figure 2.38: Exact solution, Jacobi approximation with the absolute error for $M = 5$ for Example 2.18.
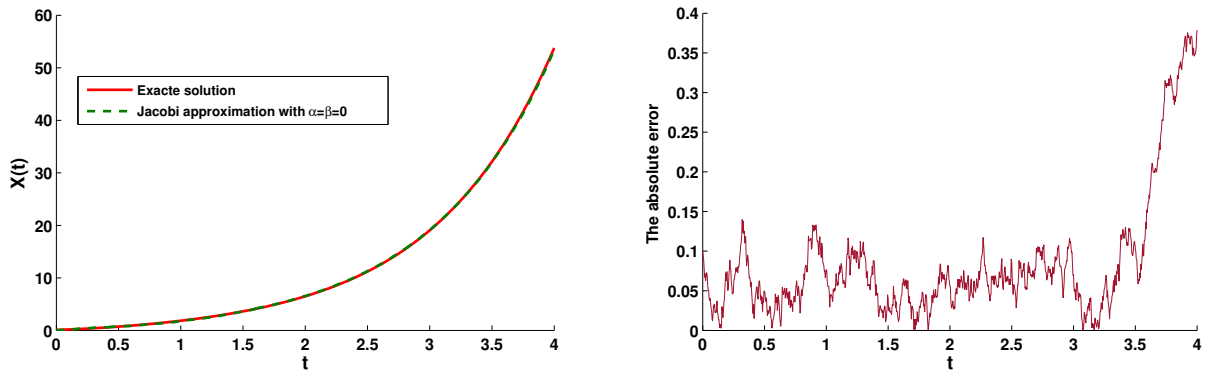
Figure 2.39: Exact solution, Jacobi approximation with the absolute error for $M = 7$ for Example 2.18.
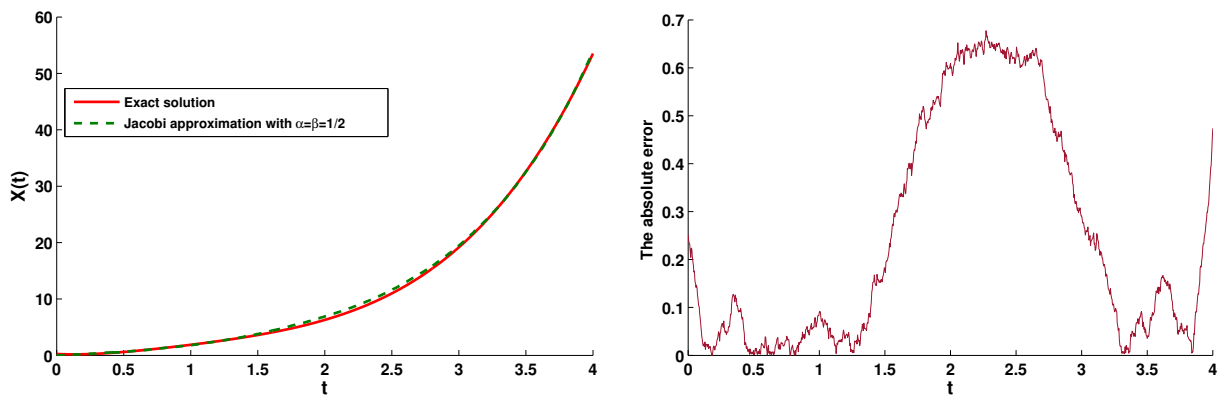
Figure 2.40: Exact solution, Jacobi approximation ($M = 7$) for Example 2.18.

2.6   Polynomial interpolation for solving nonlinear stochastic integral equations

This section is the subject of our work which have been published [23]. The new method represents an accurate approach based on the Jacobi-Gauss collocation method and Lagrange basis. It's proposed for solving a class of nonlinear stochastic Itô-Volterra integral equation Eq.(2.96). This technique effectively transforms the considered problem into system of algebraic equations. The resulting algebraic system is solved by Newton's method to construct approximate solution of the stochastic Volterra integral equation. The theoretical study and convergence analysis of this technique are detailed in [23].

2.6.1   Stability analysis

In this subsection, we discuss the stability of the presented technique.

Theorem 2.4 *Let $X_M \in \mathcal{P}_{M-1}$ be the approximate solution given by the proposed method. Assume that $\bar{X}$ and $\bar{p}$ are the errors of X_M and p ($\bar{p}$ is a small perturbation of p).Then, we have*

$$\|\bar{X}\|_{L^2(0,T)}^2 \leq C \max_{t\in[0,T]} E|\bar{p}(t)|^2, \tag{2.109}$$

where C is a constant and $\mathcal{P}_{M-1}$ is the space of polynomials of degree at least $M-1$.

Proof. We have

$$(X_M + \bar{X})(t) = (p_M + \bar{p})(t) + \int_0^t W_1(t,s)\psi_1((X_M + \bar{X})(s))ds$$
$$+ \int_0^t W_2(t,s)\psi_2((X_M + \bar{X})(s))d\mathcal{B}(s), \tag{2.110}$$

where

$$X_M(t) = p_M(t) + \int_0^t W_1(t,s)\psi_1(X_M(s))ds$$
$$+ \int_0^t W_2(t,s)\psi_2(X_M(s))d\mathcal{B}(s). \tag{2.111}$$

Subtracting equation (2.111) from (2.110), yields

$$\bar{X}(t) = \bar{p}(t) + \int_0^t W_1(t,s)(-\psi_1(X_M(s)) + \psi_1((X_M + \bar{X})(s)))ds$$
$$+ \int_0^t W_2(t,s)(-\psi_2(X_M(s)) + \psi_2((X_M + \bar{X})(s)))d\mathcal{B}(s).$$

Then

$$E|\bar{X}(t)|^2 = E\left|\bar{p}(t) + \int_0^t W_1(t,s)(-\psi_1(X_M(s)) + \psi_1((X_M + \bar{X})(s)))ds\right.$$
$$\left. + \int_0^t W_2(t,s)(-\psi_2(X_M(s)) + \psi_2((X_M + \bar{X})(s)))d\mathcal{B}(s)\right|^2.$$

By using Itô isometry, Holder's inequality and Lipschitz conditions, we obtain

$$E|\bar{X}(t)|^2 \le 2\max_{t\in[0,T]} E|\bar{p}(t)|^2 + 4TE\int_0^t |W_1(t,s)|^2|-\psi_1(X_M(s)) + \psi_1((X_M + \bar{X})(s))|^2 ds$$
$$+ 4E\int_0^t |W_2(t,s)|^2|-\psi_2(X_M(s)) + \psi_2((X_M + \bar{X})(s))|^2 ds$$
$$\le 2\max_{t\in[0,T]} E|\bar{p}(t)|^2 + 4(TM_1^2 L_1^2 + L_2^2 M_2^2)\int_0^t E|\bar{X}(s)|^2 ds$$

Applying Gronwall's lemma

$$E|\bar{X}(t)|^2 \le 2\max_{t\in[0,T]} E|\bar{p}(t)|^2 exp\left(\int_0^t 4(TM_1^2 L_1^2 + L_2^2 M_2^2)ds\right)$$
$$\le 2\max_{t\in[0,T]} E|\bar{p}(t)|^2 exp\left(4T(TM_1^2 L_1^2 + L_2^2 M_2^2)\right)$$

Thus

$$E|\bar{X}(t)|^2 \le C\max_{t\in[0,T]} E|\bar{p}(t)|^2. \tag{2.112}$$

So if $E|\bar{p}(t)|^2 \to 0$, then $E|\bar{X}(t)|^2 \to 0$.   ∎

2.6.2   Numerical tests

This subsection examines the results obtained from the presented method on several test problems by analyzing the absolute errors at specific points for each corresponding test equation.

Example 2.19 *([75]) Consider the linear stochastic integral equation*

$$X(t) = X_0 + \int_0^t \lambda X(s)ds + \int_0^t \mu X(s)d\mathcal{B}(s), \quad 0 \le t \le T, \tag{2.113}$$

where the exact solution is given by

$$X(t) = X_0 e^{(\lambda - \frac{1}{2}\mu^2)t + \mu\mathcal{B}(t)}. \tag{2.114}$$

Setting $\lambda = -5$ and $\mu = 0.1$, we present numerical results for various selections of α, β, and X_0 in Tables 2.5-2.8. The approximate and exact solutions with the absolute errors are shown in Figures 2.41-2.44 for $T = 1$. The approximate, exact solutions and the absolute errors when $T = 120$ are represented in Figure 2.45.

Table 2.5: Different approximations of $X(t)$ for Example 2.19 with $M = 10$, $X_0 = 1$ and $k = 100$.

t	Exact solution	Proposed method			
		$\alpha = 0$ $\beta = 0$	$\alpha = -1/2$ $\beta = -1/2$	$\alpha = -3/4$ $\beta = -3/4$	$\alpha = -3/4$ $\beta = -1/2$
0	1	0.99827149	0.99761262	1.0000186	1.0000352
0.1	0.60470831	0.60589369	0.60284829	0.60819231	0.60506534
0.2	0.36596147	0.36607227	0.36778730	0.36853987	0.36659411
0.3	0.22143201	0.22254742	0.22663707	0.22264968	0.22299320
0.4	0.13412600	0.13525499	0.13417609	0.13432851	0.13536515
0.5	0.08106618	0.08253313	0.07774861	0.08028317	0.08189177
0.6	0.04906421	0.04923210	0.04851151	0.04836471	0.04975954
0.7	0.02967680	0.02858087	0.03202999	0.03011485	0.02970698
0.8	0.01801294	0.01961404	0.01949866	0.01738387	0.01589688
0.9	0.01094107	0.01149224	0.01327339	0.00974494	0.00879000
1	0.00661400	0.01115745	0.00403555	0.01031051	0.01098635

Table 2.6: The absolute errors for Example 2.19 with $X_0 = 1$, $M = 10$ and $k = 100$.

t	The absolute errors			
	$\alpha = 0$ $\beta = 0$	$\alpha = -1/2$ $\beta = -1/2$	$\alpha = -3/4$ $\beta = -3/4$	$\alpha = -3/4$ $\beta = -1/2$
0	$1.72e^{-3}$	$2.38e^{-3}$	$1.86e^{-5}$	$3.52e^{-5}$
0.1	$1.18e^{-3}$	$7.02e^{-3}$	$3.91e^{-4}$	$5.89e^{-3}$
0.2	$1.10e^{-4}$	$3.79e^{-3}$	$1.06e^{-3}$	$4.61e^{-3}$
0.3	$1.11e^{-3}$	$1.05e^{-3}$	$1.93e^{-4}$	$2.23e^{-3}$
0.4	$1.12e^{-3}$	$2.13e^{-3}$	$9.49e^{-4}$	$7.90e^{-4}$
0.5	$1.46e^{-3}$	$5.06e^{-3}$	$2.22e^{-3}$	$4.67e^{-4}$
0.6	$1.67e^{-4}$	$1.76e^{-3}$	$1.44e^{-3}$	$1.71e^{-4}$
0.7	$1.09e^{-3}$	$1.33e^{-3}$	$2.06e^{-4}$	$7.09e^{-4}$
0.8	$1.60e^{-3}$	$9.34e^{-4}$	$9.66e^{-4}$	$2.51e^{-3}$
0.9	$5.51e^{-4}$	$2.02e^{-3}$	$1.39e^{-3}$	$2.41e^{-3}$
1	$4.54e^{-3}$	$2.79e^{-3}$	$3.61e^{-3}$	$4.24e^{-3}$

Table 2.7: The absolute errors for Example 2.19 with $k = 100$, $M = 10$ and $X_0 = 0.1$.

	The absolute errors			
t	$\alpha = 0$ $\beta = 0$	$\alpha = -1/2$ $\beta = -1/2$	$\alpha = -3/4$ $\beta = -3/4$	$\alpha = -3/4$ $\beta = -1/2$
0	$3.59e^{-4}$	$1.32e^{-4}$	$6.96e^{-5}$	$7.97e^{-5}$
0.1	$7.98e^{-5}$	$2.46e^{-4}$	$2.32e^{-4}$	$1.25e^{-4}$
0.2	$7.65e^{-5}$	$9.55e^{-6}$	$8.39e^{-5}$	$1.32e^{-4}$
0.3	$1.35e^{-4}$	$1.001e^{-4}$	$3.56e^{-5}$	$2.63e^{-5}$
0.4	$1.33e^{-4}$	$2.36e^{-4}$	$7.27e^{-5}$	$4.01e^{-5}$
0.5	$3.17e^{-4}$	$2.22e^{-5}$	$2.10e^{-5}$	$5.80e^{-6}$
0.6	$7.69e^{-5}$	$1.46e^{-4}$	$2.29e^{-4}$	$1.78e^{-4}$
0.7	$7.48e^{-4}$	$7.64e^{-5}$	$2.77e^{-4}$	$4.11e^{-4}$
0.8	$1.53e^{-4}$	$1.20e^{-4}$	$7.55e^{-5}$	$1.59e^{-4}$
0.9	$3.94e^{-4}$	$6.05e^{-5}$	$1.51e^{-5}$	$5.88e^{-5}$
1	$7.67e^{-4}$	$3.62e^{-4}$	$2.05e^{-4}$	$1.15e^{-4}$

Table 2.8: Different approximations of $X(t)$ for Example 2.19 with $X_0 = 0.1$, $M = 10$ and $k = 100$.

		Proposed method			
t	Exact solution	$\alpha = 0$ $\beta = 0$	$\alpha = -1/2$ $\beta = -1/2$	$\alpha = -3/4$ $\beta = -3/4$	$\alpha = -3/4$ $\beta = -1/2$
0	0.1	0.09964079	0.09986706	0.09993033	0.1000797
0.1	0.06044081	0.06036095	0.06066866	0.06082283	0.06078242
0.2	0.03664619	0.03672270	0.03677857	0.03674590	0.03702819
0.3	0.02225387	0.02238897	0.02218875	0.02225417	0.02245091
0.4	0.01351795	0.01365142	0.01329326	0.01356650	0.01358980
0.5	0.00822152	0.00853867	0.00817031	0.00816948	0.00824011
0.6	0.00499715	0.00492020	0.00511675	0.00474086	0.00478733
0.7	0.00301418	0.00226604	0.00308080	0.00274527	0.00260362
0.8	0.00182879	0.00167512	0.00194699	0.00175340	0.00166763
0.9	0.00111184	0.00150676	0.00117032	0.00109513	0.00105019
1	0.00067189	0.00143971	0.00103574	0.00087669	0.00078894
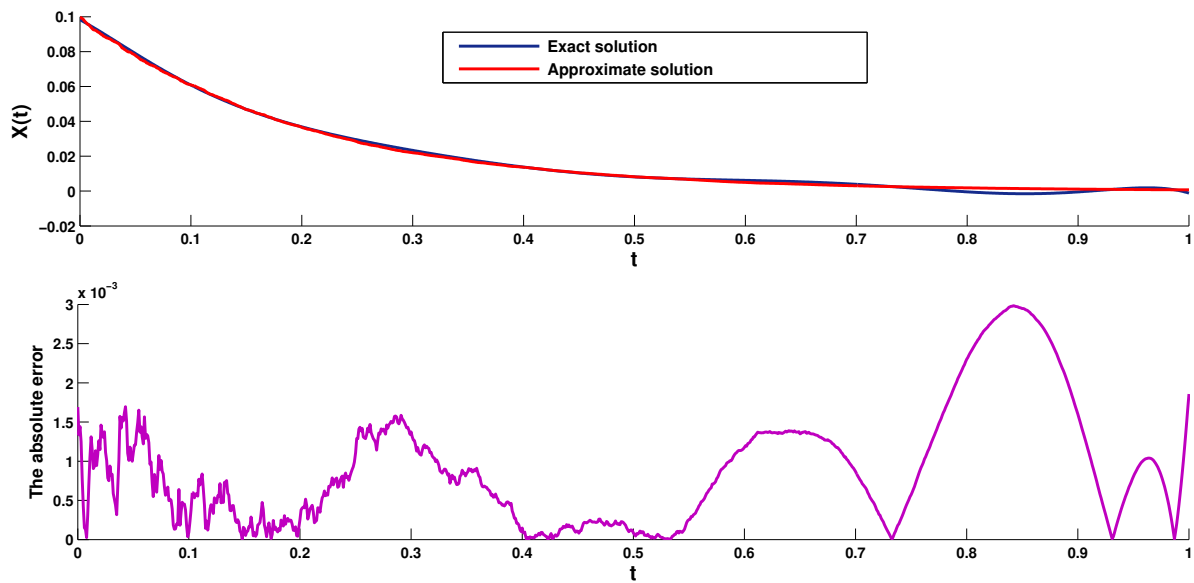
Figure 2.41: The exact and approximate solutions with the absolute error for $M = 10$, $\alpha = \beta = 0$ and $X_0 = 0.1$ for Example 2.19.
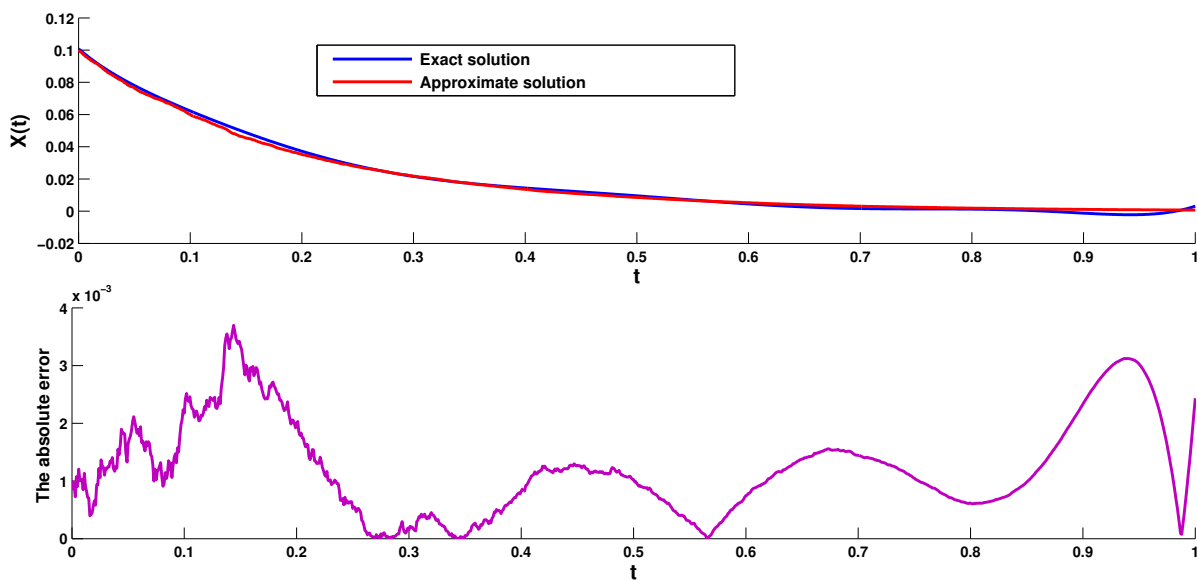
Figure 2.42: The exact and approximate solutions with the absolute error for $M = 10$, $\alpha = \beta = -1/2$ and $X_0 = 0.1$ for Example 2.19.
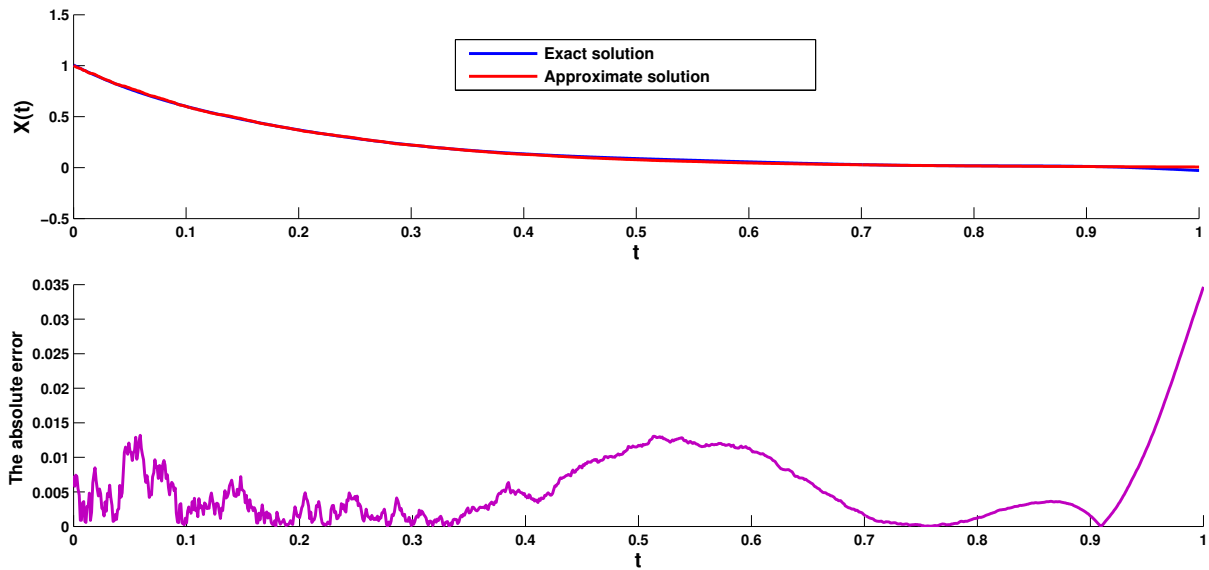
Figure 2.43: The exact and approximate solutions with the absolute error for $M = 10$, $\alpha = \beta = -3/4$ and $X_0 = 1$ for Example 2.19.
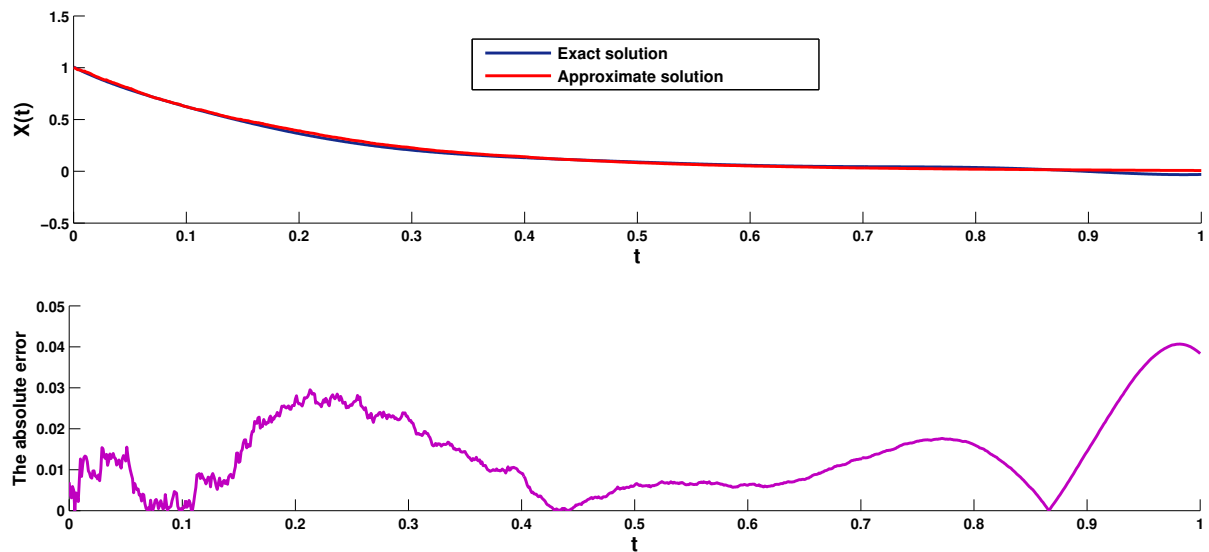
Figure 2.44: The exact and approximate solutions with the absolute error for $M = 10$, $\alpha = -3/4, \beta = -1/2$ and $X_0 = 1$ for Example 2.19.
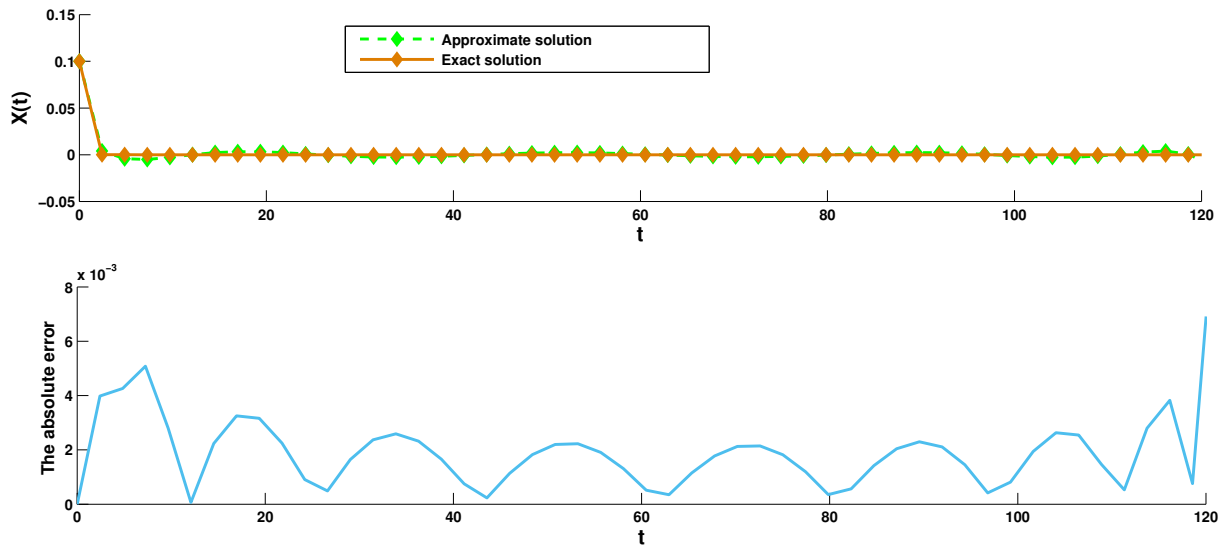
Figure 2.45: The exact and approximate solutions with the absolute error for $M = 10$, $\alpha = -3/4$, $\beta = -1/2$ and $X_0 = 0.1$ for Example 2.19.
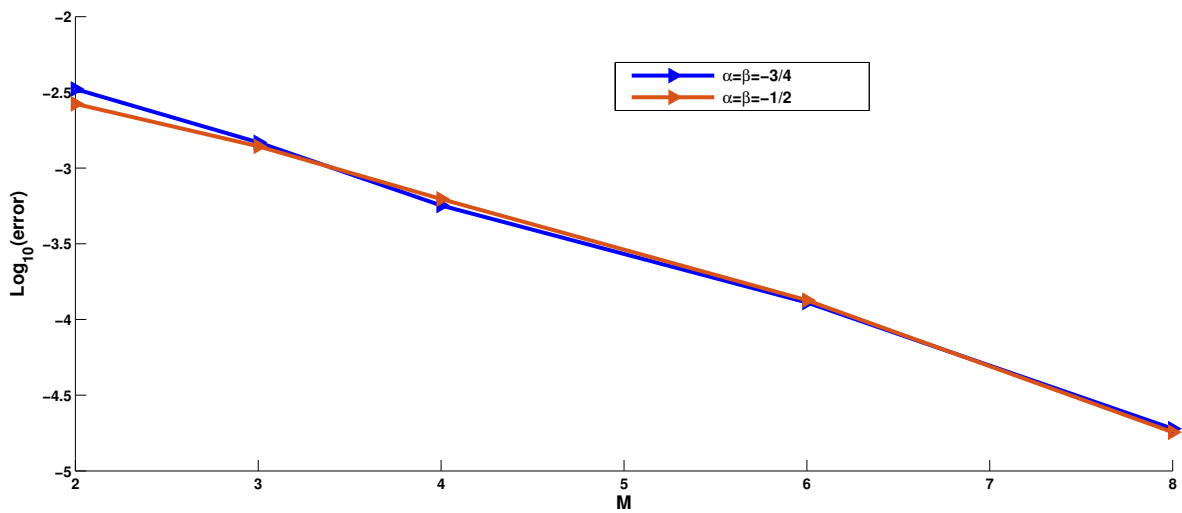
Figure 2.46: The maximum errors for $\alpha = \beta = -3/4$, $\alpha = \beta = -1/2$ and $X_0 = 0.1$ for Example 2.19.

Example 2.20 *Let take the following problem [92]*

$$X(t) = \frac{1}{20} + \int_0^t (\frac{1}{100}X(s) + \frac{1}{32}X^2(s))ds + \frac{1}{8}\int_0^t X(s)d\mathcal{B}(s), \quad 0 \le t \le T.$$

The exact solution is defined as

$$X(t) = \frac{\exp\left((\frac{1}{100} - \frac{(1/8)^2}{2})t + \frac{1}{8}\mathcal{B}(t)\right)}{20 - \frac{1}{32}\int_0^t \exp\left((\frac{1}{100} - \frac{(1/8)^2}{2})s + \frac{1}{8}\mathcal{B}(s)\right)ds}. \tag{2.115}$$

Table 2.9: Different approximations of $X(t)$ for Example 2.20 with $M = 6$.

		k=2 and M=3	Our method	
t	Exact	[121]	$\alpha = 0$	$\alpha = -3/4$
	solution		$\beta = 0$	$\beta = -3/4$
0	0.0500	0.0556	0.0501	0.0498
0.1	0.0464	0.0526	0.0524	0.0517
0.2	0.0509	0.0530	0.0524	0.0525
0.3	0.524	0.0518	0.0517	0.0532
0.4	0.0508	0.0490	0.0511	0.0538
0.5	0.0540	0.0469	0.0506	0.0541
0.6	0.0561	0.0498	0.0498	0.0538
0.7	0.0473	0.0488	0.0485	0.0530
0.8	0.0454	0.0478	0.0469	0.0520
0.9	0.0503	0.0429	0.0460	0.0523

Table 2.9 summarizes the numerical results of approximate and exact solutions for $M = 6$. Table 2.10 presents a comparison of the absolute error for $M = 6$ between the proposed method and the method detailed in [121]. For $M = 6$ and $T = 1$, the exact and approximate solutions along with their absolute errors are illustated in Figure 2.47. Figure 2.48 shows the approximate and exact solutions with the absolute errors when $T = 15$.

Example 2.21 *We examine the nonlinear SIVIE [66]*

$$X(t) = X_0 - a^2 \int_0^t X(s)(1 - X^2(s))ds + a \int_0^t (1 - X^2(s))d\mathcal{B}(s), \quad 0 \le t \le T, \tag{2.116}$$

where the analytical solution is given by

$$X(t) = \tanh(a\mathcal{B}(t) + \arctan(X_0)). \tag{2.117}$$
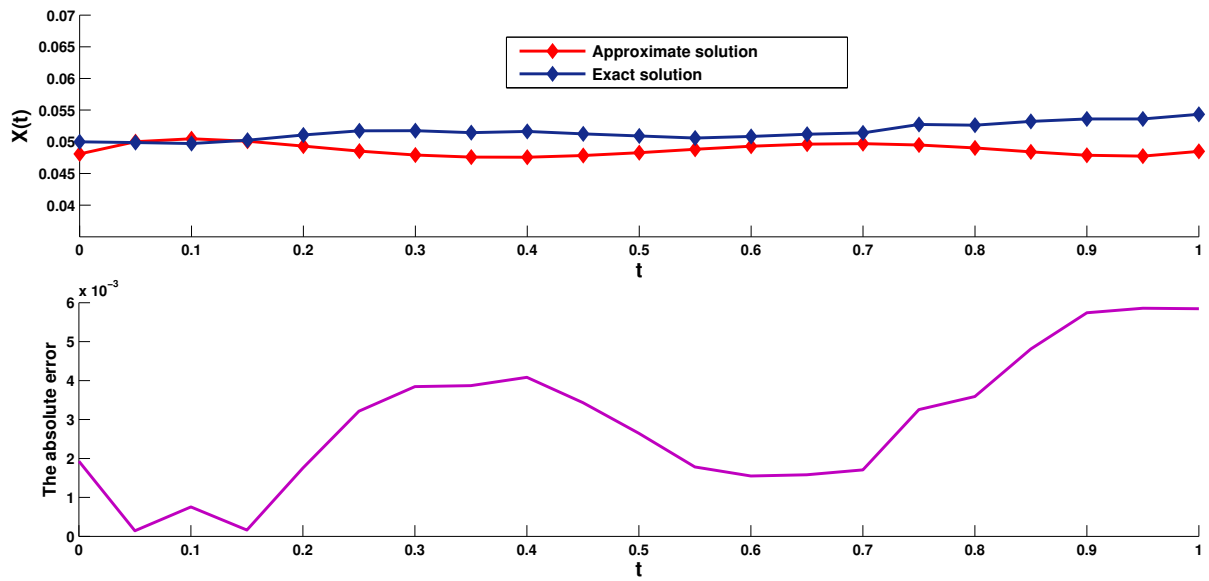
Figure 2.47: The exact and approximate solutions with the absolute error for $M = 6$ and $\alpha = \beta = -3/4$ for Example 2.20.
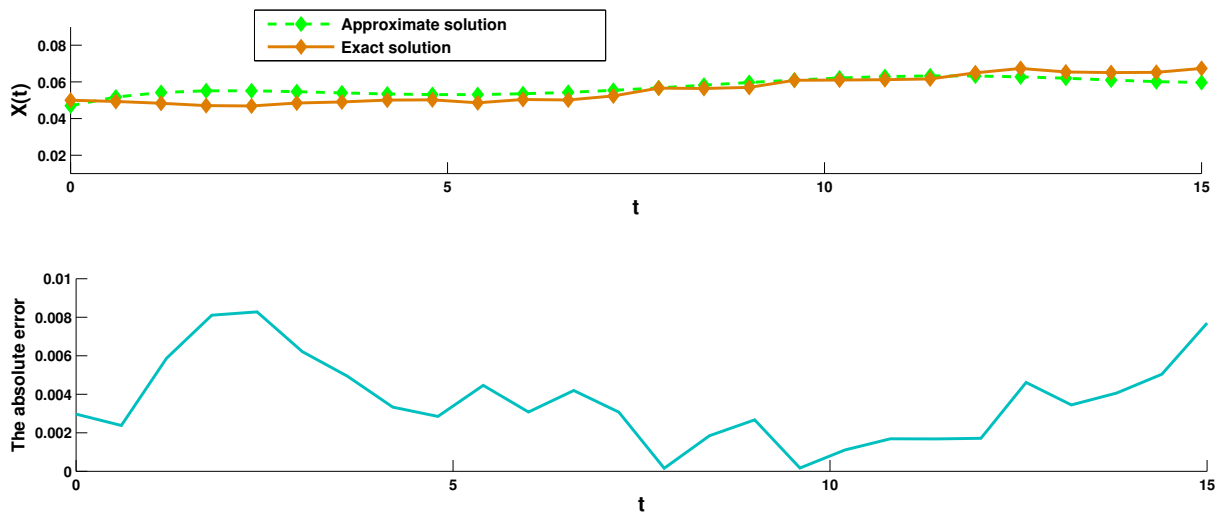
Figure 2.48: The exact and approximate solutions with the absolute error for $M = 6$, $\alpha = \beta = 0$ for Example 2.20.

Table 2.10: Absolute errors comparison for Example 2.20.

t	Error [121]	Error of our method	
		$\alpha = 0$ $\beta = 0$	$\alpha = -3/4$ $\beta = -3/4$
0	$5.58e^{-3}$	$1.17e^{-4}$	$7.08e^{-4}$
0.1	$6.19e^{-3}$	$4.55e^{-3}$	$6.04e^{-3}$
0.2	$2.09e^{-3}$	$1.19e^{-3}$	$1.48e^{-3}$
0.3	$5.67e^{-4}$	$1.49e^{-4}$	$7.00e^{-3}$
0.4	$1.79e^{-3}$	$3.27e^{-4}$	$2.95e^{-3}$
0.5	$7.14e^{-3}$	$2.01e^{-3}$	$3.43e^{-3}$
0.6	$1.03e^{-2}$	$9.49e^{-3}$	$6.32e^{-3}$
0.7	$1.48e^{-3}$	$3.26e^{-3}$	$1.18e^{-3}$
0.8	$2.47e^{-3}$	$3.66e^{-3}$	$1.47e^{-3}$
0.9	$7.35e^{-3}$	$8.08e^{-3}$	$4.33e^{-3}$

Consider $a = \frac{1}{30}$ and $X_0 = \frac{1}{10}$, for $M = 6$ and $M = 10$, the numerical results are presented in Tables 2.11 and 2.12 with 10^2 sample paths. The exact and approximate solutions with the absolute error when $M = 10$ and $T = 1$ are shown in Figures 2.49 and 2.50 with 10 sample paths. Figure 2.51 illustrates the approximate and exact solutions with the absolute errors when $T = 30$. The absolute error of the proposed method in the case $M = 10, \alpha = -3/4, \beta = -1/2$, compared with the Floater-Hormann method [84] is represented in Table 2.13.

Table 2.11: Different approximations of $X(t)$ for Example 2.21.

t	Exact solution	Proposed method for $M=6$		Proposed method for $M=10$	
		$\alpha = -1/2$ $\beta = -1/2$	$\alpha = -3/4$ $\beta = -3/4$	$\alpha = -3/4$ $\beta = -1/2$	$\alpha = -1/2$ $\beta = -1/2$
0	0.1	0.09990	0.10015	0.09998	0.09997
0.1	0.09939	0.10025	0.09755	0.10070	0.10048
0.2	0.09995	0.10056	0.09808	0.09933	0.10012
0.3	0.09832	0.10073	0.09898	0.09785	0.10017
0.4	0.09771	0.10072	0.09902	0.09849	0.10059
0.5	0.09911	0.10053	0.09812	0.09843	0.10124
0.6	0.10190	0.10024	0.09680	0.09748	0.10135
0.7	0.10205	0.09991	0.09581	0.09781	0.10077
0.8	0.10146	0.09967	0.09559	0.09931	0.10020
0.9	0.10184	0.09964	0.09584	0.09988	0.099010
1	0.10021	0.09997	0.09508	0.09912	0.09837

Table 2.12: The absolute errors for Example 2.21.

t	M=6		M=10	
	$\alpha = -1/2$ $\beta = -1/2$	$\alpha = -3/4$ $\beta = -3/4$	$\alpha = -3/4$ $\beta = -1/2$	$\alpha = -1/2$ $\beta = -1/2$
0	$9.80e^{-5}$	$1.57e^{-4}$	$1.23e^{-5}$	$2.60e^{-5}$
0.1	$1.54e^{-3}$	$5.21e^{-4}$	$1.36e^{-3}$	$1.09e^{-3}$
0.2	$5.44e^{-4}$	$2.50e^{-3}$	$7.08e^{-4}$	$1.71e^{-4}$
0.3	$2.58e^{-3}$	$3.38e^{-3}$	$7.83e^{-4}$	$1.84e^{-3}$
0.4	$2.83e^{-3}$	$3.32e^{-3}$	$5.28e^{-4}$	$2.87e^{-3}$
0.5	$2.21e^{-3}$	$2.83e^{-3}$	$1.85e^{-3}$	$2.12e^{-3}$
0.6	$9.29e^{-4}$	$2.007e^{-3}$	$4.05e^{-4}$	$5.54e^{-4}$
0.7	$1.45e^{-3}$	$7.77e^{-4}$	$1.89e^{-3}$	$1.28e^{-3}$
0.8	$1.69e^{-3}$	$7.53e^{-4}$	$3.40e^{-3}$	$1.26e^{-3}$
0.9	$3.01e^{-3}$	$2.33e^{-3}$	$4.94e^{-3}$	$2.83e^{-3}$
1	$2.58e^{-3}$	$1.44e^{-3}$	$3.93e^{-3}$	$1.83e^{-3}$
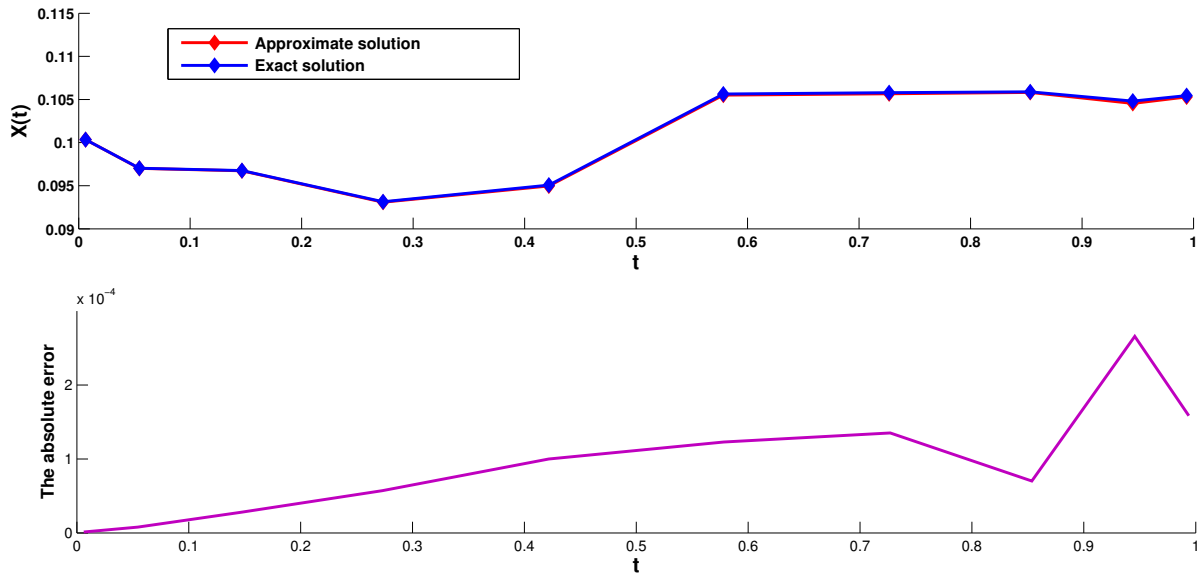
Figure 2.49: The exact and approximate solutions with the absolute error for $M = 10$ and $\alpha = \beta = -1/2$ for Example 2.21.

Table 2.13: Absolute errors comparaison of Example 2.21 for $k = 100$.

	Proposed method	Floater-Hormann method [84]
t	$M = 10, \alpha = -3/4, \beta = -1/2$	$M = 4, n = 21$
	Absolute error	error [84]
0	$1.23e^{-5}$	$4.62e^{-18}$
0.1	$1.36e^{-3}$	$3.29e^{-3}$
0.2	$7.08e^{-4}$	$3.71e^{-3}$
0.3	$7.83e^{-4}$	$5.42e^{-3}$
0.4	$5.28e^{-4}$	$5.57e^{-3}$
0.5	$1.85e^{-3}$	$7.14e^{-3}$
0.6	$4.05e^{-4}$	$7.70e^{-3}$
0.7	$1.89e^{-3}$	$7.24e^{-3}$
0.8	$3.40e^{-3}$	$8.03e^{-3}$
0.9	$4.94e^{-3}$	$7.67e^{-3}$
1	$3.93e^{-3}$	$7.94e^{-3}$
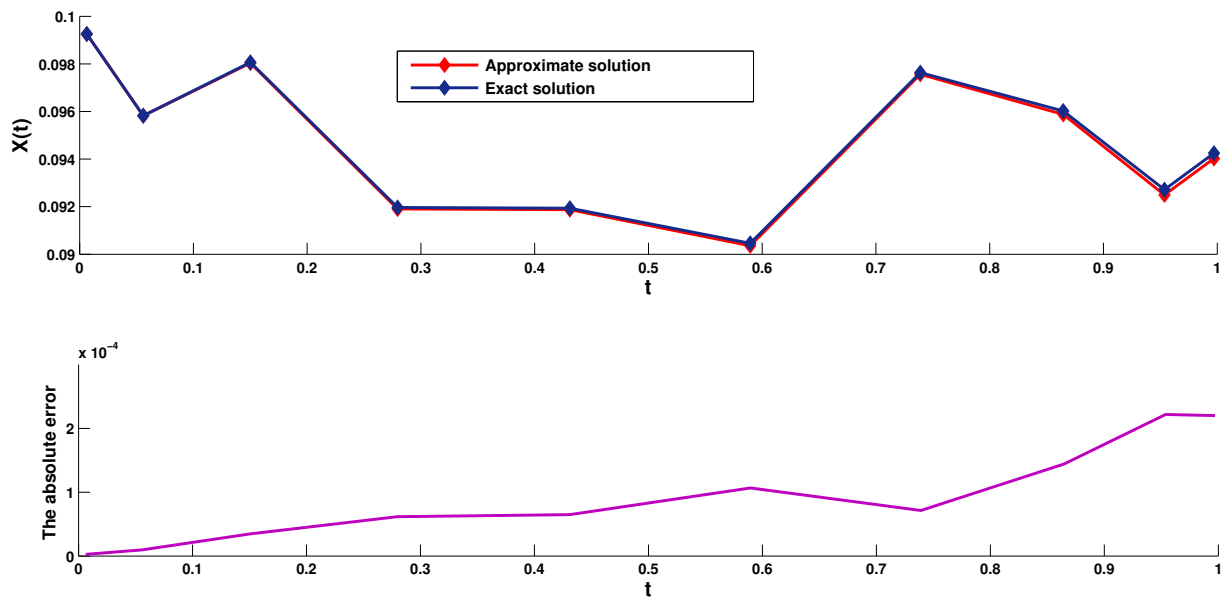
Figure 2.50: The exact and approximate solutions with the absolute error for $M = 10$, $\alpha = -3/4$ and $\beta = -1/2$ for Example 2.21.
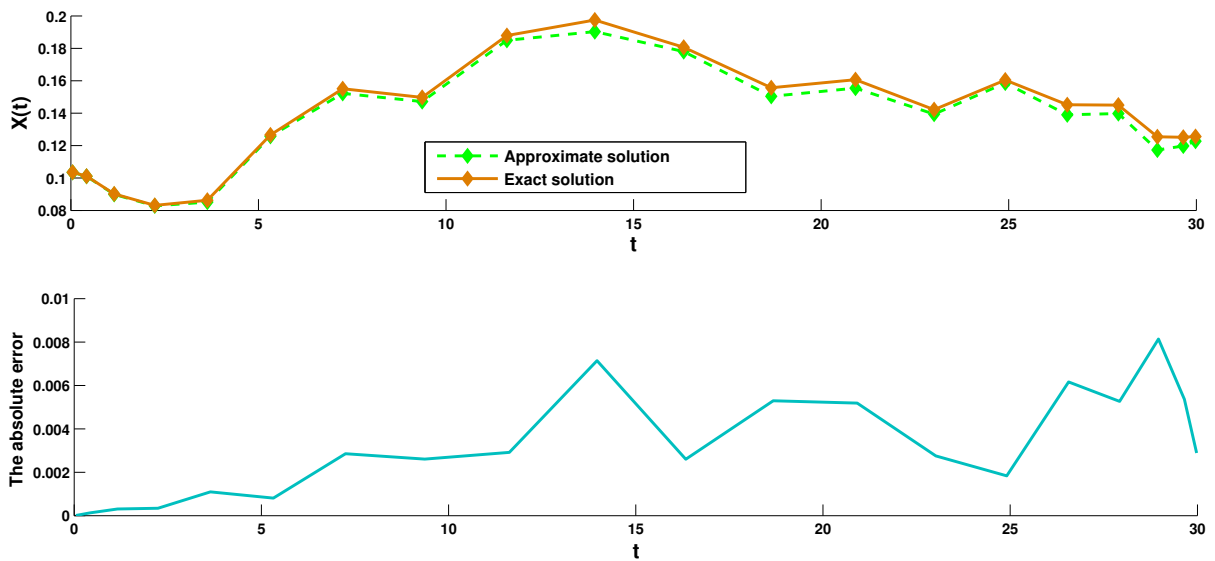
Figure 2.51: The exact and approximate solutions with the absolute error for $M = 20$, $\alpha = -3/4, \beta = -1/2$ for Example 2.21.

2.6.3   Analysis of numerical tests

In this work we have proposed an accurate spectral technique based on Lagrange polynomials and the Gauss-Jacobi collocation method for solving a class of nonlinear stochastic Volterra integral equations. This method offers several advantages, including simplicity and high accuracy achieved by varying the parameters α and β. The numerical results demonstrate that the solutions obtained through the Lagrange Jacobi-Gauss collocation method agree well with the exact solutions.

Among existing numerical methods, pseudo-spectral or collocation methods are highly effective, particularly for problems with smooth solutions. They yield precise approximations with minimal computational memory requirements. Notably, the optimal selection of interpolation points, such as Chebyshev polynomials, renders collocation methods equivalent to the Galerkin method when combined with Gaussian integration for evaluating inner products.

Furthermore, we perform convergence and error analysis for the proposed method and confirm its efficiency and a reasonable degree of accuracy through various numerical examples [23]. The advantages of our approach are manifold:

- Rapid computation, significant accuracy, and reliable convergence.

- The exponential convergence rate facilitated by the collocation approach ensures highly precise solutions.

- Transformation of the original problem into a system of linear or nonlinear algebraic equations via collocation.

- Superior accuracy compared to various existing methods.

- Attainment of well-conditioned solutions using of quadrature formulas based on Gauss-Legendre and Itô integration rules.

- Jacobi-collocation methods with Lagrange interpolation offer operational simplicity and a wide range of node choices, including Chebyshev, Legendre, etc.

- Accuracy can be enhanced with sufficiently large time intervals.

- Equidistant points are unsuitable for Lagrange interpolation; instead, Gauss quadrature nodes yield better results.

- The presented method efficiently generates accurate results using a small number of basis functions and nodal points.

3

A new accurate method to solve nonlinear stochastic Itô–Volterra integral equations

3.1 Introduction

Numerous real-world phenomena find description through stochastic integral equations (SIEs), with an increasing demand for these equations across diverse fields such as biology, chemistry, engineering, medicine, physics, social sciences, finance, economics, and mechanics, enabling the examination of complex dynamical systems (cf. [25, 37, 39, 116, 105]). Examples of SIEs arise in the stochastic formulation of challenges in reactor dynamics (cf. [27, 71, 80]), the study of biological population growth (cf. [61]), and the theory of automatic systems modeled by delay-differential equations (cf. [97]). The inherent complexity of such phenomena necessitates the use of various SIEs, particularly those dependent on a noise source, such as Gaussian white noise. Modeling these phenomena often involves stochastic differential equations (cf. [2, 28, 29, 62, 61, 63, 66, 75, 76, 98]), and in many intricate cases, stochastic integro-differential equations and stochastic Volterra integral equations (cf. [17, 34, 52, 93, 94, 142, 144, 145]).

This chapter investigates the nonlinear Itô–Volterra SIE given by

$$X(t) = h(t) + \int_0^t \gamma_1(t,s)\mu_1(X(s))ds + \int_0^t \gamma_2(t,s)\mu_2(X(s))d\mathcal{B}(s),\ t \in [0,T], \qquad (3.1)$$

where $X(t), h(t), \gamma_1(t,s)$, and $\gamma_2(t,s)$ for $t,s \in [0,T], T \in \mathbb{R}^+$ are stochastic processes defined on the filtrated probability space $(\Omega, \mathcal{F}, \mathcal{F}_t, P)$, μ_1 and μ_2 are nonlinear functions, $X(t)$ is the

unknown function, and $\mathcal{B}(t)$ is a Wiener process. As these SIEs are often too complex to be solved explicitly for most real-world problems, employing numerical techniques becomes crucial for finding their approximations. Radial basis function (RBF) methods, representing modern techniques for approximating multivariate functions, gain popularity. These methods, with nodes lacking nodal connectivity, become preferable in complex geometries. The interpolation method employing positive definite functions, such as Multiquadric RBFs and Gaussian RBFs, is employed in [89] to get approximate solution of two-dimensional linear SIEs on non-rectangular domains. An iterative method for determining the optimal number of Gaussian neurons and their locations for the RBF neural networks (RBFNN) method, ensuring efficient solving of the Fokker–Planck–Kolmogorov (FPK) equation with high accuracy, is presented in [130]. In [88], Mirzaee et al developed a numerical method based on RBFs to solve fractional stochastic integro-differential equations. More information about learning new approaches in this regard can be found in [85, 118]. Practical experience reveals that the efficacy of the previously mentioned methods in achieving satisfactory approximations is not always guaranteed. This underscores the need for advancing more effective methods, where obtaining a precise approximate solution becomes crucial for gaining valuable insights and a correct comprehension of the studied system's behavior. The challenge of approximating solutions to SIEs has been thoroughly investigated, resulting in various technique to solve both linear and nonlinear SIEs. Examples include spectral methods based on modified hat functions, Euler polynomials, Bernstein method, shifted Jacobi operational matrices, and the Fibonacci operational matrices (cf. [12, 83, 86, 110, 109, 119, 135]). Spectral methods have been widely employed for solving SIEs (cf. [92, 101, 117, 120]), offering global, continuous solutions without the need for constructing a data network. These methods typically utilize orthogonal basis functions to reduce computational costs. In response to this, the present chapter introduces a novel spectral method based on the collocation approach, applicable to the solution of various SIEs. A generalized pseudo-spectral (GPS) technique is presented in [33], it is a generalization of the conventional Lagrangian interpolation. Interpolation operators play a major role in minimizing computational costs in many spectral methods, including Galerkin and Petrov-Galerkin methods. To attain this goal, a specific set of interpolation points is chosen to create Lagrange interpolation functions, ensuring that the residual error function is adjusted to zero at these selected collocation points, coinciding with the roots of Jacobi polynomials. Since determining the degree of the polynomial

poses challenges with equidistant interpolation points, a method for selecting these points is explored. This chapter develops a new truncated interpolation method for solving SIEs by the interpolation techniques based on the combination of the Jacobi collocation nodes and the generalized Lagrange functions with a suitable Gauss-Legendre quadrature. The three significant contributions of this study are as follows:

- **Efficient Pseudospectral Method:** The study provides an efficient pseudospectral method for solving a more general family of nonlinear stochastic Volterra integral equations. Notably, the method extends Lagrange interpolation to weighted L_2 space, employing interpolation points as the zeros of orthogonal polynomials, such as Jacobi polynomials. The interpolation formula exhibits excellent numerical stability, capable of achieving machine-precision approximations for arbitrary smooth functions. The proposed technique is validated by demonstrating its ability to generate accurate approximate solutions for the considered problems.

- **Jacobi–Gauss Collocation Method:** The study introduces the Jacobi–Gauss collocation method for stochastic differential equations, selecting a set of distinct and optimal interpolation points, namely Jacobi Gauss points. This represents a novel contribution to the field, and the accuracy of the proposed method is demonstrated through test problems, showcasing the typical exponential convergence behavior of spectral approximations.

- **Generalized Lagrange Functions:** The study explores various new generalized Lagrange functions suitable for solving different types of stochastic integral equations. These functions enable the transformation of the original problem into linear or nonlinear algebraic systems, enhancing the versatility and applicability of the proposed method.

The new spectral method presented in this chapter addresses the limitations of existing techniques and offers valuable contributions in terms of efficiency, accuracy, and versatility for solving a broader range of stochastic differential and integral equations.

Before delving into the computational method, let's introduce some fundamental definitions.

Generalized Lagrange functions

Generalized Lagrange functions are defined as follows

$$G_j^L(t) = \prod_{i=1,i\neq j}^{M} \frac{L(t) - L(t_i)}{L(t_j) - L(t_i)}, \ 1 \leq j \leq M, \tag{3.2}$$

where $L(t)$ is a smooth function, $t_1 < t_2 < \cdots < t_M$ are the interpolation points and $L(t_j) \neq L(t_i)$ for all $i \neq j$. The Generalized Lagrange functions have the following properties:

- if $\lim_{t\to\infty} L(t) = c < \infty$, then $\lim_{t\to\infty} G_j^L(t) < \infty \ \forall \ 1 \leq j \leq M$;

- $G_j^L(t_i) = \delta_{ij}$ at any point t_i, where δ_{ij} is the Kronecker delta

- $\sum_{j=1}^{M} G_j^L(t) = 1$.

This chapter introduces a collocation spectral method using generalized Lagrange basis functions with Jacobi collocation nodes to tackle the aforementioned problem.

This method proves to be highly adapted, capable of accurately approximating various types of equations (cf. [3, 18, 19, 20, 35, 36, 113, 96]). Hence, instead of developing approximation results for individual pairs of indexes α and β, a systematic investigation into Jacobi collocation points might offer valuable generalizations. It's noteworthy that even with a small selection of collocation points, this method consistently produces remarkable numerical results.

3.2 The new proposed technique

For a nonlinear Itô–Volterra SIE given in (3.1). The proposed technique consists of the following steps, which are illustrated in the flowchart (Figure 1).

- **Step 1:** Collocate Eq.(3.1) at t_i points as follows:

$$X(t_i) = h(t_i) + \underbrace{\int_0^{t_i} \gamma_1(t_i, s)\mu_1(X(s))ds}_{(I)} + \underbrace{\int_0^{t_i} \gamma_2(t_i, s)\mu_2(X(s))d\mathcal{B}(s)}_{(II)}, \tag{3.3}$$

where $t_i, \ 1 \leq i \leq M$ are the roots of the Mth Jacobi's polynomial.

- **Step 2:** Interpolate the state variable using a generalized Lagrange function as follows:

$$X(t) \simeq \widehat{X_M}(t) = \sum_{j=1}^{M} X(t_j) G_j^L(t) = (X(t_1) \; X(t_2) \; ... \; X(t_M)) \begin{pmatrix} G_1^L(t) \\ G_2^L(t) \\ \vdots \\ G_M^L(t) \end{pmatrix} = X'G^L(t).$$

(3.4)

- **Step 3:** Apply the Gauss-Legendre quadrature rule to approximate both integrals (I) and (II) in equation (3.3) as below

  - Approximate the integral (I) in (3.3), we get

$$\int_0^{t_i} \gamma_1(t_i, s)\mu_1(X(s)) ds = \frac{1}{2}t_i \sum_{j=1}^{n_1} A_j \gamma_1 \left(t_i, \frac{1}{2}t_i s_j + \frac{1}{2}t_i\right) \mu_1 \left(X\left(\frac{1}{2}t_i s_j + \frac{1}{2}t_i\right)\right)$$

$$= \frac{1}{2}t_i \sum_{j=1}^{n_1} A_j \gamma_1 \left(t_i, \frac{1}{2}t_i s_j + \frac{1}{2}t_i\right) \mu_1 \left(X'G^L\left(\frac{1}{2}t_i s_j + \frac{1}{2}t_i\right)\right),$$

(3.5)

  where s_j are the Gauss Legendre roots on $[-1, 1]$ and A_j are the weights of Gauss quadrature.

  - Using integration by parts for each $w \in \Omega$, the integral (II) in equation (3.3) yields

$$\int_0^{t_i} \gamma_2(t_i, s)\mu_2(X(s)) d\mathcal{B}(s)$$

$$= [\gamma_2(t_i, s)\mu_2(X(s))\mathcal{B}(s)]_0^{t_i} - \int_0^{t_i} \mathcal{B}(s)\frac{d[\gamma_2(t_i, s)\mu_2(X(s))]}{ds} ds$$

$$= \gamma_2(t_i, t_i)\mu_2(X(t_i))\mathcal{B}(t_i) - \int_0^{t_i} \mathcal{B}(s)\frac{d[\gamma_2(t_i, s)\mu_2(X(s))]}{ds} ds$$

$$= \gamma_2(t_i, t_i)\mu_2(X'G^L(t_i))\mathcal{B}(t_i) - \underbrace{\int_0^{t_i} \mathcal{B}(s)\frac{d[\gamma_2(t_i, s)\mu_2(X'G^L(s))]}{ds} ds}_{(J)}.$$

By using the Gauss-Legendre quadrature to approximate the integral (J), we get

$$\int_0^{t_i} \gamma_2(t_i, s)\mu_2(X(s)) d\mathcal{B}(s) = \gamma_2(t_i, t_i)\mu_2\left(X'G^L(t_i)\right)\mathcal{B}(t_i)$$

$$- \frac{1}{2}t_i \sum_{j=1}^{n_2} \tilde{A}_j \mathcal{B}\left(\frac{1}{2}t_i \tilde{s}_j + \frac{1}{2}t_i\right) \left(\frac{d[\gamma_2(t_i, s)\mu_2(X'G^L(s))]}{ds}\right)\left(\frac{1}{2}t_i \tilde{s}_j + \frac{1}{2}t_i\right).$$

(3.6)

- **Step 4:** Replacing Eqs.(3.4), (3.5) and (3.6) in Eq.(3.3), we obtain the following nonlinear algebraic system

$$
X'G^H(t_i) = h(t_i) + \gamma_2(t_i, t_i)\mu_2(X'G^L(t_i))\mathcal{B}(t_i)
$$
$$
+ \frac{1}{2}t_i \sum_{j=1}^{n_1} A_j \gamma_1 \left(t_i, \frac{1}{2}t_i s_j + \frac{1}{2}t_i \right) \mu_1 \left(X'G^L \left(\frac{1}{2}t_i s_j + \frac{1}{2}t_i \right) \right)
$$
$$
- \frac{1}{2}t_i \sum_{j=1}^{n_2} \tilde{A}_j \mathcal{B} \left(\frac{1}{2}t_i \tilde{s}_j + \frac{1}{2}t_i \right) \left(\frac{d\left[\gamma_2(t_i, s)\mu_2(X'G^L(s)) \right]}{ds} \right) \left(\frac{1}{2}t_i \tilde{s}_j + \frac{1}{2}t_i \right).
$$

$$(3.7)$$

- **Step 5:** Solving the algebraic system (3.7).

- **Step 6:** To obtain the approximate solution of the Itô–Volterra stochastic integral equation, replace the value achieved of X' into Eq. (3.4) as $X(t) \simeq \widehat{X_M}(t) = X'G^L(t)$.

It's important to note that the new proposed technique is totally different from existing works, such as those detailed in [12, 83, 86, 110, 119]. In these approaches, operational matrices for each polynomial are presented, and Newton-Cotes collocation nodes are employed. For instance, in [83], Fibonacci polynomials outperformed techniques utilizing Block pulse functions and Bernstein polynomials. The authors improved upon these results in [86] by incorporating Euler polynomials. More recently, Sharafi et al. [119] introduced an algorithm based on hat functions, demonstrating superior performance when the step size h is sufficiently small, this results in an increase in m (the number of basis approximations) and large CPU time.

In contrast, Ray et al. [110] utilized Jacobi polynomials with their operational matrix, employing Jacobi nodes and Newton-Cotes as collocation points. The numerical results, as presented in Section 4, of the new proposed approach demonstrate the significant advantage of employing generalized basis functions for solving equations of this type. The main strengths of the new technique lie in its simplicity, reduced CPU time compared to existing methods, and the flexibility of parameter choices for α and β, allowing for optimal selection and achieving optimal approximate solutions.

Input: the interval $[0, T]$, the number of Jacobi points M, the number of simulation k, Jacobi polynomials $\mathcal{J}_M^{\alpha, \beta}(t)$, the parameters α, $\beta \geq -1$, the functions $\gamma_1(t, s)$, $\mu_1(X(s))$, $\gamma_2(t, s)$, $\mu_2(X(s))$ and $h(t)$.

Solve $\mathcal{J}_{T,M}^{(\alpha, \beta)}(t) = 0$ and get the collocation points t_i.

Define the generalized Lagrange function $G^L(t)$ given in (3.2) and use it to approximate the solution X in (3.1).

Collocating the SIE (3.1) at t_i points.

Get equation (3.3).

Approximate each integrals (I) and (II) in (3.3).

Get the algebraic system given in (3.7).

Extract the algebraic system (3.7) and solve it.

Replace the value achieved for X' into (3.4) to get the final new approximate solution.

Figure 3.1: The new proposed technique for solving SIEs.

3.3 The convergence of our technique

The theorem below outlines the sufficient conditions under which the estimation error converges to zero.

Theorem 3.1 *Suppose that $X(t)$ is the exact solution of nonlinear Itô–Volterra SIE (3.1) and $\widehat{X_M}(t)$ is the approximate solution obtained by the new proposed method. Assume that μ_1 and μ_2 are Lipschitzian functions with constants Q_1 and Q_2, respectively, and the functions γ_i, $i = 1, 2$ satisfy the following conditions*

$$|\gamma_i(t, s)| \leq Z_i, \ i = 1, 2, \forall (t, s) \in [0, T]^2, \tag{3.8}$$

where Z_i, $i = 1, 2$ are positive constants. Then, we get

$$\left\| X(t) - \widehat{X_M}(t) \right\|_{L^2(0,T)}^2 = E \left| X(t) - \widehat{X_M}(t) \right|^2 \to 0 \ \text{as } M \to \infty. \tag{3.9}$$

Proof. From equation (3.1), we get

$$X(t_i) = h(t_i) + \int_0^{t_i} \gamma_1(t_i, s)\mu_1(X(s))ds + \int_0^{t_i} \gamma_2(t_i, s)\mu_2(X(s))d\mathcal{B}(s)$$

and

$$\widehat{X_M}(t_i) = h_M(t_i) + \int_0^{t_i} \gamma_1(t_i, s)\mu_1\left(\widehat{X_M}(s)\right)ds + \int_0^{t_i} \gamma_2(t_i, s)\mu_2\left(\widehat{X_M}(s)\right)d\mathcal{B}(s) - er_1^i - er_2^i, \tag{3.10}$$

where er_1^i and er_2^i represent the errors corresponding to integrals (I) and (II) in equation (3.3), respectively, defined as follows:

$$er_1^i = \int_0^{t_i} \gamma_1(t_i, s)\mu_1\left(\widehat{X_M}(s)\right)ds - \frac{1}{2}t_i \sum_{j=1}^{n1} A_j \gamma_1\left(t_i, \frac{1}{2}t_i s_j + \frac{1}{2}t_i\right)\mu_1\left(X'G^L\left(\frac{1}{2}t_i s_j + \frac{1}{2}t_i\right)\right) \tag{3.11}$$

and

$$er_2^i = \int_0^{t_i} \gamma_2(t_i, s)\mu_2\left(\widehat{X_M}(s)\right)d\mathcal{B}(s) - \gamma_2(t_i, t_i)\mu_2\left(X'G^L(t_i)\right)\mathcal{B}(t_i)$$
$$+ \frac{1}{2}t_i \sum_{j=1}^{n2} \tilde{A}_j \mathcal{B}\left(\frac{1}{2}t_i \tilde{s}_j + \frac{1}{2}t_i\right)\left[\gamma_2(t_i, s)\mu_2\left(X'G^L(s)\right)\right]'\left(\frac{1}{2}t_i \tilde{s}_j + \frac{1}{2}t_i\right). \tag{3.12}$$

Then, we have

$$E\left|X(t) - \widehat{X_M}(t)\right|^2 \leq E\left[\left|(h(t) - h_M(t)) + \int_0^{t_i} \gamma_1(t, s)(\mu_1(X(s)) - \mu_1(\widehat{X_M}(s)))ds\right.\right.$$
$$\left.\left. + \int_0^t \gamma_2(t, s)(\mu_2(X(s)) - \mu_2(\widehat{X_M}(s)))d\mathcal{B}(s) + er_1 + er_2 \right|^2\right]. \tag{3.13}$$

Since $(k_1 + k_2 + k_3)^2 \leq 4k_1^2 + 4k_2^2 + 4k_3^2$, then we get

$$E|X(t) - \widehat{X_M}(t)|^2 \leq 4E|h(t) - h_M(t)|^2 + 4E\left[\left|\int_0^t \gamma_1(t,s)(\mu_1(X(s)) - \mu_1(\widehat{X_M}(s)))ds\right.\right.$$

$$+ \int_0^t \gamma_2(t,s)(\mu_2(X(s)) - \mu_2(\widehat{X_M}(s)))d\mathcal{B}(s)\left.\left.\right|^2\right] + 4E|er_1 + er_2|^2$$

$$\leq 4E|h(t) - h_M(t)|^2 + 8E\left|\int_0^t \gamma_1(t,s)(\mu_1(X(s)) - \mu_1(\widehat{X_M}(s)))ds\right|^2$$

$$+ 8E\left|\int_0^t \gamma_2(t,s)(\mu_2(X(s)) - \mu_2(\widehat{X_M}(s)))d\mathcal{B}(s)\right|^2 + 4E|er_1 + er_2|^2. \quad (3.14)$$

Using Itô isometry, Lipschitz conditions, Holder's inequality and the boundedness of γ_1 and γ_2, we get

$$E|X(t) - \widehat{X_M}(t)|^2 \leq 4E|h(t) - h_M(t)|^2 + 8tE\int_0^t |\gamma_1(t,s)|^2|\mu_1(X(s)) - \mu_1(\widehat{X_M}(s))|^2 ds$$

$$+ 8E\int_0^t \gamma_2^2(t,s)|\mu_2(X(s)) - \mu_2(\widehat{X_M}(s))|^2 ds + 4E|er_1 + er_2|^2,$$

$$\leq 4E|h(t) - h_M(t)|^2 + 8TQ_1^2Z_1^2 \int_0^t E|Y(s) - \widehat{X_M}(s)|^2 ds$$

$$+ 8Q_2^2Z_2^2 \int_0^t E|X(s) - \widehat{X_M}(s)|^2 ds + 8E|er_1|^2 + 8E|er_2|^2$$

$$\leq (8TQ_1^2Z_1^2 + 8Q_2^2Z_2^2) \int_0^t E|X(s) - \widehat{X_M}(s)|^2 ds$$

$$+ 4E|h(t) - h_M(t)|^2 + 8E|er_1|^2 + 8E|er_2|^2. \quad (3.15)$$

Applying Gronwall's lemma, we obtain

$$E|X(t) - \widehat{X_M}(t)|^2 \to 0 \ \text{ as } M \to +\infty. \quad (3.16)$$

∎

3.4   Evaluation of the accuracy of the new proposed technique

This section assesses the efficacy of the newly proposed technique by employing various Lagrange functions and adjusting parameters such as α, β, and M. The evaluation includes a comparison with established methods widely used in the field, namely modified hat function (MHF), Fibonacci operational matrices (FOM), Euler polynomials (EP), shifted Jacobi operational matrices (SJOM), and the Bernstein method. To examine the efficacy of the newly proposed technique, various types of stochastic integral equations with different

types of exact solutions are used. The algorithm is implemented using MATLAB (R2014a). These experiments provide valuable insights into the efficiency and reliability of the proposed technique in comparison to established methods, helping to validate its applicability across different scenarios.

Example 3.1 *Consider the nonlinear Itô–Volterra SIE in [66]*

$$X(t) = \frac{1}{8} - 0.015625 \int_0^t X(s)(1 - X^2(s))ds + 0.125 \int_0^t (1 - X^2(s))d\mathcal{B}(s), \ 0 \le t \le 1, \quad (3.17)$$

with the exact solution

$$X_{Exact}(t) = \frac{9}{9\, e^{0.125\mathcal{B}(t)} + 7}\, e^{0.25\mathcal{B}(t)} - \frac{7}{9\, e^{0.125\mathcal{B}(t)} + 7}. \quad (3.18)$$

Table 3.1 presents the analytical solution via (3.18) and the approximate solutions obtained by the proposed technique, using various Lagrange functions $L_1(t) = 1 - 2e^{-\frac{t}{100}}$ and $L_2(t) = 2\tanh(t) - 1$ and different values of α and β ($\alpha = \beta = 0$), ($\alpha = \beta = -0.75$), ($\alpha = \beta = -0.5$) and ($\alpha = -0.75\beta = -0.5$) for $0 \le t \le 0.9$, $M = 8$ and 10^2 sample paths.

Table 3.1: Numerical results of the exact solution and approximate solutions for Example 3.1.

t	Exact solution $Y(t) = \frac{9\, e^{0.25\mathcal{B}(t)} - 7}{9\, e^{0.125\mathcal{B}(t)} + 7}$	Approximate solutions			
		$L_1(t) = 1 - 2e^{-\frac{t}{100}}$		$L_2(t) = 2\tanh(t) - 1$	
		$\alpha = \beta = 0$	$\alpha = \beta = -0.75$	$\alpha = \beta = -0.5$	$\alpha = -0.75, \beta = -0.5$
0	0.12500000	0.12812630	0.12376224	0.12439152	0.12411194
0.1	0.12455492	0.12534476	0.12855858	0.12839622	0.12423431
0.2	0.12972764	0.12706921	0.12890479	0.12919038	0.12557322
0.3	0.13032644	0.12793268	0.12599189	0.12479003	0.12969632
0.4	0.11675846	0.12796429	0.12358697	0.12334069	0.12804461
0.5	0.11114545	0.12889378	0.12283510	0.12346982	0.12678623
0.6	0.12381948	0.13122039	0.12241042	0.12215894	0.13013486
0.7	0.11889557	0.1330032	0.12106677	0.12019059	0.13359992
0.8	0.11875911	0.13130259	0.11971906	0.11975725	0.13189005
0.9	0.11111908	0.12717650	0.12026580	0.12040455	0.12743390

Absolute errors $\xi(t) = mean|X_{Exact}(t) - X_{Approximate}(t)|$, are given in Figure 3.2 using generalized Lagrange function $L_1(t) = 1 - 2e^{-\frac{t}{100}}$ for 2 trajectories, $\alpha = \beta = -0.75$ and $M = 20$.
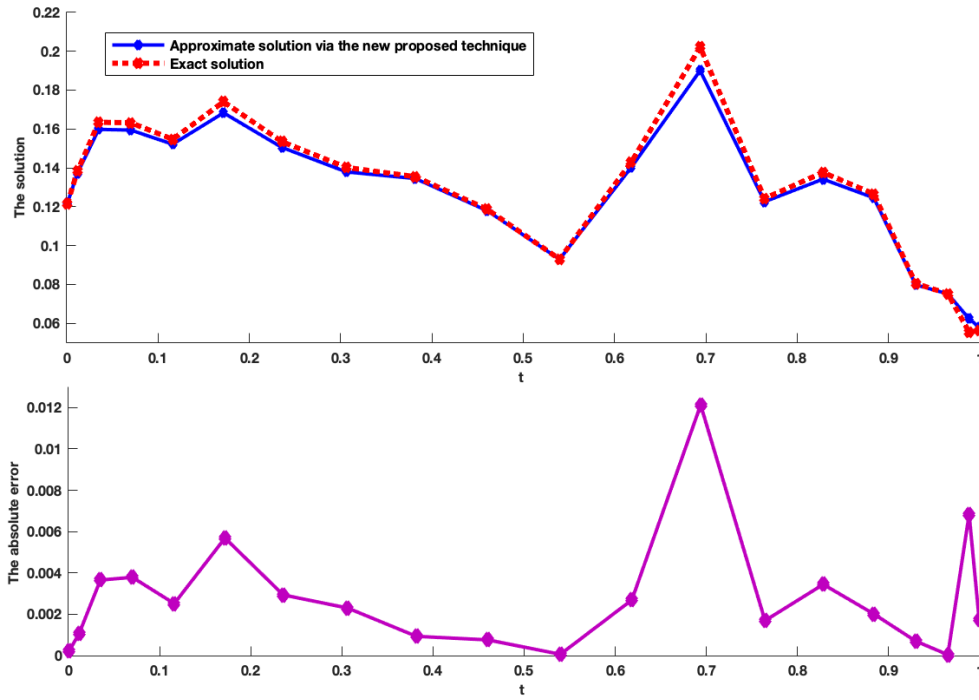
Figure 3.2: Numerical results obtained by the proposed technique for Example 3.1.

Table 3.2 presents a comparison between our technique and the FOM technique in [83].

Table 3.2: Comparaison of the absolute errors of the FOM technique and the generalized Lagrange technique for Example 3.1.

| t | Error using the FOM in [83] | $L_1(t) = 1 - 2e^{-\frac{t}{100}}$ | | $L_2(t) = 2\tanh(t) - 1$ | |
		$\alpha = \beta = 0$	$\alpha = \beta = -0.75$	$\alpha = \beta = -0.5$	$\alpha = -0.75, \beta = -0.5$
0	9.35×10^{-3}	3.12×10^{-3}	1.23×10^{-3}	6.08×10^{-4}	8.88×10^{-4}
0.1	3.12×10^{-2}	1.81×10^{-3}	6.54×10^{-3}	6.38×10^{-3}	7.02×10^{-4}
0.2	4.10×10^{-2}	2.75×10^{-3}	1.23×10^{-2}	1.26×10^{-2}	1.25×10^{-3}
0.3	4.87×10^{-2}	2.25×10^{-3}	8.94×10^{-3}	7.73×10^{-3}	4.95×10^{-4}
0.4	5.51×10^{-2}	6.17×10^{-4}	4.76×10^{-3}	4.51×10^{-3}	6.97×10^{-4}
0.5	6.10×10^{-2}	5.56×10^{-3}	4.67×10^{-3}	5.31×10^{-3}	7.67×10^{-3}
0.6	6.65×10^{-2}	5.10×10^{-3}	5.06×10^{-4}	2.55×10^{-4}	6.18×10^{-3}
0.7	7.47×10^{-2}	3.68×10^{-3}	4.66×10^{-4}	1.34×10^{-3}	3.09×10^{-3}
0.8	8.40×10^{-2}	4.32×10^{-3}	2.66×10^{-3}	2.62×10^{-3}	3.74×10^{-3}
0.9	9.72×10^{-2}	1.21×10^{-2}	5.06×10^{-3}	4.92×10^{-3}	1.18×10^{-2}

For better understanding, Figure 3.3 indicates a comparison between the exact solution, the approximate solution calculated by the present method with Lagrange function $L_1(t) = 1 - 2e^{-\frac{t}{100}}$ for $M = 8$ and $\alpha = \beta = -0.75$ and using the FOM technique in [83].
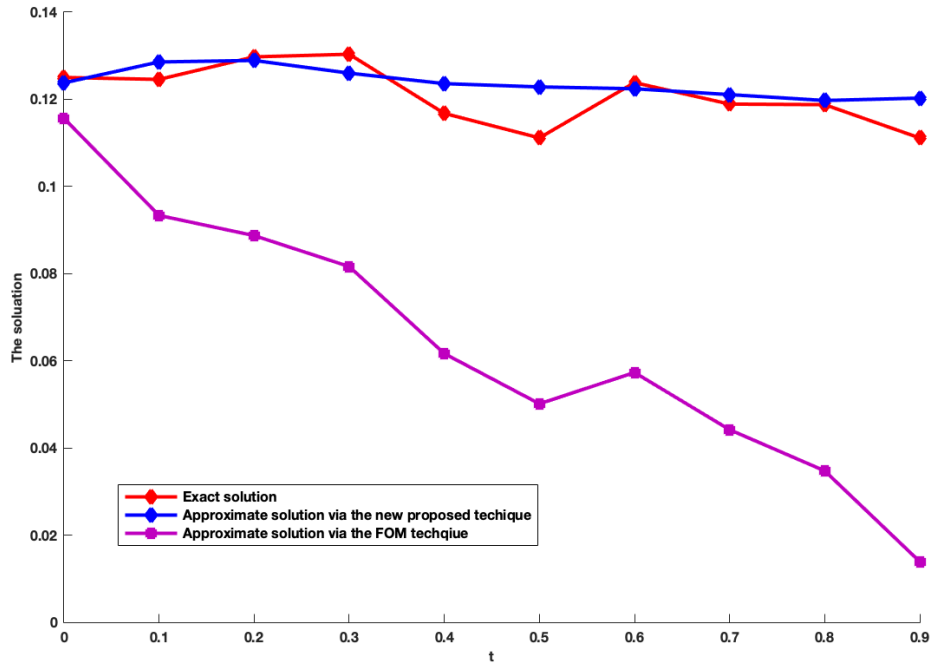
Figure 3.3: Comparaison of the results of the generalized Lagrange solution and the FOM technique with the exact solution for Example 3.1.

From Tables 3.1 and 3.2 and Figures 3.2 and 3.3 we conclude that:

- *The new method gives us solutions that are very similar to the exact ones for any values of t, Lagrange function, α, and β. This means that the approximate solution behaves just like the exact solution in equation (1.32) and can be considered as an accurate representative solution of the nonlinear stochastic Itô–Volterra integral equation in (3.17).*

- *The approximate solutions based on the generalized Lagrange technique are better than the approximate solutions obtained by the FOM technique in [83] for any t, Lagrange function, α and β, where*

$$\xi_{new}(L, \alpha, \beta; t) < \xi_{FOM}(t), \text{ for any } L, \alpha, \beta, t.$$

More Precisly, for $0 \leq t \leq 0.9$ we have

$$
\begin{cases}
0.0093 \leq \xi_{FOM}(t) \leq 0.0972. \\
0.0004 \leq \xi_{new}(L_1, -0.75, -0.75; t) \leq 0.0089. \\
0.0006 \leq \xi_{new}(L_1, 0, 0; t) \leq 0.0121. \\
0.0003 \leq \xi_{new}(L_2, -0.5, -0.5; t) \leq 0.0126. \\
0.0005 \leq \xi_{new}(L_2, -0.5, 0.667; t) \leq 0.0118.
\end{cases}
$$

Example 3.2 *Let given the following nonlinear Itô–Volterra SIE in [83]*

$$
X(t) = 1 + \int_0^t X(s) \left(\frac{1}{32} - X^2(s) \right) ds + 0.25 \int_0^t X(s) d\mathcal{B}(s), \ 0 \leq t \leq 1, \tag{3.19}
$$

with the exact solution

$$
X_{Exact}(t) = \frac{e^{0.25\mathcal{B}(t)}}{\sqrt{1 + 2 \int_0^t e^{0.5\mathcal{B}(s)} ds}}. \tag{3.20}
$$

Table 3.3 shows the analytical solutions via (3.20) and the approximate solutions given by the proposed technique, using various Lagrange functions $L_1(t) = t$, $L_2(t) = 2\tanh(t) - 1$ and $L_3(t) = 1 - 2e^{-t}$ and different values of α and β ($\alpha = \beta = -0.75$), ($\alpha = \beta = 0$) and ($\alpha = 0, \ \beta = -5/6$) for $0 \leq t \leq 0.9$, $M = 8$ and 10^2 sample paths.

Table 3.3: Numerical results of the exact solution and approximate solutions for Example 3.2.

t	Exact solution $Y(t) = \frac{e^{0.25\mathcal{B}(t)}}{\sqrt{1+2\int_0^t e^{0.5\mathcal{B}(s)}ds}}$	$L_1(t) = t$ $\alpha = \beta = -0.75$	$L_2(t) = -1 + 2\tanh(t)$ $\alpha = \beta = 0$	$\alpha = 0, \beta = -5/6$	$L_3(t) = 1 - 2e^{-t}$ $\alpha = \beta = 0$	$\alpha = 0, \beta = -5/6$
0	1.0	1.001423	1.027262	0.999345	0.979067	1.001771
0.1	0.918945	0.921487	0.917016	0.911177	0.913172	0.930352
0.2	0.854198	0.851411	0.858504	0.851796	0.839501	0.858175
0.3	0.791579	0.793812	0.796184	0.806006	0.791913	0.801717
0.4	0.746896	0.747737	0.755605	0.749902	0.745678	0.767293
0.5	0.711232	0.710177	0.728305	0.702221	0.704470	0.732648
0.6	0.665611	0.678215	0.694829	0.674294	0.67414	0.691860
0.7	0.652236	0.650551	0.653132	0.651000	0.651024	0.656214
0.8	0.609760	0.627179	0.615321	0.612777	0.62806	0.633083
0.9	0.606999	0.605938	0.590884	0.560159	0.604471	0.608415

The mean of absolute error $\xi(t) = mean|X_{Exact}(t) - X_{Approximate}(t)|$, is given in Figure 3.4 using the generalized Lagrange function $L_2(t)$ for 50 trajectories, $\alpha = \beta = 0$ and $M = 20$.
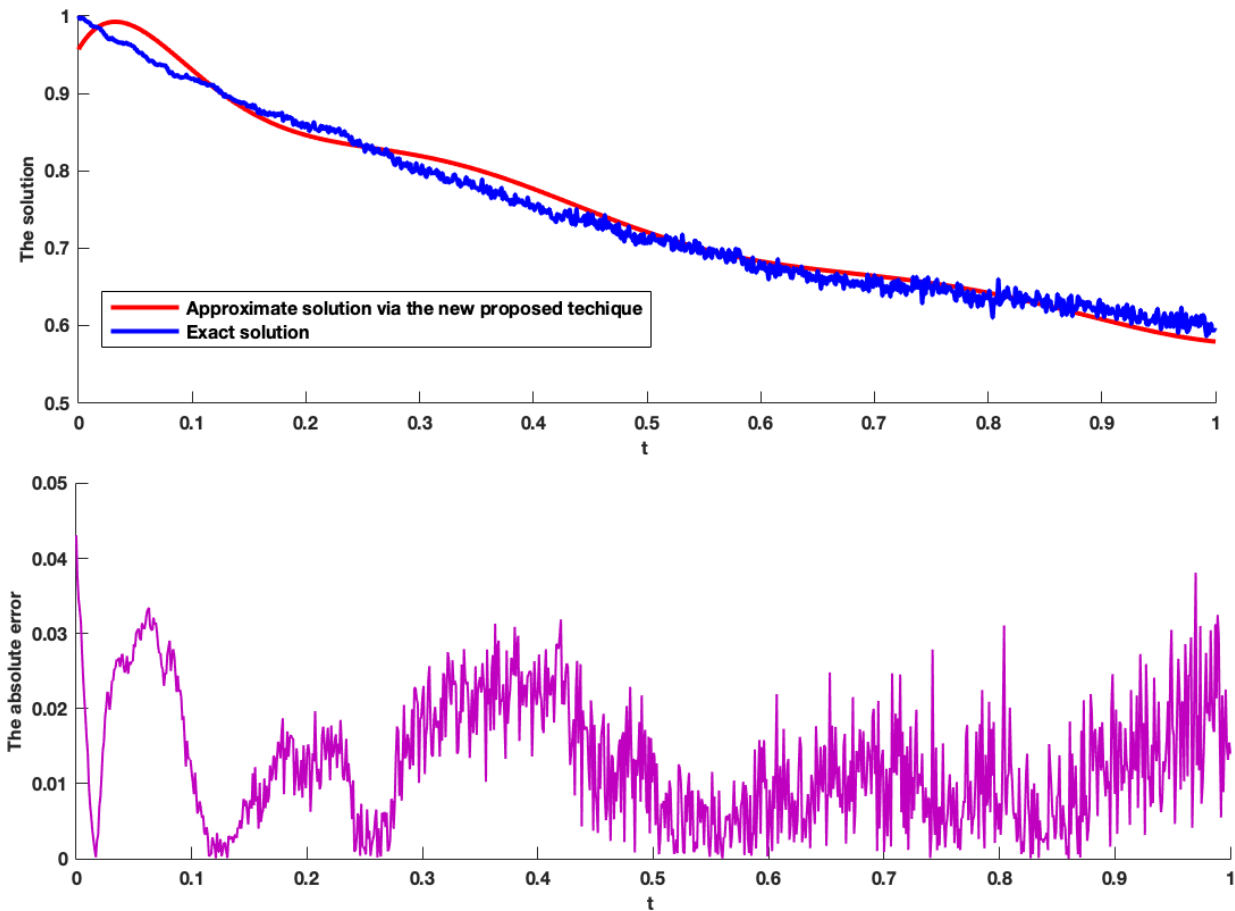
Figure 3.4: Numerical results obtained by the proposed technique for Example3.2.

Table 3.4 presents a comparison between our technique, the MHF technique in [119], the EP technique in [86] and the FOM technique in [83], where $\xi_2(t)$ is the error using $L_1(t)$ for $\alpha = \beta = -0.75$ and $M = 8$ and $\xi_3(t)$ is the error for $L_2(t)$, $\alpha = \beta = 0$ and $M = 8$. For more comprehension, Figure 3.5 indicates a comparison study between the exact solutions, the approximate solutions calculated by the EP technique in [86], the approximate solutions using the FOM technique in [83], the approximate solutions using the MHF technique in [119] and the approximate solutions using the generalized Lagrange technique via the Lagrange function $L_3(t)$ for $\alpha = 0, \beta = -5/6$ and $M = 8$.

Table 3.4: Comparaison of the absolute errors of the EP technique, the MHF technique, the proposed method and the FOM technique for Example 3.2.

t	EP technique in [86]	MHF techniquein [119]	FOM technique in [83]	New proposed technique	
				ξ_2	ξ_3
0	2.76×10^{-2}	2.31×10^{-2}	0.135	1.42×10^{-3}	2.72×10^{-2}
0.1	2.51×10^{-2}	1.03×10^{-2}	9.45×10^{-2}	2.54×10^{-3}	3.37×10^{-3}
0.2	2.59×10^{-2}	2.21×10^{-2}	6.56×10^{-2}	2.78×10^{-3}	1.88×10^{-3}
0.3	3.06×10^{-2}	1.02×10^{-2}	4.62×10^{-2}	2.23×10^{-3}	1.47×10^{-3}
0.4	3.84×10^{-2}	3.19×10^{-2}	3.69×10^{-2}	8.40×10^{-4}	1.14×10^{-3}
0.5	4.87×10^{-3}	3.69×10^{-2}	4.04×10^{-2}	1.05×10^{-3}	1.11×10^{-2}
0.6	6.08×10^{-2}	5.98×10^{-2}	5.16×10^{-2}	1.26×10^{-2}	7.68×10^{-3}
0.7	7.42×10^{-2}	6.88×10^{-2}	6.62×10^{-2}	1.68×10^{-3}	1.88×10^{-3}
0.8	8.89×10^{-2}	7.73×10^{-2}	8.23×10^{-2}	1.74×10^{-2}	3.85×10^{-3}
0.9	0.105	9.81×10^{-2}	0.1	1.06×10^{-3}	2.37×10^{-2}
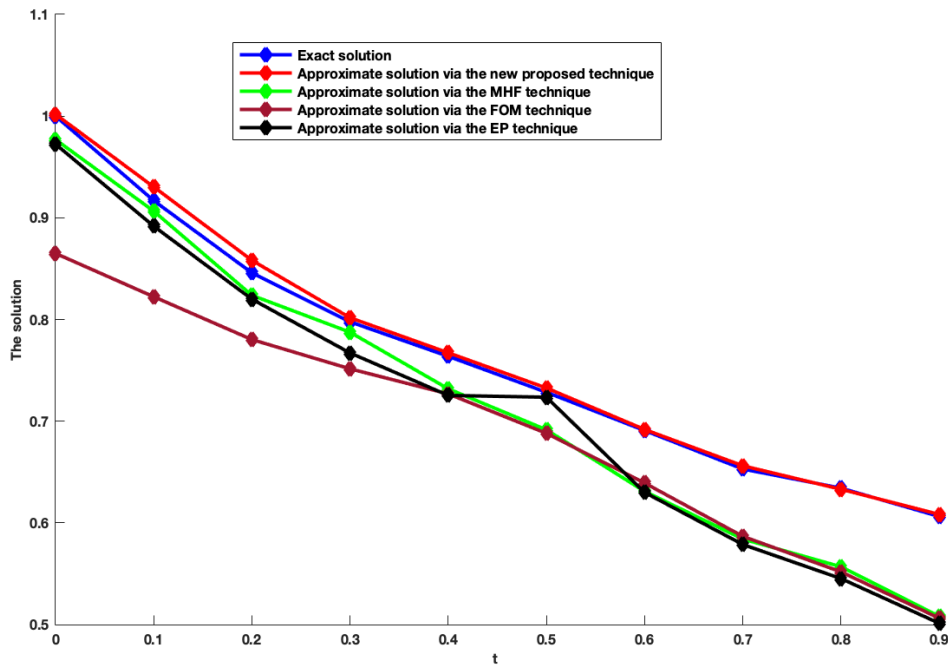
Figure 3.5: Comparaison of the results of the FOM technique, MHF technique, proposed method and the EP technique with the exact solution for Example 3.2.

Moreover, Table 3.5 gives the maximum absolute error and the CPU time of the new proposed

technique using the Lagrange function $L(t) = 1 - 2e^{-\frac{t}{100}}$ for $\alpha = \beta = 0$, $M = 8$ and 20 simulations compared with the MHF technique in [119], the FOM technique in [83] and the Bernstein technique in [12].

Table 3.5: The maximum error and CPU time for Bernstein technique, the MHF technique, new proposed technique and EP technique for Example 3.2.

The used techniques	CPU time	Maximum error
New proposed technique	169.8	0.06805
MHF technique in [119]	803.8	0.1342
Bernstein technique in [12]	1492.4	0.1366
EP technique in [83]	899.4	0.1363

From Tables 3.3, 3.4 and 3.5 and Figures 3.4 and 3.5, we conclude that:

- *The new method gives us solutions that are very similar to the exact ones for any values of t, Lagrange function, α, and β. This means that the approximate solution behaves just like the exact solution in equation (3.20) and can be considered as an accurate representative solution of the nonlinear stochastic Itô–Volterra integral equation in (3.19).*

- *The approximate solutions based on the new proposed technique are better than the approximate solutions based on the EP technique in [86], the MHF technique in [119] and the FOM method in [83] for any t, Lagrange function $L_1(t)$ for $\alpha = \beta = -0.75$ where*

$$\xi_{new}(t) < \xi_{EP}(t), \; \xi_{new}(t) < \xi_{MHF}(t), \; \xi_{new}(t) < \xi_{FOM}(t), \; \text{for any } t.$$

To be more specific, for $0 \leq t \leq 0.9$ we have

$$
\begin{cases}
0.0369 \leq \xi_{FOM} \leq 0.135. \\
0.0981 \; \leq \xi_{MHF} \leq 0.102. \\
0.0487 \leq \xi_{EP} \leq 0.105. \\
0.000840 \leq \xi_{new} \leq 0.0174.
\end{cases}
\tag{3.21}
$$

- *The required time (denoted as Γ) of the new proposed technique is much less than the required time of the MHF technique in [119], Bernstein technique in [12] and FOM technique in [83]. In some circumstances, the existing techniques take more than 8 times as long as the new proposed technique, where*

$$\Gamma_{new} = 169.8 < \Gamma_{MHF} = 803.8 < \Gamma_{PE} = 899.4 < \Gamma_{Bernstein} = 1492.4.$$

Moreover,

$$\max(\xi_{new}) < \max(\xi_{MHF}) < \max(\xi_{PE}) < \max(\xi_{Bernstein}).$$

Example 3.3 *Consider the following nonlinear Itô–Volterra SIE in [60]*

$$X(t) = \frac{1}{12} + \int_0^t \cos(s)X(s)ds + \int_0^t \sin(s)X(s)d\mathcal{B}(s), \ 0 \le t \le 0.5, \quad (3.22)$$

with the exact solution

$$X_{Exact}(t) = \frac{1}{12}\exp\left(-\frac{t}{4}\sin(t) + \frac{\sin(2t)}{8} + \int_0^t \sin(s)d\mathcal{B}(s)\right). \quad (3.23)$$

Table 3.6 illustrates the analytical solutions via (3.23) and the approximate solutions obtained by the proposed technique using various Lagrange functions $L_1(t) = 1 - 2e^{-t}$, $L_2(t) = -1 + 2\tanh(t)$ and $L_3(t) = 2t^2 - 1$ and different values of α and β ($\alpha = -0.75$, $\beta = -0.5$), ($\alpha = \beta = -0.5$), ($\alpha = \beta = 0$) and ($\alpha = -\beta = 0.5$) for $0 \le t \le 0.5$, $M = 5$ and 10^2 sample path. The mean absolute error $\xi(t) = mean|X_{Exact}(t) - X_{Approximate}(t)|$, are given in Figure 3.6 using the generalized Lagrange function $L_3(t)$ for 10^2 trajectories, $\alpha = \beta = 0$ and $M = 5$. Table 3.7 gives a comparison study between the generalized Lagrange technique and the SJOM technique in [110]. For more understanding, Figure 3.7 shows a comparison study between the exact solutions, the approximate solutions using the SJOM technique in [110] and the approximate solutions using the new proposed technique via the Lagrange function $L_2(t)$ for $\alpha = -0.75$, $\beta = -0.5$ and $M = 5$.

From Tables 3.6 and 3.7 and Figures 3.6 and 3.7, we conclude that:

- *The new method gives us solutions that are very similar to the exact ones for any values of t, Lagrange function, α, and β. This means that the approximate solution can be considered as an accurate representative solution of the nonlinear stochastic Itô–Volterra integral equation in (3.22).*

- *The approximate solutions based on the new proposed technique are more better than the approximate solutions based on the SJOM technique in [110] for any t, Lagrange function $L_2(t)$ and $\alpha = -0.75, \beta = -0.5$ where*

$$\xi_{new}(t) < \xi_{SJOM}(t), \ \textit{for any } t.$$

To be more specific, for $0 \le t \le 0.9$ we have

$$\begin{cases} 0.00134 \le \xi_{SJOM} \le 0.06007. \\ 0.000965 \le \xi_{new} \le 0.02008. \end{cases} \quad (3.24)$$

Table 3.6: Numerical results of the exact solution and approximate solutions for Example 3.3.

t	Exact solution	New approximate solutions via different parameters				
		$L_1(t) = 1 - 2e^{-t}$	$L_2(t) = -1 + 2\tanh(t)$		$L_3(t) = 2t^2 - 1$	
		$\alpha = -0.75,\ \beta = -0.5$	$\alpha = -0.75,\ \beta = -0.5$	$\alpha = \beta = -0.5$	$\alpha = \beta = 0$	$\alpha = -\beta = 0.5$
0	0.0833333	0.080346	0.0838326	0.0860746	0.0849288	0.0840893
0.05	0.0875073	0.0906386	0.0870375	0.0847848	0.0866409	0.0863398
0.1	0.0922140	0.0928989	0.0919553	0.0922183	0.0911313	0.0918855
0.15	0.0965564	0.0945836	0.0976023	0.1005236	0.0968281	0.0979178
0.2	0.1015327	0.0990577	0.1034996	0.1057918	0.1021902	0.1021081
0.25	0.1067153	0.1069682	0.1096368	0.1077977	0.1068317	0.1049321
0.3	0.1123379	0.1172533	0.1163963	0.1094383	0.1121089	0.1105140
0.35	0.1226227	0.1278727	0.1244509	0.1159563	0.1201832	0.1235821
0.4	0.1268072	0.1363243	0.1346472	0.1340524	0.1302893	0.1394374
0.45	0.1313347	0.1400012	0.1478892	0.1709888	0.1306597	0.1231503
0.5	0.1351400	0.1364274	0.1650334	0.2337728	0.0842698	-0.02649076

Table 3.7: Absolute errors comparaison for Example 3.3.

t	SJOM technique in [110]	Approximate solution				
		$L_1(t) = 1 - 2e^{t}$	$L_2(t) = -1 + 2\tanh(t)$		$L_3(t) = 2t^2 - 1$	
		$\alpha = -0.75,\ \beta = -0.5$	$\alpha = -0.75,\ \beta = -0.5$	$\alpha = \beta = -0.5$	$\alpha = \beta = 0$	$\alpha = -\beta = 0.5$
0	$1.39e^{-8}$	2.98×10^{-3}	4.99×10^{-4}	2.74×10^{-3}	1.59×10^{-3}	2.80×10^{-4}
0.05	1.34×10^{-3}	3.07×10^{-3}	6.57×10^{-4}	2.71×10^{-3}	8.38×10^{-4}	2.80×10^{-3}
0.1	5.95×10^{-3}	8.56×10^{-4}	3.87×10^{-4}	6.27×10^{-4}	1.05×10^{-3}	2.80×10^{-4}
0.15	4.01×10^{-3}	2.80×10^{-3}	2.70×10^{-4}	3.72×10^{-3}	3.89×10^{-4}	2.80×10^{-4}
0.2	3.34×10^{-3}	3.62×10^{-3}	1.63×10^{-4}	3.82×10^{-3}	5.77×10^{-4}	2.80×10^{-4}
0.25	1.30×10^{-2}	2.36×10^{-3}	9.65×10^{-4}	7.16×10^{-4}	2.39×10^{-3}	2.80×10^{-3}
0.3	7.24×10^{-3}	1.006×10^{-4}	7.18×10^{-4}	4.17×10^{-3}	2.90×10^{-3}	2.80×10^{-3}
0.35	2.19×10^{-2}	4.96×10^{-3}	2.21×10^{-3}	2.62×10^{-3}	4.09×10^{-4}	2.80×10^{-3}
0.4	1.87×10^{-2}	1.32×10^{-3}	4.92×10^{-3}	5.58×10^{-3}	3.85×10^{-3}	2.80×10^{-2}
0.45	5.08×10^{-2}	3.45×10^{-3}	1.16×10^{-2}	3.72×10^{-2}	3.88×10^{-3}	2.80×10^{-2}
0.5	6.007×10^{-2}	1.46×10^{-2}	2.008×10^{-2}	9.46×10^{-2}	6.30×10^{-2}	2.80×10^{-1}
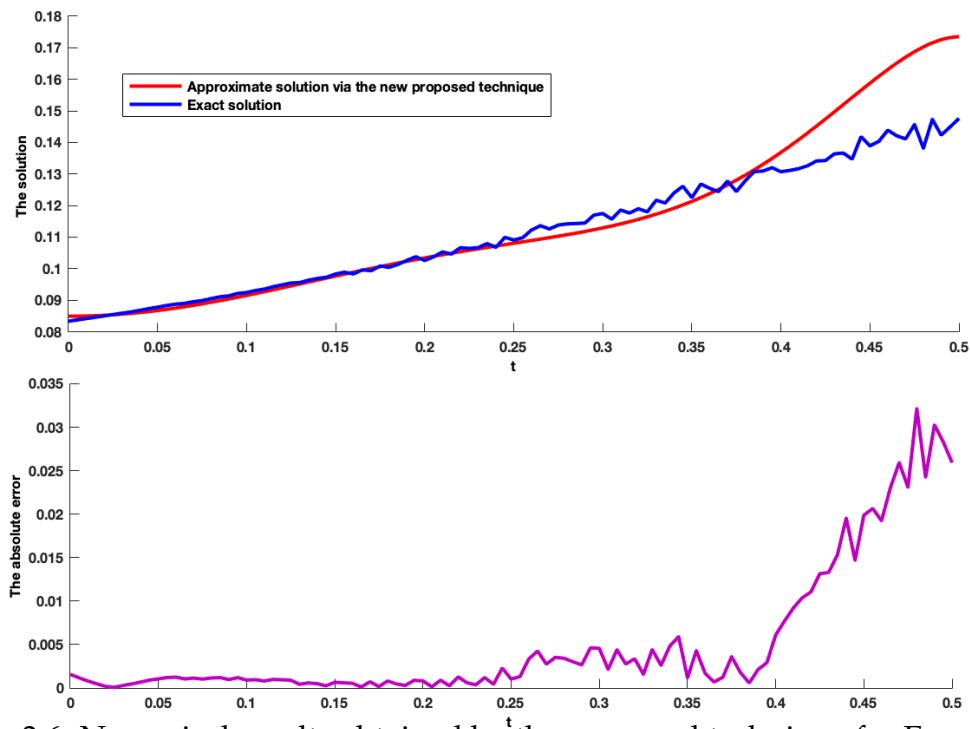
Figure 3.6: Numerical results obtained by the proposed technique for Example 3.3.
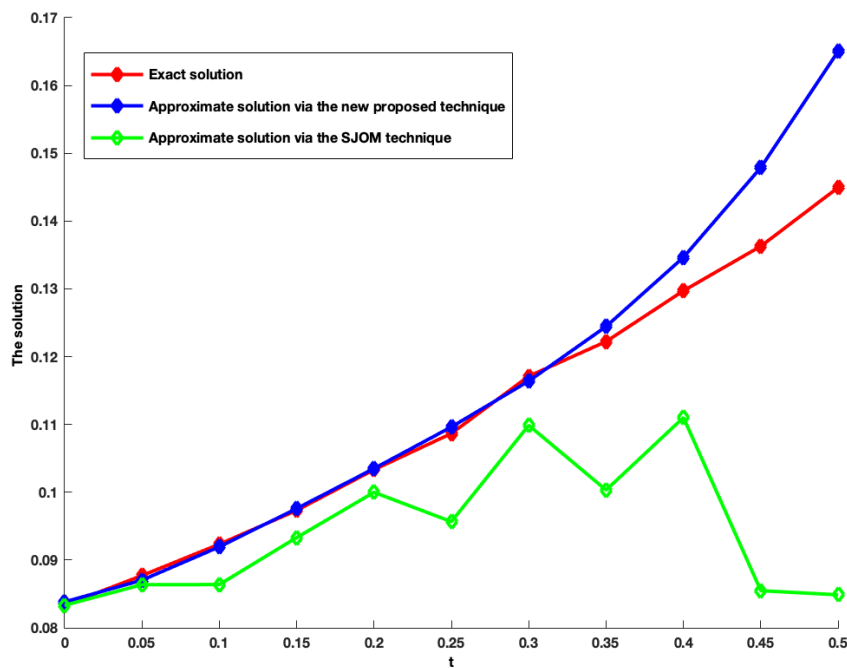
Figure 3.7: Comparaison of the results of the generalized Lagrange solution and the SJOM technique with the exact solution for Example 3.3.

Example 3.4 *Let the following nonlinear Itô–Volterra SIE in [66]*

$$X(t) = \frac{1}{20} + \frac{1}{400} \int_0^t \cos(X(s)) \sin^3(X(s)) ds + a \int_0^t \sin^2(X(s)) d\mathcal{B}(s), \ \ 0 \leq t \leq 1, \quad (3.25)$$

with the exact solution

$$X_{Exact}(t) = arccot\left(\frac{1}{20}\mathcal{B}(t) + cot\left(\frac{1}{20}\right)\right). \quad (3.26)$$

Table 3.8 shows the analytical solutions via (3.26) and the approximate solutions obtained by the proposed technique using various Lagrange functions $L_1(t) = 1 - 2e^{-\frac{t}{100}}$ and $L_2(t) = \frac{t-1}{t+1}$ and different values of α and β ($\alpha = \beta = -0.5$), ($\alpha = \beta = -0.75$) and ($\alpha = \beta = 0$) for $0 \leq t \leq 0.9$, $M = 6$ and 10^2 sample paths.

Table 3.8: The approximate and exact solutions for Example 3.4.

t	Exact solution	Approximate solutions			
		$L_1(t) = 1 - 2e^{-\frac{t}{100}}$		$L_2(t) = \frac{t-1}{t+1}$	
		$\alpha = \beta = -0.5$	$\alpha = \beta = -0.75$	$\alpha = \beta = 0$	$\alpha = \beta = -0.75$
0	0.05	0.05000131	0.04999960	0.05002543	0.04999657
0.1	0.04999959	0.04999114	0.04999397	0.04999338	0.04999919
0.2	0.04999799	0.04998969	0.04999620	0.05000307	0.04998586
0.3	0.04999651	0.04999059	0.04999871	0.05000515	0.04998351
0.4	0.04999736	0.04999067	0.04999907	0.05000313	0.04998663
0.5	0.04999649	0.04998908	0.04999812	0.05000327	0.04998932
0.6	0.05000140	0.04998649	0.04999810	0.05000711	0.04998960
0.7	0.05000353	0.04998424	0.05000091	0.05001280	0.04998823
0.8	0.05000189	0.04998356	0.05000623	0.05001708	0.04998713
0.9	0.05000315	0.04998475	0.05000983	0.05001662	0.04998843
1	0.05000519	0.04998640	0.05000183	0.05000862	0.04999397

Mean of absolute error $\xi(t) = mean|X_{Exact}(t) - X_{Approximate}(t)|$, is given in Figure 3.8 using generalized Lagrange function $L_1(t)$ for 10 trajectories, $\alpha = -0.75$, $\beta = -0.5$ and $M = 6$.

Table 3.9 represents the absolute errors of the proposed technique using $L_1(t)$ and $L_2(t)$ for $M = 6$. From Tables 3.8 and 3.9 and Figure 3.8 we conclude that:

- *The new method gives us solutions that are very similar to the exact ones for any values of t, the adopted Lagrange function $L_2(t)$, $\alpha = -0.75$, $\beta = -0.75$. This indicates that the*

Table 3.9: The absolute errors of the generalized Lagrange technique for Example 3.4.

| t | Error via the new proposed technique | | | |
| | $L_1(t) = 1 - 2e^{-\frac{t}{100}}$ | | $L_2(t) = \frac{t-1}{t+1}$ | |
	$\alpha = \beta = -0.5$	$\alpha = \beta = -0.75$	$\alpha = \beta = 0$	$\alpha = \beta = -0.75$
0	1.31×10^{-6}	3.97×10^{-7}	2.54×10^{-5}	3.24×10^{-6}
0.1	8.44×10^{-6}	4.68×10^{-6}	3.41×10^{-6}	1.57×10^{-6}
0.2	8.29×10^{-6}	1.03×10^{-5}	4.23×10^{-6}	1.15×10^{-5}
0.3	5.91×10^{-6}	4.25×10^{-6}	3.98×10^{-6}	1.35×10^{-5}
0.4	6.68×10^{-6}	3.02×10^{-6}	4.24×10^{-6}	1.34×10^{-5}
0.5	7.41×10^{-6}	1.20×10^{-5}	3.41×10^{-6}	5.69×10^{-6}
0.6	1.49×10^{-5}	1.32×10^{-5}	2.19×10^{-6}	1.24×10^{-5}
0.7	1.92×10^{-5}	1.99×10^{-5}	5.96×10^{-6}	8.66×10^{-6}
0.8	1.83×10^{-5}	1.81×10^{-5}	6.50×10^{-6}	9.84×10^{-6}
0.9	1.84×10^{-5}	1.92×10^{-5}	8.01×10^{-7}	7.37×10^{-9}

approximate solution behaves just like the exact solution in equation (3.26) and can be seen as an accurate representative solution of the nonlinear stochastic Itô–Volterra integral equation in (3.25), where

$$7.37 \times 10^{-9} \leq \xi_{new} \leq 1.35 \times 10^{-5}, \text{ for } 0 \leq t \leq 0.9.$$
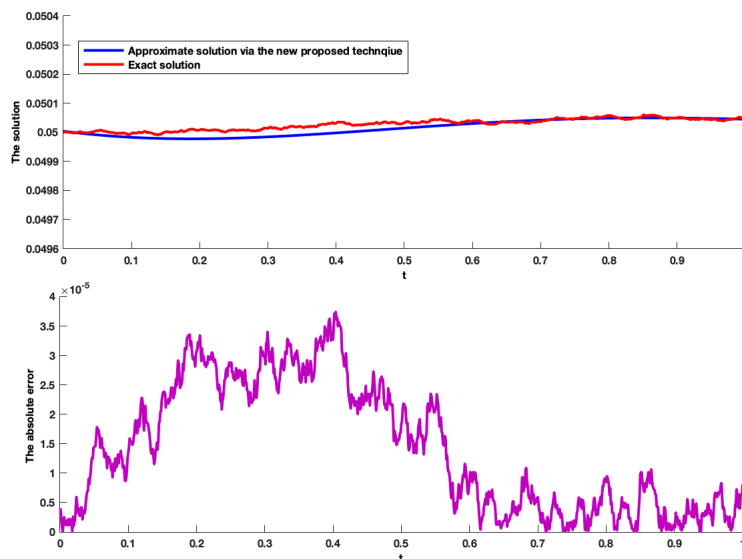
Figure 3.8: Numerical results obtained by the generalized Lagrange technique for Example 3.4.

Remark 3.1 *Now comes to mind the following logical question:* What are the effects of the selected Lagrange functions and the values of α and β on the accuracy of the new proposed technique? *To answer this significant question, Figures 3.9-3.12 give the approximate solutions via the new proposed technique of the above-mentioned nonlinear equations in Examples 1-5, respectively using different Lagrange functions $L(s)$ and different values of α and β. From Figures 3.9-3.12, we can conclude that:*

- *In Figure 3.9, $\alpha = \beta = 1/2$ (Chebyshev interpolation points) and different generalized functions are taken to get approximate solutions. The results show that, all the choices gives acceptable results. In the case $L(s) = s$, the approximate solution is in a good agreement with exact solution of Example 1. Secondly, for $L(s) = 1 - 2e^{\frac{-s}{100}}$, the best choice to approximate exact solution for all mentioned α and β is $\alpha = \beta = 0.5$.*

- *The choices $L(s) = -1 + 2tan(s)$ and $L(s) = s$ for $\alpha = \beta = 0$ are good choices to approximate exact solution for Example 2. For $L(s) = -1 + 2tan(s)$ and $t \in [0, 0.9]$, all choices of α and β can be used to estimate the analytical solution. For $t \in [0.9, 1]$, among all the values of α and β, the best options to estimate the exact solution are $(\alpha = -0.75, \beta = -0.5)$, $(\alpha = 3, \beta = -0.25)$ and $\alpha = -5/7, \beta = 0$.*

- *In Figure 3.11, all the numerical experiments for the Lagrange function $L(s) = -1 + 2tan(s)$ for the most different values of α, β and $t \in [0, 0.5]$ shows the good agreement between exact and approximate solutions for Example 3, and for $t \in [0.5, 1]$ the best choices are $(\alpha = \beta = 0)$, $(\alpha = \beta = 0.5)$ and $\alpha = 0, \beta = 1/3$. For a fixed $\alpha = \beta = 0.5$, the approximate solutions obtained by all Lagrange functions agree well with the exact solution except the case $L(s) = 2s^2 - 1$.*

- *For all Lagrange functions or for all values of α and β, the approximate solutions are in a good agreement with the exact solution of Example 4.*
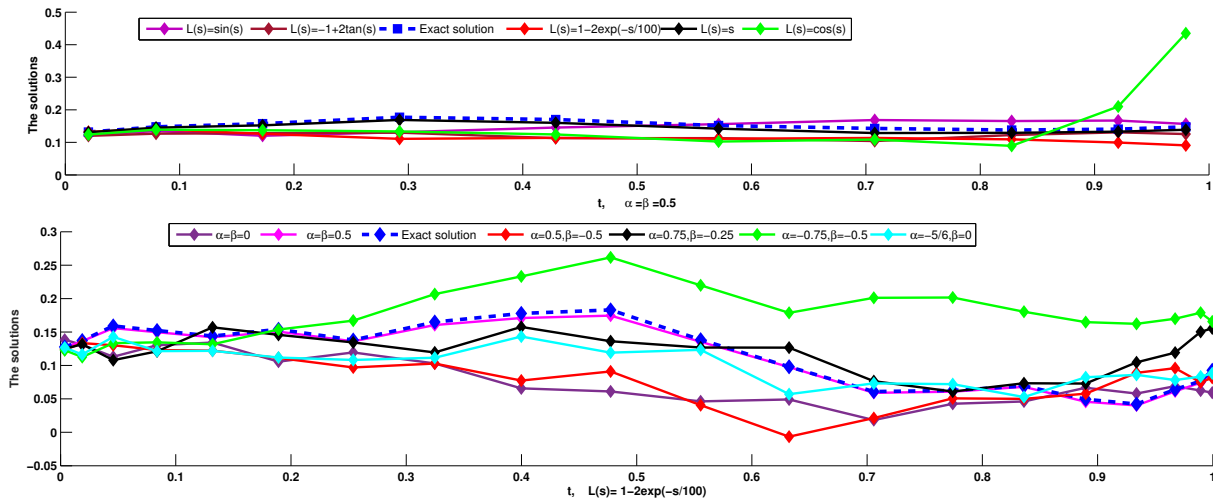
Figure 3.9: The exact solution and approximate solutions using different values of α and β and a different Lagrange functions $L(s)$ for Example 3.1.
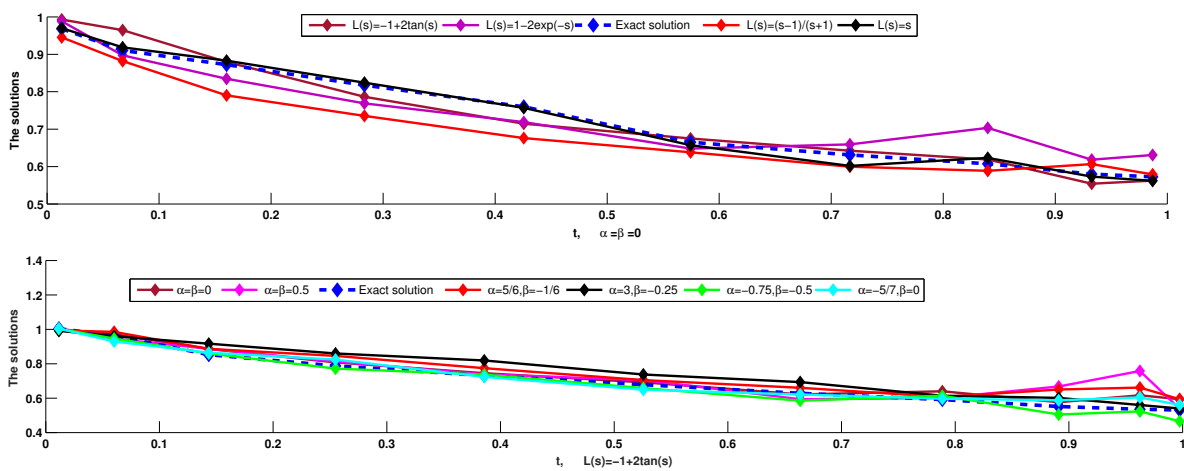
Figure 3.10: The exact solution and approximate solutions using different values of α and β and a different Lagrange functions $L(s)$ for Example 3.2.
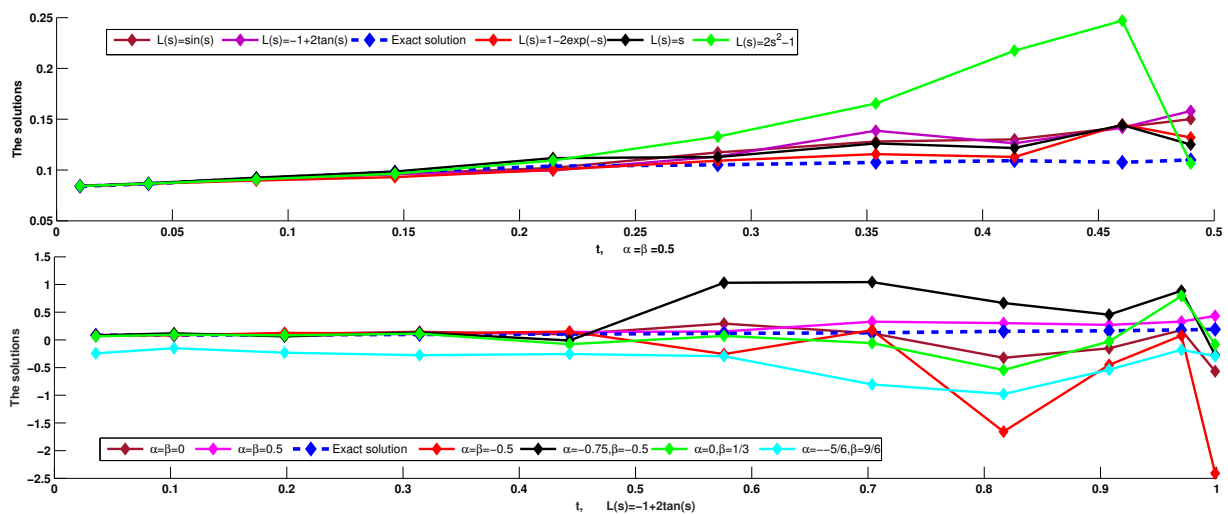
Figure 3.11: The exact solution and approximate solutions using different values of α and β and a different Lagrange functions $L(s)$ for Example 3.3.
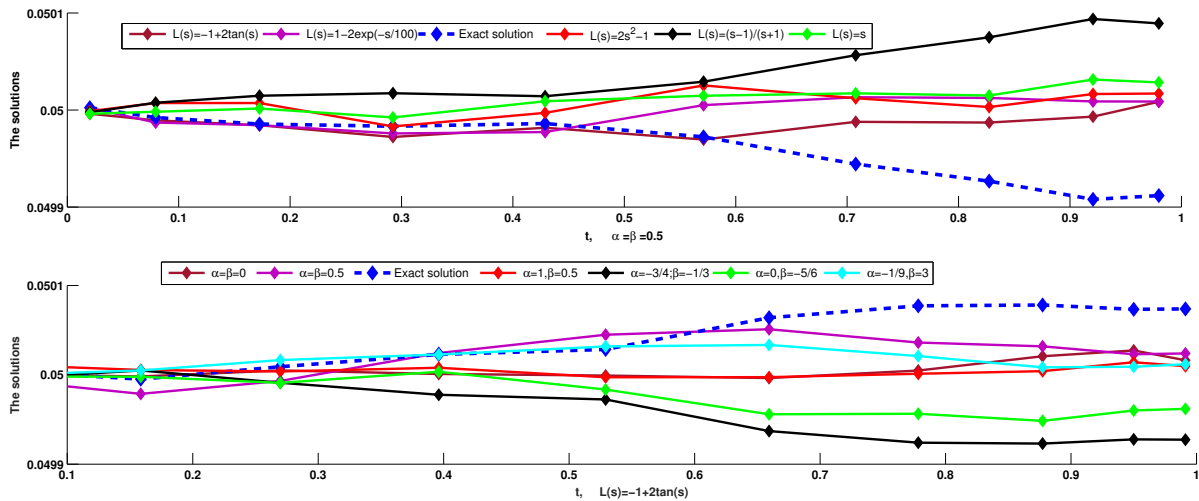
Figure 3.12: The exact solution and approximate solutions using different values of α and β and a different Lagrange functions $L(s)$ for Example 3.4.

3.5   Analysis of the proposed technique

The proposed technique leverages the generalized Lagrange interpolated polynomial with a new way, showcasing advantages over existing methods such as the Fibonacci method in [83], Euler polynomials in [86], hat functions in [119], and Jacobi polynomials in [110]. The approximate solutions obtained through the new proposed technique demonstrate excellent agreement with exact solutions across various choices of generalized Lagrange functions. Some advantages of the proposed technique include:

- **Applicability to Smooth Solutions**: The method performs well when a smooth solution is anticipated, utilizing low-degree polynomials through a spectral approach.

- **Adaptability to Problem Characteristics**: The flexibility to select basis functions tailored to specific problem characteristics enhances the method's versatility.

- **Stability and Efficiency**: The proposed spectral method proves to be more stable, suitable, and less time-consuming than certain existing numerical methods.

- **Efficiency Across Various Solutions**: The algorithm exhibits efficiency across diverse exact solutions employed as test functions.

The novelty lies in the utilization of a new concept for approximating Itô stochastic integral equations through integration by parts and Gauss quadrature for each trajectory of Brown-

ian motion. Moreover, the accuracy of the technique can be explored for sufficiently large T, providing feasibility for numerical experiments in terms of speed and memory within the developed framework.

Conclusion and Perspectives

Stochastic differential equations (SDEs) governed by Brownian motion and by a jump diffusion are important tools in a wide range of applications, including biology, chemistry, mechanics, economics, and physics. They are becoming more and more attractive due to their application for simulating stochastic phenomena in various fields.

These equations are explained and interpreted in the context of the Itô calculus. Unfortunately, there is frequently no analytical solution to these equations, and we are obliged to use numerical approximations. Broadly speaking, there are two basic ways to derive these approximations. When the sample trajectories of the solutions need to be approximated, mean square convergence is employed, and the methods thus derived are called strong. When we are interested only in the moments or other functionals of the solution, which involve a much weaker form of convergence.

The purpose of this dissertation is to provide a brief overview of the different numerical methods for solving stochastic differential equations and to propose a new methodology that improves some existing techniques. It can be seen that the discretization step size plays an important role in the accuracy for each method through the simulation of Itô-Taylor schemes and in particular by the examination of the effectiveness of some schemes for the approximation of the solutions of SDE. When the step size is kept very small, good results can be attained. Conversely, the computational complexity is very high when we increase the order of the schemes.

We have proposed two numerical approaches that can be used for finding approximate solutions of stochastic integral equations. Interpolation by Lagrange polynomials and zeros of Jacobi polynomials are used to reduce the considered problem of stochastic Volterra integral equations to an algebraic system of equations. Approximate solutions of the stochastic

Volterra integral equations are then obtained. A theoretical investigation is also carried out to confirm the error and convergence analysis of these methods. The spectral convergence rate for the developed method is established. In order to prove the suitability and accuracy of our methods several related numerical examples with different simulations of Brownian motion are included. The numerical results of the presented methods are also compared with the results of other numerical techniques.

The second new technique is based on combining Jacobi-Gauss collocation points and generalized Lagrange functions. The accuracy and consistency of the new technique are evaluated and compared with some techniques. In addition, sufficient conditions are given to ensure that the estimation error tends to zero. The new technique shows surprising efficiency over the existing techniques in terms of needed time, computational, and approximation performance. The accuracy of the solution derived by the new technique is significantly higher than that of the existing methods.

We are optimistic that it will be possible to generalize the proposed method to a broader class of problems while maintaining the efficiency and accuracy of the method. Extending our work represents an interesting topic for future work, which we can identify as follows

- The ability to extend the approximation to higher dimensions.

- Our results leave the door open for future developments, including the extension of the current research to stochastic differential equations driven by other stochastic processes.

- According to the approach presented in this dissertation, in a future research, one can think about the application of the proposed technique to stochastic integro-differential or partial equations.

Bibliography

[1] Abdulle, Assyr, Grigorios A. Pavliotis, and Urbain Vaes. "Spectral methods for multi-scale stochastic differential equations." SIAM/ASA Journal on Uncertainty Quantification 5, no. 1 (2017): 720-761.

[2] Abdulle, Assyr, and Adrian Blumenthal. "Stabilized multilevel Monte Carlo method for stiff stochastic differential equations." Journal of Computational Physics 251 (2013): 445-460.

[3] Abdelkawy, M. A., António M. Lopes, and Mohammed M. Babatin. "Shifted fractional Jacobi collocation method for solving fractional functional differential equations of variable order." Chaos, Solitons & Fractals 134 (2020): 109721.

[4] Abu Arqub, Omar, and Hasan Rashaideh. "The RKHS method for numerical treatment for integrodifferential algebraic systems of temporal two-point BVPs." Neural Computing and Applications 30 (2018): 2595-2606.

[5] Ahmad, Sk Safique, Nigam Chandra Parida, and Soumyendu Raha. "The fully implicit stochastic-α method for stiff stochastic differential equations." Journal of Computational Physics 228, no. 22 (2009): 8263-8282.

[6] Alcock, Jamie, and Kevin Burrage. "A note on the balanced method." BIT Numerical Mathematics 46 (2006): 689-710.

[7] Alcock, Jamie, and Kevin Burrage. "Stable strong order 1.0 schemes for solving stochastic ordinary differential equations." BIT Numerical Mathematics 52 (2012): 539-557.

[8] Ali, Khalid K., Mohamed A. Abd El salam, and Emad MH Mohamed. "A numerical technique for a general form of nonlinear fractional-order differential equations with the linear functional argument." International Journal of Nonlinear Sciences and Numerical Simulation 22, no. 1 (2021): 83-91.

[9] Ali, Khalid K., Mohamed A. Abd El Salam, Emad MH Mohamed, Bessem Samet, Sunil Kumar, and M. S. Osman. "Numerical solution for generalized nonlinear fractional integro-differential equations with linear functional arguments using Chebyshev series." Advances in Difference Equations 2020, no. 1 (2020): 1-23.

[10] Arnold, L. "Stochastic differential equations: Theory and applications(Book)." New York, Wiley-Interscience, 1974. 243 p (1974).

[11] Ascher, Uri M., and Chen Greif, eds. A first course on numerical methods. Society for Industrial and Applied Mathematics, 2011.

[12] Asgari, Mahnaz, Elham Hashemizadeh, Morteza Khodabin, and Khosrow Maleknejad. "Numerical solution of nonlinear stochastic integral equation by stochastic operational matrix based on Bernstein polynomials." Bulletin mathématique de la Société des Sciences Mathématiques de Roumanie (2014): 3-12.

[13] Baccouch, Mahboub, Helmi Temimi, and Mohamed Ben-Romdhane. "A discontinuous Galerkin method for systems of stochastic differential equations with applications to population biology, finance, and physics." Journal of Computational and Applied Mathematics 388 (2021): 113297.

[14] Bachelier, Louis. "Théorie de la spéculation." In Annales scientifiques de l'École normale supérieure, vol. 17, pp. 21-86. 1900.

[15] Bathe, Klaus-Jürgen. Finite element procedures. Klaus-Jurgen Bathe, 2006.

[16] Baxter, Martin, and Andrew Rennie. Financial calculus: an introduction to derivative pricing. Cambridge university press, 1996.

[17] Berger, Marc A., and Victor J. Mizel. "Volterra equations with itô integrals—I." The Journal of Integral Equations (1980): 187-245.

[18] Bhrawy, Ali H. "A Jacobi spectral collocation method for solving multi-dimensional nonlinear fractional sub-diffusion equations." Numerical Algorithms 73 (2016): 91-113.

[19] Bhrawy, Ali H., and Abdulaziz S. Alofi. "A Jacobi–Gauss collocation method for solving nonlinear Lane–Emden type equations." Communications in Nonlinear Science and Numerical Simulation 17, no. 1 (2012): 62-70.

[20] Bhrawy, A. H., E. H. Doha, M. A. Abdelkawy, and R. A. Van Gorder. "Jacobi–Gauss–Lobatto collocation method for solving nonlinear reaction–diffusion equations subject to Dirichlet boundary conditions." Applied Mathematical Modelling 40, no. 3 (2016): 1703-1716.

[21] Billingsley, Patrick. Probability and measure. John Wiley & Sons, 2017.

[22] Boukhelkhal, Ikram, Rebiha Zeghdane, and A. M. Elsawah. "A novel efficient technique for solving nonlinear stochastic Itô–Volterra integral equations." Expert Systems with Applications 238 (2024): 121626.

[23] Boukhelkhal, Ikram, and Rebiha Zeghdane. "Lagrange interpolation polynomials for solving nonlinear stochastic integral equations." Numerical Algorithms (2023): 1-36.

[24] Burrage, Pamela Marion. "Runge-Kutta methods for stochastic differential equations." (1999).

[25] Cao, Yang, Daniel T. Gillespie, and Linda R. Petzold. "Adaptive explicit-implicit tau-leaping method with automatic tau selection." The Journal of chemical physics 126, no. 22 (2007).

[26] Carletti, Margherita, Kevin Burrage, and Pamela M. Burrage. "Numerical simulation of stochastic ordinary differential equations in biomathematical modelling." Mathematics and Computers in Simulation 64, no. 2 (2004): 271-277.

[27] Cioica, Petru A., and Stephan Dahlke. "Spatial Besov regularity for semilinear stochastic partial differential equations on bounded Lipschitz domains." International Journal of Computer Mathematics 89, no. 18 (2012): 2443-2459.

[28] Cortés, Juan Carlos, Lucas Jódar, and L. Villafuerte. "Mean square numerical solution of random differential equations: facts and possibilities." Computers & Mathematics with Applications 53, no. 7 (2007): 1098-1106.

[29] Cortés, Juan Carlos, Lucas Jódar, and Laura Villafuerte. "Numerical solution of random differential equations: a mean square approach." Mathematical and Computer Modelling 45, no. 7-8 (2007): 757-765.

[30] Courtault, Jean-Michel, Youri Kabanov, Bernard Bru, Pierre Crépel, Isabelle Lebon, and Arnaud Le Marchand. "Louis Bachelier on the centenary of Théorie de la spéculation." Mathematical Finance 10, no. 3 (2000): 339-353.

[31] Deb, Manas Kumar. Solution of stochastic partial differential equations (SPDEs) using Galerkin method: theory and applications. The University of Texas at Austin, 2000.

[32] Debrabant, Kristian, and Anne K. "Stochastic Taylor expansions: Weight functions of B-series expressed as multiple integrals." Stochastic analysis and applications 28, no. 2 (2010): 293-302.

[33] Delkhosh, Mehdi, and Kourosh Parand. "Generalized pseudospectral method: theory and applications." Journal of Computational Science 34 (2019): 11-32.

[34] Djordjević, Jasmina, and Svetlana Janković. "On a class of backward stochastic Volterra integral equations." Applied Mathematics Letters 26, no. 12 (2013): 1192-1197.

[35] Doha, E. H., M. A. Abdelkawy, A. Z. M. Amin, and Dumitru Baleanu. "Spectral technique for solving variable-order fractional Volterra integro-differential equations." Numerical Methods for Partial Differential Equations 34, no. 5 (2018): 1659-1677.

[36] Doha, Eid H., Mohamed A. Abdelkawy, A. Z. M. Amin, and António M. Lopes. "Shifted Jacobi–Gauss-collocation with convergence analysis for fractional integro-differential equations." Communications in Nonlinear Science and Numerical Simulation 72 (2019): 342-359.

[37] Ehler, Martin. "Shrinkage rules for variational minimization problems and applications to analytical ultracentrifugation." (2011): 593-614.

[38] Einstein, Ann. "On the movement of small particles suspended in a stationary liquid demanded by the molecular-kinetic theory of heat (English translation, 1956)." Investigations on the theory of the Brownian movement (1905).

[39] Elworthy, K. D., A. Truman, H. Z. Zhao, and J. G. Gaines. "Approximate travelling waves for generalized KPP equations and classical mechanics." Proceedings of the Royal Society of London. Series A: Mathematical and Physical Sciences 446, no. 1928 (1994): 529-554.

[40] Ghanem, Roger G., and Pol D. Spanos. Stochastic finite elements: a spectral approach. Courier Corporation, 2003.

[41] Gikhman, Iosif Ilyich, Anatoli Vladimirovich Skorokhod, Iosif Ilyich Gikhman, and Anatoli Vladimirovich Skorokhod. Stochastic differential equations. Springer Berlin Heidelberg, 2007.

[42] Haghighi, Amir, and S. Mohammad Hosseini. "A class of split-step balanced methods for stiff stochastic differential equations." Numerical Algorithms 61 (2012): 141-162.

[43] Haworth, D. C., and S. B. Pope. "A second-order Monte Carlo method for the solution of the Ito stochastic differential equation." Stochastic Analysis and Applications 4, no. 2 (1986): 151-186.

[44] Hespanha, Joao P. "Modelling and analysis of stochastic hybrid systems." IEE Proceedings-Control Theory and Applications 153, no. 5 (2006): 520-535.

[45] Higham, Desmond J. "An algorithmic introduction to numerical simulation of stochastic differential equations." SIAM review 43, no. 3 (2001): 525-546.

[46] Ikeda, Nobuyuki, and Shinzo Watanabe. Stochastic differential equations and diffusion processes. Elsevier, 2014.

[47] Itô, Kiyosi. "Differential equations determining Markov processes." Zenkoku Sizyo Sugaku Danwakai-si (J. Pan-Japan Math. Coll) 244, no. 1077 (1942): 1352-1400.

[48] Itô, Kiyosi. "109. stochastic integral." Proceedings of the Imperial Academy 20, no. 8 (1944): 519-524.

[49] Itô, Kiyosi. "On a stochastic integral equation." Proceedings of the Japan Academy 22, no. 1-4 (1946): 32-35.

[50] Itô, Kiyosi. "On a formula concerning stochastic differentials." Nagoya Mathematical Journal 3 (1951): 55-65.

[51] Itô, Kiyosi. "Multiple wiener integral." Journal of the Mathematical Society of Japan 3, no. 1 (1951): 157-169.

[52] Janković, Svetlana, and Dejan Ilić. "One linear analytic approximation for stochastic integrodifferential equations." Acta Mathematica Scientia 30, no. 4 (2010): 1073-1085.

[53] John, D., and J. R. Anderson. "Computational fluid dynamics: the basics with applications." Mechanical engineering series (1995): 261-262.

[54] Kahl, Christian, and Henri Schurz. "Balanced Milstein methods for ordinary SDEs." Monte Carlo Methods Appl. 12, no. 2 (2006): 143-170.

[55] Karatzas, Ioannis, and Steven Shreve. Brownian motion and stochastic calculus. Vol. 113. Springer Science & Business Media, 2012.

[56] Kawada, Yukiyosi, and Kiyosi Itô. "On the probability distribution on a compact group. I." Proceedings of the Physico-Mathematical Society of Japan. 3rd Series 22, no. 12 (1940): 977-998.

[57] Kendall, Maurice George, and A. Bradford Hill. "The analysis of economic time-series-part i: Prices." Journal of the Royal Statistical Society. Series A (General) 116, no. 1 (1953): 11-34.

[58] Khalaf, Sanaa L., and Hadeer S. Flayyih. "Analysis, predicting, and controlling the COVID-19 pandemic in Iraq through SIR model." Results in Control and Optimization 10 (2023): 100214.

[59] Khalaf, Sanaa L., Mohammed S. Kadhim, and Ayad R. Khudair. "Studying of COVID-19 fractional model: Stability analysis." Partial Differential Equations in Applied Mathematics 7 (2023): 100470.

[60] Khan, Sami Ullah, Mushtaq Ali, and Ishtiaq Ali. "A spectral collocation method for stochastic Volterra integro-differential equations and its error analysis." Advances in Difference Equations 2019, no. 1 (2019): 1-14.

[61] Khodabin, M., K. Maleknejad, M. Rostami, and M. Nouri. "Interpolation solution in generalized stochastic exponential population growth model." Applied Mathematical Modelling 36, no. 3 (2012): 1023-1033.

[62] Khodabin, Morteza, Khosrow Maleknejad, M. Rostami, and Mostafa Nouri. "Numerical approach for solving stochastic Volterra–Fredholm integral equations by stochastic operational matrix." Computers & Mathematics with Applications 64, no. 6 (2012): 1903-1913.

[63] Khodabin, Morteza, Khosrow Maleknejad, M. Rostami, and Mostafa Nouri. "Numerical solution of stochastic differential equations by second order Runge–Kutta methods." Mathematical and computer Modelling 53, no. 9-10 (2011): 1910-1920.

[64] Klebaner, Fima C. Introduction to stochastic calculus with applications. World Scientific Publishing Company, 2012.

[65] Kloeden, Peter, and Andreas Neuenkirch. "Convergence of numerical methods for stochastic differential equations in mathematical finance." In Recent Developments in Computational Finance: Foundations, Algorithms and Applications, pp. 49-80. 2013.

[66] Kloeden, Peter E., Eckhard Platen. Stochastic differential equations. Springer Berlin Heidelberg, 1992.

[67] Kloeden, Peter E., and Eckhard Platen. "Stratonovich and Itô stochastic taylor expansions." Mathematische Nachrichten 151, no. 1 (1991): 33-50.

[68] Kolmogorov, A. N. "Statistical Theory of Oscillations with continuous spectrum In: Selected Works of AN Kolmogorov, Volume II, Probability Theory and Mathematical Statistics." (1992).

[69] Kurttila, Mikko, Mauno Pesonen, Jyrki Kangas, and Miika Kajanus. "Utilizing the analytic hierarchy process (AHP) in SWOT analysis—a hybrid method and its application to a forest-certification case." Forest policy and economics 1, no. 1 (2000): 41-52.

[70] Lebesgue, Henri. "Intégrale, longueur, aire." Annali di Matematica Pura ed Applicata (1898-1922) 7, no. 1 (1902): 231-359.

[71] Levin, J. J., and J. A. Nohel. "On a system of integrodifferential equations occurring in reactor dynamics." Journal of Mathematics and Mechanics (1960): 347-368.

[72] Li, Zenghu, and Leonid Mytnik. "Strong solutions for stochastic differential equations with jumps." In Annales de l'IHP Probabilités et statistiques, vol. 47, no. 4, pp. 1055-1067. 2011.

[73] Luo, Yi. Numerical Solutions for Stochastic Differential Equations and Some Examples. Brigham Young University, 2009.

[74] Luo, Wuan. Wiener chaos expansion and numerical solutions of stochastic partial differential equations. California Institute of Technology, 2006.

[75] Maleknejad, Khosrow, Morteza Khodabin, and M. Rostami. "A numerical method for solving m-dimensional stochastic Itô–Volterra integral equations by stochastic operational matrix." Computers & Mathematics with Applications 63, no. 1 (2012): 133-143.

[76] Maleknejad, Khosrow, Morteza Khodabin, and M. Rostami. "Numerical solution of stochastic Volterra integral equations by a stochastic operational matrix based on block pulse functions." Mathematical and computer Modelling 55, no. 3-4 (2012): 791-800.

[77] Mardones, H. A., and C. M. Mora. "First-order weak balanced schemes for stochastic differential equations." Methodology and Computing in Applied Probability 22 (2020): 833-852.

[78] Marzban, H. R., H. R. Tabrizidooz, and M. Razzaghi. "A composite collocation method for the nonlinear mixed Volterra–Fredholm–Hammerstein integral equations." Communications in Nonlinear Science and Numerical Simulation 16, no. 3 (2011): 1186-1194.

[79] Méléard, Sylvie. Aléatoire: Introduction à la théorie et au calcul des probabilités. Editions Ecole Polytechnique, 2010.

[80] Miller, R. K. "On a system of integro-differential equations occurring in reactor dynamics." SIAM J. Appl. Math 14 (1966): 446-452.

[81] Milstein, Grigorii Noikhovich. Numerical integration of stochastic differential equations. Vol. 313. Springer Science & Business Media, 2013.

[82] Milstein, Grigori N., Eckhard Platen, and Henri Schurz. "Balanced implicit methods for stiff stochastic systems." SIAM Journal on Numerical Analysis 35, no. 3 (1998): 1010-1019.

[83] Mirzaee, Farshid, and Seyede Fatemeh Hoseini. "Numerical approach for solving nonlinear stochastic Itô-Volterra integral equations using Fibonacci operational matrices." Scientia Iranica 22, no. 6 (2015): 2472-2481.

[84] Mirzaee, Farshid, Shiva Naserifar, and Erfan Solhi. "Accurate and stable numerical method based on the Floater-Hormann interpolation for stochastic Itô-Volterra integral equations." Numerical Algorithms (2023): 1-18.

[85] Mirzaee, Farshid, Shadi Rezaei, and Nasrin Samadyar. "Numerical solution of two-dimensional stochastic time-fractional Sine–Gordon equation on non-rectangular domains using finite difference and meshfree methods." Engineering Analysis with Boundary Elements 127 (2021): 53-63.

[86] Mirzaee, Farshid, Nasrin Samadyar, and Seyede Fatemeh Hoseini. "Euler polynomial solutions of nonlinear stochastic Itô–Volterra integral equations." Journal of Computational and Applied Mathematics 330 (2018): 574-585.

[87] Mirzaee, Farshid, and Nasrin Samadyar. "Numerical solution of two dimensional stochastic Volterra–Fredholm integral equations via operational matrix method based on hat functions." SeMA Journal 77, no. 3 (2020): 227-241.

[88] Mirzaee, Farshid, and Nasrin Samadyar. "On the numerical solution of fractional stochastic integro-differential equations via meshless discrete collocation method based on radial basis functions." Engineering Analysis with Boundary Elements 100 (2019): 246-255.

[89] Mirzaee, Farshid, and Nasrin Samadyar. "Using radial basis functions to solve two dimensional linear stochastic integral equations on non-rectangular domains." Engineering Analysis with Boundary Elements 92 (2018): 180-195.

[90] Mohamed, Emad MH, K. R. Raslan, Khalid K. Ali, and Mohamed A. Abd El Salam. "On general form of fractional delay integro-differential equations." Arab journal of basic and applied sciences 27, no. 1 (2020): 313-323.

[91] Momani, Shaher, Omar Abu Arqub, and Banan Maayah. "Piecewise optimal fractional reproducing kernel solution and convergence analysis for the Atangana–Baleanu–Caputo model of the Lienard's equation." Fractals 28, no. 08 (2020): 2040007.

[92] Mousavi, Bibi Khadijeh, Ataollah Askari Hemmat, and Mohammad Hossien Heydari. "Wilson wavelets for solving nonlinear stochastic integral equations." Wavelet and Linear Algebra 4, no. 2 (2017): 33-48.

[93] Murge, M. G., and B. G. Pachpatte. "On second order Ito type stochastic integrodifferential equations." Analele Stiintifice ale Universitatii. I. Cuza din Iasi, Mathematica 30, no. 5 (1984): 25-34.

[94] Murge, M. G., and B. G. Pachpatte. "Successive approximations for solutions of second order stochastic integro-differential equations of Ito type." Indian J. Pure Appl. Math 21, no. 3 (1990): 260-274.

[95] Nadja, Jafar Saberi, Omid Reza Navid Samadi, and Emran Tohidi. "Numerical solution of two-dimensional Volterra integral equations by spectral Galerkin method." Journal of Applied Mathematics and Bioinformatics 1, no. 2 (2011): 159.

[96] Nemati, S., P. M. Lima, and S. Sedaghat. "Legendre wavelet collocation method combined with the Gauss–Jacobi quadrature for solving fractional delay-type integro-differential equations." Applied Numerical Mathematics 149 (2020): 99-112.

[97] Oguztoreli, M. Namik. Time-lag control systems. Vol. 24. New York: Academic Press, 1966.

[98] Oksendal, Bernt. Stochastic differential equations: an introduction with applications. Springer Science & Business Media, 2013.

[99] Pais, Abraham. Subtle is the Lord: The Science and the Life of Albert Einstein: The Science and the Life of Albert Einstein. Oxford University Press, USA, 1982.

[100] Papoulis, Athanasios. Probability, Random Variables, and Stochastic Processes: Solutions to the Problems in Probability, Random Variables and Stochastic Processes. McGraw-Hill, 1965.

[101] Parand, Kourosh, and Mehdi Delkhosh. "The generalized fractional order of the Chebyshev functions on nonlinear boundary value problems in the semi-infinite domain." Nonlinear Engineering 6, no. 3 (2017): 229-240.

[102] Pellegrini, Clément. "Existence, uniqueness and approximation of the jump-type stochastic Schrödinger equation for two-level systems." Stochastic Processes and their Applications 120, no. 9 (2010): 1722-1747.

[103] Perrin, Jean. "Mouvement brownien et réalité moléculaire." In Annales de Chimie et de Physique, vol. 18, pp. 1-114. 1909.

[104] Parvizi, Maryam, and M. R. Eslahchi. "The convergence and stability analysis of the Jacobi collocation method for solving nonlinear fractional differential equations with integral boundary conditions." Mathematical Methods in the Applied Sciences 39, no. 8 (2016): 2038-2056.

[105] Platen, Eckhard, and Nicola Bruti-Liberati. Numerical solution of stochastic differential equations with jumps in finance. Vol. 64. Springer Science & Business Media, 2010.

[106] Ramu, S. Anantha, and R. Ganesan. "A Galerkin finite element technique for stochastic field problems." Computer Methods in Applied Mechanics and Engineering 105, no. 3 (1993): 315-331.

[107] Raslan, K. R., and Khalid K. Ali. "A new structure formulations for cubic B-spline collocation method in three and four-dimensions." Nonlinear Engineering 9, no. 1 (2020): 432-448.

[108] Raslan, K. R., and Khalid K. Ali. "On n-dimensional quadratic B-splines." Numerical Methods for Partial Differential Equations 37, no. 2 (2021): 1057-1071.

[109] Ray, S. Saha, and S. Singh. "Numerical solution of nonlinear stochastic Itô–Volterra integral equation driven by fractional Brownian motion." Engineering Computations 37, no. 9 (2020): 3243-3268.

[110] Ray, S. Saha, and P. Singh. "Numerical solution of stochastic Itô-Volterra integral equation by using Shifted Jacobi operational matrix method." Applied Mathematics and Computation 410 (2021): 126440.

[111] Reshniak, V., A. Q. M. Khaliq, D. A. Voss, and G. Zhang. "Split-step Milstein methods for multi-channel stiff stochastic differential systems." Applied Numerical Mathematics 89 (2015): 1-23.

[112] Resnick, Sidney I. Adventures in stochastic processes. Springer Science & Business Media, 2013.

[113] Rezazadeh, Tohid, and Esmaeil Najafi. "Jacobi collocation method and smoothing transformation for numerical solution of neutral nonlinear weakly singular Fredholm integro-differential equations." Applied Numerical Mathematics 181 (2022): 135-150.

[114] Rößler, Andreas. "Rooted tree analysis for order conditions of stochastic Runge-Kutta methods for the weak approximation of stochastic differential equations." Stochastic analysis and applications 24, no. 1 (2006): 97-134.

[115] Rong, S. Theory of stochastic differential equations with jumps and applications: mathematical and analytical techniques with applications to engineering. Springer Science & Business Media, 2006.

[116] Rué, Pau, Jordi Villà-Freixa, and Kevin Burrage. "Simulation methods with extended stability for stiff biochemical kinetics." BMC Systems Biology 4 (2010): 1-13.

[117] Saha Ray, S., and S. Singh. "New stochastic operational matrix method for solving stochastic Itô–Volterra integral equations characterized by fractional Brownian motion." Stochastic Analysis and Applications 39, no. 2 (2020): 224-234.

[118] Samadyar, Nasrin, and Farshid Mirzaee. "Numerical solution of two-dimensional weakly singular stochastic integral equations on non-rectangular domains via radial basis functions." Engineering Analysis with Boundary Elements 101 (2019): 27-36.

[119] Sharafi, Fatemeh, and Behrooz Basirat. "Numerical solution of nonlinear stochastic Itô–Volterra integral equation by stochastic modified hat function operational matrices." Results in Applied Mathematics 14 (2022): 100260.

[120] Shen, Jie, Tao Tang, and Li-Lian Wang. Spectral methods: algorithms, analysis and applications. Vol. 41. Springer Science & Business Media, 2011.

[121] Shiralashetti, S. C., and Lata Lamani. "Bernoulli wavelets operational matrices method for the solution of nonlinear stochastic Itô-Volterra integral equations." Earthline Journal of Mathematical Sciences 5, no. 2 (2021): 395-410.

[122] Shreve, Steven E. Stochastic calculus for finance II: Continuous-time models. Vol. 11. New York: springer, 2004.

[123] Tao, Xia, Ziqing Xie, and Xiaojun Zhou. "Spectral Petrov-Galerkin methods for the second kind Volterra type integro-differential equations." Numerical Mathematics: Theory, Methods and Applications 4, no. 2 (2011): 216-236.

[124] Thiele, Thorvald N. Sur la compensation de quelques erreurs quasi-systématiques par la méthode des moindres carrés. Reitzel, 1880.

[125] Tian, Tianhai, and Kevin Burrage. "Implicit Taylor methods for stiff stochastic differential equations." Applied Numerical Mathematics 38, no. 1-2 (2001): 167-185.

[126] Ville, Jean. Etude critique de la notion de collectif. Paris: Gauthier-Villars, 1939.

[127] Wang, Peng, and Zhenxin Liu. "Split-step backward balanced Milstein methods for stiff stochastic systems." Applied Numerical Mathematics 59, no. 6 (2009): 1198-1213.

[128] Wang, Peng, and Yong Li. "Split-step forward methods for stochastic differential equations." Journal of computational and applied mathematics 233, no. 10 (2010): 2641-2651.

[129] Wang, Xiaojie, Siqing Gan, and Desheng Wang. "A family of fully implicit Milstein methods for stiff stochastic differential equations with multiplicative noise." BIT Numerical Mathematics 52 (2012): 741-772.

[130] Wang, Xi, Jun Jiang, Ling Hong, Lincong Chen, and Jian-Qiao Sun. "On the optimal design of radial basis function neural networks for the analysis of nonlinear stochastic systems." Probabilistic Engineering Mechanics (2023): 103470.

[131] Wagner, W. "On a Taylor formula for a class of Ito processes." Proba. and Math. Statist. 3 (1982): 37-51.

[132] Wan, Zhengsu, Yanping Chen, and Yunqing Huang. "Legendre spectral Galerkin method for second-kind Volterra integral equations." Frontiers of Mathematics in China 4 (2009): 181-193.

[133] Wen, Haining. "Convergence rates of full-implicit truncated Euler–Maruyama method for stochastic differential equations." Journal of Applied Mathematics and Computing 60, no. 1-2 (2019): 147-168.

[134] Wiener, N. "Collected Works—Vol. 1,(ed.) P. Masani." (1976): 453.

[135] Wu, Jieheng, Guo Jiang, and Xiaoyan Sang. "Numerical solution of nonlinear stochastic Itô–Volterra integral equations based on Haar wavelets." Advances in Difference Equations 2019, no. 1 (2019): 1-14.

[136] Xi, Fubao, and Chao Zhu. "Jump type stochastic differential equations with non-Lipschitz coefficients: non-confluence, Feller and strong Feller properties, and exponential ergodicity." Journal of Differential Equations 266, no. 8 (2019): 4668-4711.

[137] Xie, Ziqing, Xianjuan Li, and Tao Tang. "Convergence analysis of spectral Galerkin methods for Volterra type integral equations." Journal of Scientific Computing 53 (2012): 414-434.

[138] Xiu, Dongbin, and George Em Karniadakis. "The Wiener–Askey polynomial chaos for stochastic differential equations." SIAM journal on scientific computing 24, no. 2 (2002): 619-644.

[139] Xiu, Dongbin, and Jie Shen. "Efficient stochastic Galerkin methods for random diffusion equations." Journal of Computational Physics 228, no. 2 (2009): 266-281.

[140] Yang, Yin, and Yanping Chen. "Jacobi spectral Galerkin and iterated methods for nonlinear Volterra integral equation." (2016).

[141] Yang, Yin, and Yunqing Huang. "Spectral Jacobi–Galerkin methods and iterated methods for Fredholm integral equations of the second kind with weakly singular kernel." Discrete Contin. Dyn. Syst. Ser. S 12 (2019): 685-702.

[142] Yong, Jiongmin. "Backward stochastic Volterra integral equations and some related problems." Stochastic Processes and their Applications 116, no. 5 (2006): 779-795.

[143] Zeghdane, Rebiha. "Numerical solution of stochastic integral equations by using Bernoulli operational matrix." Mathematics and Computers in Simulation 165 (2019): 238-254.

[144] Zhang, Xicheng. "Euler schemes and large deviations for stochastic Volterra equations with singular kernels." Journal of Differential Equations 244, no. 9 (2008): 2226-2250.

[145] Zhang, Xicheng. "Stochastic Volterra equations in Banach spaces and stochastic partial differential equation." Journal of Functional Analysis 258, no. 4 (2010): 1361-1425.